SHREDDED TIRES AS AN URBAN LOCAL ROAD DRAINAGE LAYER MATERIAL

Thesis Submitted to the College of

Graduate Studies and Research

in Partial Fulfillment of the Requirements

for the Degree of Masters of Science

in the Department of Civil and Geological Engineering

University of Saskatchewan

Saskatoon

By

Ganiu Abdul Rahman

PERMISSION TO USE

In presenting this thesis in partial fulfillment of the requirements for a Postgraduate degree from the University of Saskatchewan, the author has agreed that the Libraries of this University may make it freely available for inspection. The author has further agreed that permission for copying of this thesis in any manner, in whole or in part, for scholarly purposes may be granted by the professor or professors who supervised the thesis work or, in their absence, by the Head of the Department or the Dean of the College in which the thesis work was done. It is understood that any copying, publication, or use of this thesis or parts thereof for financial gain shall not be allowed without the author's written permission. It is also understood that due recognition shall be given to the author and to the University of Saskatchewan in any scholarly use which may be made of any material in this thesis.

Requests for permission to copy or to make other use of material in this thesis in whole or part should be addressed to:

Head of the Department of Civil Engineering

University of Saskatchewan

Saskatoon, Saskatchewan S7N 5A9

ABSTRACT

Roads in many northern climates like Saskatchewan can undergo structural failure caused by frost action and substructure moisture problems. Frost action can be efficiently controlled by eliminating at least one of the following conditions: moisture; freezing temperatures; and frost susceptible soils. However, effective use of shredded tire material could provide an environmentally sustainable solution for waste tires and could relieve pressure on limited quality aggregate resources.

The City of Saskatoon has successfully incorporated crushed rock and crushed recycled concrete as a subsurface road drainage layer to mitigate substructure drainage and frost issues. However, the price of crushed high value aggregates can be cost prohibitive and at times these materials are not available in quantities required. Previous research has documented that shredded tires are efficient in controlling frost action by providing thermal insulation and free drainage, but shredded tires performed poorly as a structural support layer with low mechanical stiffness and high compressibility properties.

The goal of this research was to provide improved pavement performance with respect to road substructure moisture drainage and frost mitigation. The specific objectives of this research were to:

- Quantify the mechanical properties of shredded tires and investigate the mechanical behavior of mixes of shredded tires with and without sand blended into the tire matrix as compared to conventional subbase and base coarse materials;
- Determine the permeability of shredded tires and investigate the effect of sand on the permeability of shredded tire/sand mixes as compared to conventional granular base and subbase materials, and;
- Compare the structural primary response behavior and capital cost of alternate road structures constructed with shredded tires and mixes of shredded tire and sand as a free draining subbase material compared to conventional drainage layers and road structures.

The hypothesis of this research was that the mechanical behavior of shredded tire material, used as a road substructure layer, can be improved by blending it with free draining sand. It was also hypothesized that blending shredded tire with free draining sand will have improved drainage compared to conventional granular subbase and base course materials.

Volumetric and mechanistic material properties and structural performance behavior of shredded tires and shredded tire/sand mixes in the mix ratios (by volume) of 1Tire:1Sand, 1Tire:2Sand and 1Tire:3Sand were evaluated and compared to City of Saskatoon subbase materials: crushed rock and granular base; as well as Saskatchewan Ministry of Highways and Infrastructure (SMHI) Type 6 subbase.

Laboratory characterization showed that 100% shredded tire materials were uniformly graded indicating high amounts of voids. The addition of sand resulted in a reduction of interparticle air voids. Results from strength and stiffness characterization tests indicated that 100% shredded tires exhibited low structural stiffness, but this behavior was improved as the quantity of sand in the shredded tire was increased. The 100% shredded tire material was determined to have a dynamic modulus value of 5MPa, whereas shredded tires/sand blends at the ratios of 1Tire:1Sand, 1Tire:2Sand and 1Tire:3Sand gave dynamic moduli values of 30MPa, 110 MPa and 158MPa, respectively. For comparison, SMHI Type 6 subbase, City of Saskatoon crushed rock and granular base exhibited dynamic moduli values of 94MPa, 174MPa and 471MPa, respectively.

Permeability characterization indicated that the 100% shredded tire materials were free draining at 1.42cm/s. Permeability decreased from 1.42cm/s with 100% shredded tire to 0.0026cm/s with 1Tire:3Sand. However, the shredded tire/sand mixes maintained permeability values higher than sand (0.0013cm/s). SMHI Type 6 subbase and granular materials were found to have a permeability of 0.0018cm/s and 0.000025cm/s, respectively, while crushed rock was free draining with a permeability of 1.12cm/s.

Structural behavior of 100% shredded tire, shredded tire/sand mixes and City of Saskatoon subbase materials were studied in road models using a 3-D numerical road modeling software that encoded triaxial material constitutive relationships determined in this research. A typical City of Saskatoon road structure was assumed for all road structures considered in this

study with varying subbase material so as to directly compare the structural effect of the shredded tire with conventional road materials under primary load limits. Modeled results of the 100% shredded tire and crushed rock roads showed peak surface deflections of 2.19mm and 0.73mm, respectively. Peak surface deflection under primary load limits was found to decrease with an increase in sand quantity within the shredded tire layer. Based on the modeling results, 1Tire:2Sand and 1Tire:3Sand yielded peak surface deflections of 1.01mm and 0.96mm, respectively. For comparative purposes, road structures with SMHI Type 6 subbase deflected at 1.14mm.

Field test sections were constructed at Adolph Way in Saskatoon to compare the structural performance of shredded tire to crushed rock (currently specified by City of Saskatoon for drainage layers) in a typical residential road in Saskatoon. Unfortunately, both crushed rock (control) and shredded tire sections were found to deflect above acceptable limits due to high moisture conditions within the deep subgrade. Therefore, deeper excavation was required and the test sections were not constructed. The Adolph Way field experimentation of shredded tire showed that shredded tire road systems can be effectively constructed in the field, but showed the same sensitivity to poor subgrade conditions as crushed rock.

Capital cost analysis showed the 100% shredded tire and shredded tire/sand subbase layers to be less expensive than City of Saskatoon specified crushed rock drainage layers. The 100% shredded tire layer was estimated at a total cost of $\$2.93/m^2$ while 1Tire:1Sand, 1Tire:2Sand and 1Tire:3Sand were estimated at $\$4.39/m^2$, $\$4.88/m^2$ and $\$5.12/m^2$, respectively. SMHI Type 6 subbase, crushed rock and granular base layers were estimated at a total cost of $\$5.85/m^2$, $\$13.95/m^2$ and $\$9.00/m^2$, respectively for equivalent thickness.

From the structural, permeability and economic perspective of this research, the 1Tire:2Sand and 1Tire:3Sand materials proved to be cost efficient as well as technically viable options for mitigating frost action as compared with City of Saskatoon crushed rock materials evaluated. The use of shredded tire/sand mixes of 1Tire:2Sand and 1Tire:3Sand in urban local road structures with low traffic volumes are therefore recommended as a cost effective subbase drainage layer material.

ACKNOWLEDGEMENTS

All praises to God Almighty for His guidance and protection throughout my years of studies in the University of Saskatchewan. My gratitude to my lovely wife and mom for their love and support.

Special thanks to the staff of Civil Engineering Department: Debbie Forgie, Cynthia Hanke, and Alison Beattty for their assistance.

My sincere gratitude goes to my Advisory Committee for their guidance in my research: Dr. Gordon Putz, Dr. Gordon Sparks, and Dr. Peter Park.

Special thanks and acknowledgement to my research supervisor, Dr. Curtis Berthelot, for his guidance throughout my years of studies.

TABLE OF CONTENTS

LIST OF FIGURES

LIST OF TABLES

List of Abbreviations

AAA	-	American Automobile Association
AASHTO	-	Association of State Highway and Transportation Officials
ARMA	-	Alberta Recycling Management Authority
ASTM	-	American Society for Testing and Materials
CAA	-	Canadian Automobile Association
CalTrans	-	California Department of Transportation
CBR	-	California Bearing Ratio
CCME	-	Canadian Council of Ministers of the Environment
COE	-	Corps of Engineers
COS	-	City of Saskatoon
EQG	-	Environmental Quality Guidelines
HMAC	-	Hot Mix Asphalt Concrete
HWD	-	Heavy Weight Deflectometer
LVDTs	-	Linear Variable Displacement Transducers
PCC	-	Portland Cement Concrete
RAP	-	Recycled Asphalt Pavement
RaTT	-	Rapid Triaxial Tester
SHRP	-	Strategic Pavement Research Programme
SHWEC	-	Solid & Hazardous Waste Education Centre
SMHI	-	Saskatchewan Ministry of Highway and Infrastructure
SPS-9A	-	Specific Pavement Studies 9A
SSTC	-	Saskatchewan Scrap Tire Corporation
USCS	-	Unified Soil Classification System

CHAPTER 1 INTRODUCTION

1.1 Background

Over recent years, road agencies have experienced an increase in registered vehicles as well as an increase in traffic volumes (American Automobile Association (AAA) 2009; Canadian Automobile Association (CAA) 2009). This increase in traffic volumes has led to an increase in the number of scrap tires generated (Saskatchewan Scrap Tire Corporation (SSTC) 2009). About 2,000,000 scrap tires are generated in Saskatchewan annually (SSTC 2012). As a result, government regulatory bodies are faced with the problem of recycling or properly disposing of scrap tires.

Scrap tires are non-degradable and bulky, making their disposal a significant problem and high cost. The most common means of disposal of old tires is land filling. However, scrap tires are voluminous and take up valuable landfill air space (as seen in Figure 1.1). They also serve as breeding grounds for mosquitoes causing health related problems (SSTC 2009). These tires also contain combustible materials that expose landfills to fire and other environmental hazards if ignited. To illustrate, Figure 1.2 shows a fire incident in 1990 in the small community of Hagersville, Ontario, where 14 million scrap tires piled in a landfill caught fire and burned for 17 days causing an extensive amount of pollution and also costing the province of Ontario $12 million to extinguish (SSTC 2009).

Coupled with growing traffic on the road infrastructure of many Canadian cities (Prang 2009), frost action in northern climates can result in significant heaving of road pavements. Frost action in frost susceptible soils causes roads to heave in winter generating cracks and pavement failure. In the spring, the melting of ice lenses releases moisture and causes the subbase and subgrade materials to weaken due to loss in bearing capacity, which results in accelerated pavement deterioration (Figure 1.3 and 1.4).

Figure 1.1 Scrap Tires in a Landfill (SSTC 2012)

Figure 1.2 Fire Hazard in Hagersville, Ontario (Buthe 1990)

Figure 1.3 Frost Heave Failure of Saskatchewan Rural Road – Highway 22

Figure 1.4 Frost Induced Failure of Urban Road on Calder Crescent, Saskatoon

Substructure moisture issues in the City of Saskatoon have caused failures on local roads. As an initiative to mitigate subsurface moisture through environmentally sustainable solutions, the City of Saskatoon Green Street Infrastructure Project adopted and successfully implemented the use of crushed recycled concrete and crushed rock as drainage layer material.

Frost action is caused by three conditions: freezing temperatures, available water in sufficient quantities, and frost susceptible soil. Provided at least one of the above conditions is mitigated, frost action ceases to occur (Doré and Zubeck 2008). Based on this phenomenon, previous research experiments have incorporated the use of various materials including shredded tires to mitigate at least one of the aforementioned conditions. Other materials that were used in previous research experiments included sawdust and styrofoam as a thermal insulating medium (Konrad et al 1996).

Shredded tires have been found to provide higher drainage and thermal insulation than conventional road materials. Andersland and Ladanyi (1994) found the thermal conductivity of dry soil to be 1.1W/m.K and that of shredded tires to be 0.23W/m.K which is approximately 80% less than dry soil. Based on results obtained from the bulk density characterization of shredded tires conducted by Das (1995), these materials were found to be three times lighter than conventional granular materials and clay. The lightweight property of shredded tires makes them suitable for use as a fill material on unstable subgrades and slope stability applications. Furthermore, shredded tires contain larger air voids than conventional granular aggregates even under high compressive state, thereby resulting in higher drainage performance than conventional aggregates. The constant head permeability test conducted by California Department of Transportation (CalTrans) found the permeability coefficient of shredded tire to be at an average of 10,000 ft/day (3.47cm/s) (Dresher et al. 1992). The above mentioned properties make shredded tire materials a much more suitable material for use as a drainage layer material in roads for mitigating frost action and substructure moisture problems than conventional granular materials.

However, shredded tire material have low mechanical stiffness compared to conventional aggregates and are generally found to provide poor structural support when used as a pavement layer material due to higher air voids (Lawrence et al 1999). Field experiments conducted by Lawrence et al. (1999) reported that test sections constructed with shredded tires as subbase

(drainage layer) material mitigated frost penetration by a greater extent but performed poorly in providing structural support as compared to an adjacent control section constructed with conventional subbase material.

Environmental impact analysis relating to water-quality effects of shredded tires placed above the water level has been carried out in previous research. This analysis indicates that metals and organic compounds released from shredded tire materials used in road construction are in trace amounts and the leaching of these substances have insignificant effect on groundwater quality (Humphrey and Katz 2000; Humphrey et al 1997).

This research proposes to investigate the feasibility of improving the mechanistic structural performance of shredded tire road systems while providing substructure drainage and thermal insulation to mitigate frost penetration. The use of shredded tires as aggregates would also serve as a less expensive substitute to natural coarse aggregates, which are being depleted in many regions of Saskatchewan.

1.2 Research Goal

The goal of this research was to improve substructure drainage and mitigate frost action in urban roads in Saskatchewan field state conditions.

1.3 Research Objectives

The objectives of this research were to:

- Quantify the mechanical properties of shredded tires and investigate the mechanical behavior of mixes of shredded tires with and without sand blended into the tire matrix as compared to conventional subbase and base coarse materials;
- Determine the permeability of shredded tires and investigate the effect of sand on the permeability of shredded tire/sand mixes as compared to conventional granular base and subbase materials, and;
- Compare the structural primary response behavior and capital cost of alternate road structures constructed with shredded tires and mixes of shredded tire and sand as a free draining subbase material compared to conventional drainage layers and road structures.

1.4 Research Hypothesis

It was hypothesized that the mechanical behavior of shredded tires can be improved by blending them with free draining sand. It is also hypothesized that shredded tire/sand mixes will serve as a drainage and structural layer for Saskatchewan field state conditions relative to conventional road drainage materials.

1.5 Scope

The scope of this research considered the technical feasibility of using shredded tires as a subbase drainage material in urban road construction. This research considered mechanistic based laboratory characterization, structural field investigation, and finite element structural modeling of shredded tire road structures. Tire shreds used in this research were manufactured by Shercom industries of Saskatoon, were irregularly shaped, and varied in sizes. Most of them ranged between 50mm and 150mm with steel fibres still embedded in them.

Laboratory test protocols designed for characterizing granular materials will not be able to efficiently quantify the mechanistic and physical properties of shredded tires in their raw state due to sample size ratio limitation. Fabricating larger test apparatus for characterizing shredded tire in their raw state is cost prohibitive. For the purpose of this research, tire shreds obtained were reduced to smaller pieces of sizes ranging between 12.5mm to 25mm. The modification of tire shreds was done to make them slightly similar to the nominal sizes of granular materials for which test protocols were designed.

Laboratory tests were conducted on prepared samples of 100% shredded tire and shredded tire/sand mixes in the ratios (by volume) of 1Tire:1Sand, 1Tire:2Sand and 1Tire:3Sand. Laboratory characterization of the shredded tire and shredded tire/sand mixes in this research were for the sole purpose of determining and comparing the effect of the quantity of sand on the road structural and subsurface drainage properties of the various shredded tire/sand mixes. Laboratory tests used included grain size distribution, California bearing ratio, vertical confined compressive strength, confined frequency sweep and permeability tests. Six repeat samples were characterized for each of the prepared 100% shredded tire and shredded tire/sand mixes using California bearing ratio, vertical confined compressive strength, and permeability tests. Three repeated samples were characterized using the confined frequency sweep test. The limited

number of repeat samples was due to difficulty involved in reducing shredded tire sizes. Only three repeat samples were tested in RaTT cell for each material due to the risk of damaging test apparatus.

Three dimensional non-linear finite element structural modeling was used to predict and compare the structural performance of 100% shredded tire and shredded tire/sand mixes used as subbase layer materials to City of Saskatoon conventional subbase layer materials in a typical City of Saskatoon local road structure. Structural performance measures used in the comparison included peak surface deflection, horizontal tensile strains at the bottom of asphalt overlay, vertical compressive strain on the top of subgrade and shear stains in all structural layers.

In order to ensure direct comparison of the structural performance of the subbase materials, standard City of Saskatoon road materials and design geometry were used for base layers (120mm thick) and overlays (50mm thick) for all road models. Road models were named according to the subbase material. For instance, a 1Tire:1Sand road represents a road constructed with 50mm asphalt overlay, 120mm base and a 225mm subbase layer composed of shredded tire and sand in the mix ratio of 1:1 by volume.

Field experimentation involved the construction of a 100% shredded tire and a crushed rock test section at Adolph Way in Saskatoon to compare the structural response behavior of the materials as a subbase later material. A typical City of Saskatoon local road design composed of 50 mm asphalt overlay, 120mm Recycled Asphalt Pavement (RAP) base layer and a 225mm subbase layer was used for both sections. Each section was 50m long and 10m wide. Both sections were built up to the base layer and structurally evaluated through proof rolling. Finite element structural modelling was further used to model the structural behavior of both sections.

Capital cost analysis for this research involved analysis of the cost of subbase material used in the shredded tire and shredded tire/sand mix roads as compared to conventional City of Saskatoon materials: SMHI Type 6; crushed rock; and, granular base roads.

No environmental impact analysis was carried out in this research as it was considered outside the scope of this research.

1.6 Methodology

This research will include the following project elements and tasks.

Project Element 1: Literature Review

Task 1: Review of literature related to scrap tire recycling.

Task 2: Review of shredded tire processing and material properties.

Task 3: Frost action and its effect on road performance.

Task 4: Review of laboratory test procedures used in the characterization of shredded tires in previous research.

Task 5: Review of laboratory test procedures to be used in this research.

Project Element 2: Shredded Tire Material Sampling

Task 1: Sampling of tire shreds from Shercom Industries of Saskatoon.

Task 2: Sampling of clean drainage sand readily available in Saskatoon area to be used as a blend material with shredded tire.

Project Element 3: Laboratory Characterization of Samples

Task 1: Tire shreds will be cut into chips for test sample preparation.

Task 2: Prepare samples of:

- Shredded tires;
- 1:1 Shredded tire-sand mix;
- 1:2 Shredded tire-sand mix;
- 1:3 Shredded tire/sand mix (by volume); and,
- Sand.

Task 3: Grain size distribution as specified in American Society for Testing and Materials (ASTM D442) on prepared samples.

Task 4: Standard Proctor compaction of samples (ASTM D698).

Task 5: California Bearing Ratio (CBR) test as specified in ASTM D1883 on compacted samples.

Task 6: Confined vertical compression test on compacted samples.

Task 7: Free drainage test on compacted samples.

Task 8: Confined frequency sweep testing on confined compacted samples at room temperature and load frequency of 5Hz.

Project Element 4: *Finite Element Structural Modeling Road Sections*

Task 1: Determine model input variables for shredded tire roads and City of Saskatoon local roads to be evaluated: design load, road geometry and mechanistic layer material properties.

Task 2: Model the peak surface deflection and 3D strain responses of shredded tire and shredded tire/sand roads together with City of Saskatoon subbase roads.

Task 3: Compare and analyze all road models.

Project Element 5: Design and Construction of Test Section

Task 1: Design of pavement structural thicknesses based on the anticipated traffic loading, City of Saskatoon design standards, and laboratory results and mechanistic material constituent properties.

Task 2: Design of pavement structure of shredded tire test section and City of Saskatoon conventional crushed rock section based on recommendations from literature, City of Saskatoon design criteria and proposed budget.

Task 3: Construction of the two road sections on 100 m long residential road section (Adolph Way, Saskatoon).

Task 4: Use of woven geotextile as subbase separation medium together with geogrid for structural reinforcement on both sections.

Project Element 6: Capital Cost Evaluation

Task 1: Determine the unit cost of materials.

Task 2: Estimate quantities of materials from road section design.

Task 3: Determine the total capital cost for each subbase layer.

Project Element 7: Summary, Conclusions, and Future Recommendations

The research map and work plan for this research is illustrated in Appendix A.

1.7 Benefits of Research

The use of shredded tires as a frost mitigation and drainage subbase material for roads may serve as a cost effective substitute for high value crushed drainage aggregates. The use of shredded tires will also help reduce the number of scrap tires in landfills throughout Saskatchewan. The effective use of scrap tires will significantly improve the state of health and sanitary conditions related to the disposal of tires. Incorporating shredded tire in roads could use approximately 370,000 waste tires per km for a two lane roadway (Lawrence et al 1999).

The long term benefits of this research include the development of road structures with improved drainage and resistance to frost penetration while maintaining a high level of road structural performance in Saskatchewan field state conditions.

1.8 Layout of Thesis

Chapter 1 introduced the background, goal, objectives, and methodology of this research. Chapter 2 gives a literature overview of scrap tire recycling in Saskatchewan. In addition, this chapter reviews the various recycling processes involved in the production of shredded tires from scrap tires and looks at the engineering properties of these products. A review of the mechanism of frost action and an analysis of methods used by previous researchers to mitigate frost action was also considered. Chapter 3 presents laboratory characterization results and analysis. This chapter gives a description of the laboratory test protocols used to characterize shredded tire materials. Chapter 4 involves structural performance modeling and evaluation of road sections constructed using shredded tire, shredded tire/sand mixes and conventional subbase materials. Chapter 5 presents the field test section construction and observations made using shredded tire materials. Chapter 6 provides capital cost analysis for comparing the economics between shredded tire subbase layers and conventional City of Saskatoon local subbase layers. Chapter 7 provides a conclusion, summary and recommendations of the research.

CHAPTER 2 LITERATURE REVIEW

This chapter reviews scrap tire recycling in Saskatchewan and the manufacture of shredded tires from scrap tires. A brief review of the physical and mechanical properties of shredded tires characterized in previous research is also documented.

Frost action is a major contributing factor that causes accelerated pavement deterioration and road failure in northern climates like Canada (Dore and Zubeck 2008). This chapter also reviews the mechanism of frost action and how it could be mitigated by incorporating shredded tires as a subbase drainage layer material in roads.

2.1 Physical Properties of Shredded Tires

Shredded tires are irregularly shaped materials of nominal length mostly ranging from 50 to 305mm (ASTM 1998) depending on the intended use. Shredded tires usually have cord wire and fabric still embedded in them and could be seen along the edges of the shreds as shown in Figure 2.1. Shredded tires can be produced in various shapes and sizes depending on the size of screen used during the shredding process. They are generally durable, coarse grained and of lighter weight as compared to granular materials. Shredded tires are obtained from processing scrap tires.

2.2 Physical and Chemical Composition of Scrap Tire

Scrap tires are composed of three main physical components: rubber, cord wire and fabric. About 80% of the weight of the tire is rubber whereas the cord wire and fabric each takes up 10% of the remaining weight depending on the type of tire (Cosentino et al 1995; Russel 1992).

The technical and environmental properties of shredded tires are influenced by the rubber and steel wire content of scrap tire while the water absorption property is influenced by the fabric content (Russel 1992). Figure 2.2 shows a cross-sectional view of a passenger car tire.

Figure 2.1 Shredded Tire Sample

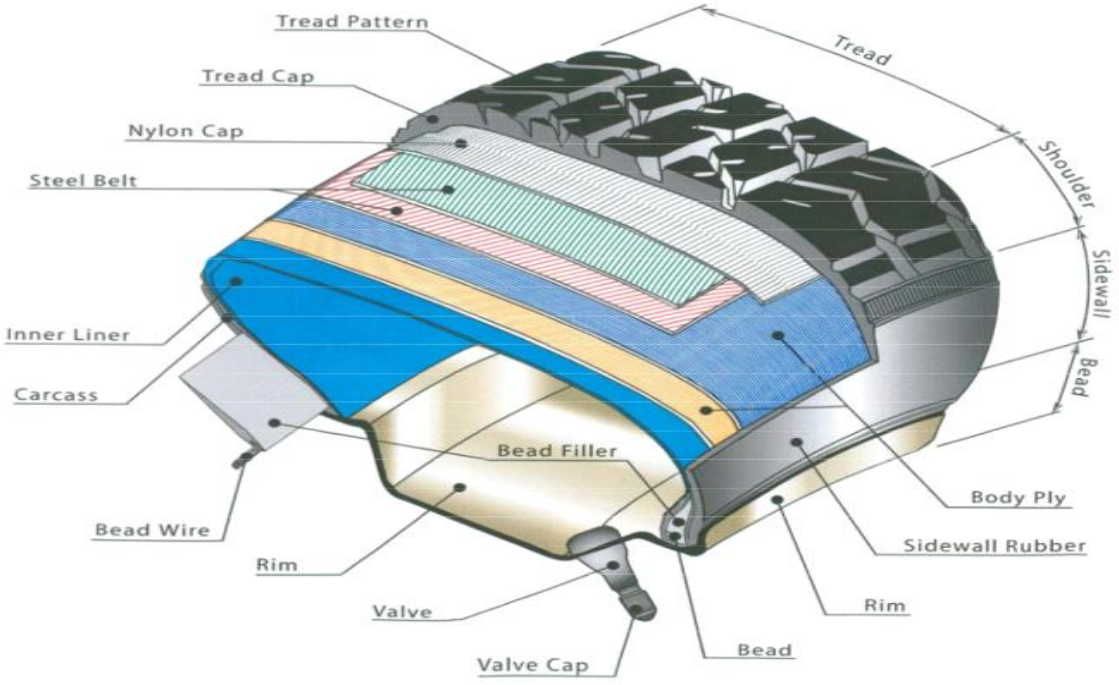

Figure 2.2 Cross-Section of a Car Tire (Anne and Ross 2006)

Tires contain reinforcing chemicals such as carbon black, silica, resin and additives (Pehlken and Essadiqi 2005). Reinforcing chemicals enhance the durability and longevity under all weather and roadway conditions (Pehlken and Essadiqi 2005).

2.3 Waste Tire Recycling

Waste tire recycling is becoming a common practice in major cities around the globe (SSTC 2010). This initiative is mostly aimed at reducing the number of tires occupying vast air space on our landfills so as to promote good sanitation and reduce possible fire hazards.

Recycling of scrap tires in Canada is managed in the various provinces by stewardship programmes. Since scrap tires are of less economic value, government funds and grants are used to promote tire recycling through stewardship programmes in each province (SSTC 2010).

In Saskatchewan, Saskatchewan Scrap Tire Corporation (SSTC), a non profit, non government organization, has recycled over 16 million waste tires since its establishment in 1995 into various useful products (SSTC 2010). Funds generated by SSTC for the collection and recycling of waste tires is mostly from recycling fees remitted to SSTC from the purchase of new tires by consumers. Waste tires recycled are typically from municipal landfills and private stockpiles in backyards and farmlands. A three-phase project launched by the SSTC managed the recycling of more than 6.7 million pounds of scrap tire in its second phase of the project (SSTC 2010). The third phase dubbed "The Black Gold Rush" saw the collection and recycling of more than 2.8 million pounds of waste tire from backyards and farmlands in 48 municipalities (SSTC 2010). Figure 2.3 below shows the number of various tires recycled under the management of SSTC in 2010.

In Alberta, a total of six million scrap tires are disposed each year and the tire stewardship programme in Alberta has recycled an estimated 58 million scrap tires since its establishment in 1992 (Alberta Recycling Management Authority (ARMA) 2009). In September 2009, Ontario launched the Used Tire Stewardship Program to recycle scrap tires within the province that were previously disposed in landfills (Ontario Tire Stewardship 2009).

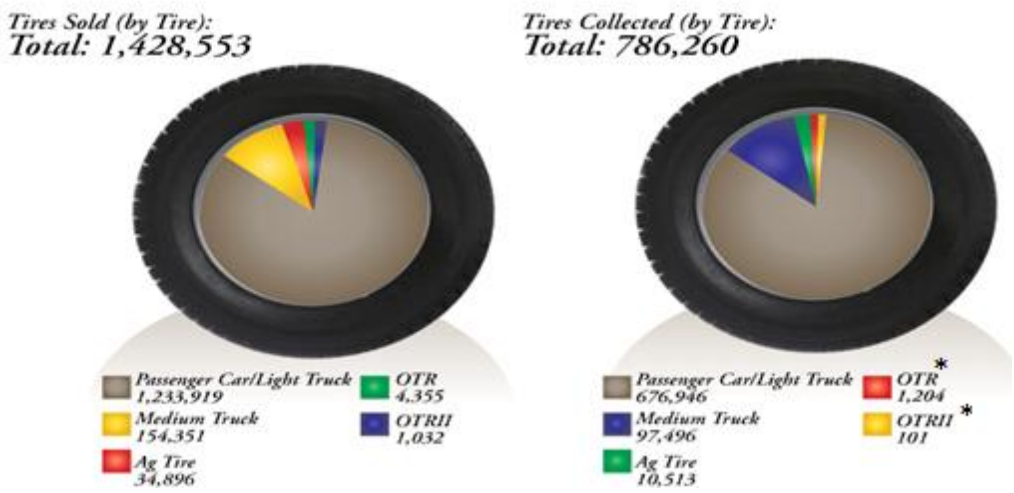

OTR* – Off the Road, OTRII* - Off the Road Retreaded

Figure 2.3 2010 Statistics of Tire Types Recycled by SSTC (SSTC 2010)

2.3.1 Processing of Shredded Tire

The shredded tire processing unit consists of tire shredding machines and conveyors. Tire shredding machines are built to house and shred waste tires fed into them. These machines consist of a series of cutting and shearing teeth built on rotating shafts (Reschner 2008) (Figure 2.4). The shredding machines and conveyor units are normally set up in a sequential order such that waste tires are fed onto the conveyor units and transported to the shredding machines which shear the tires into pieces depending on the manufacturing specifications (Reschner 2008) (Figure 2.5). A series of shredders can be used to shred tires to produce much smaller shreds. Screens are also used in the setup to remove dirt and unwanted smaller tire shreds and also separate finer shreds from coarser ones. Debris such as wood and other foreign materials are removed by hand or fan blowers while scrap metal is removed by magnetic separation. Products from the shredding machines are then transported out by conveyor units to the dumping section or returned for further processing (Reschner 2008).

The stages in shredded tire processing can be broken into primary and secondary shredding. End products of primary shredding, depending on the manufacturer specifications and intended use, usually range from 300 to 450mm, down to 100 to 150mm in length (Solid & Hazardous Waste Education Centre (SHWEC) 2012, Rubber Manufacturers Association 2011, Scrap Tire Council 1995). Tire shreds produced from primary shredding can further be processed

into smaller equidimensional chips of sizes ranging from 75mm to 12mm in the secondary shredding stage (Baker et al 2003). Tire shreds and chips produced by the primary and secondary shredding mostly contain steel fibres still embedded in them (Rubber Manufacturers Association 2011).

The end products of secondary shredding can be further processed into finer material of more economic value using machines equipped with magnets and grinders (Robert 1991). Tire shreds and chips fed into these machines are further broken down and the steel fibres are removed by magnets before the rubber is further ground into a product known as ground rubber (Robert 1991).

2.3.2 Other Waste Tire Products

Waste tires can be processed into several other products including whole tires, slit tires, ground rubber and crumb rubber which are used for various engineering projects (Micheal 1992). Whole tires are mostly stacked up vertically and clipped together for building retaining walls and for slope protection. Slit tires are made from recycled whole tires cut in two halves. Slit tires can also be used for building retaining walls and around road shoulders. Slit tires can further be processed into shredded tires or ground rubber. Ground rubber normally has materials of nominal size ranging between 6.4mm down to 0.85mm with all steel fibres removed (Micheal 1992). Ground rubber is used in making traffic safety products and for design in playgrounds and parks.

Ground rubber can also further be processed into crumb rubber. Crumb rubber is mostly used as an asphalt modifier to increase the viscosity of asphalt so as to reduce thermal cracking in the road construction industry (Michael 1992). Crumb rubber used for making crumb rubberised asphalt has particle sizes ranging from 0.6 to 0.15mm (Michael 1992). Rubberised asphalt processing involves mixing asphalt binder with crumb rubber at extremely temperatures. Crumb rubberised asphalt is also used in seal coat applications. Illustrated in Figure 2.6 is the amount of recycled products obtained from scrap tires under the management of SSTC in 2010.

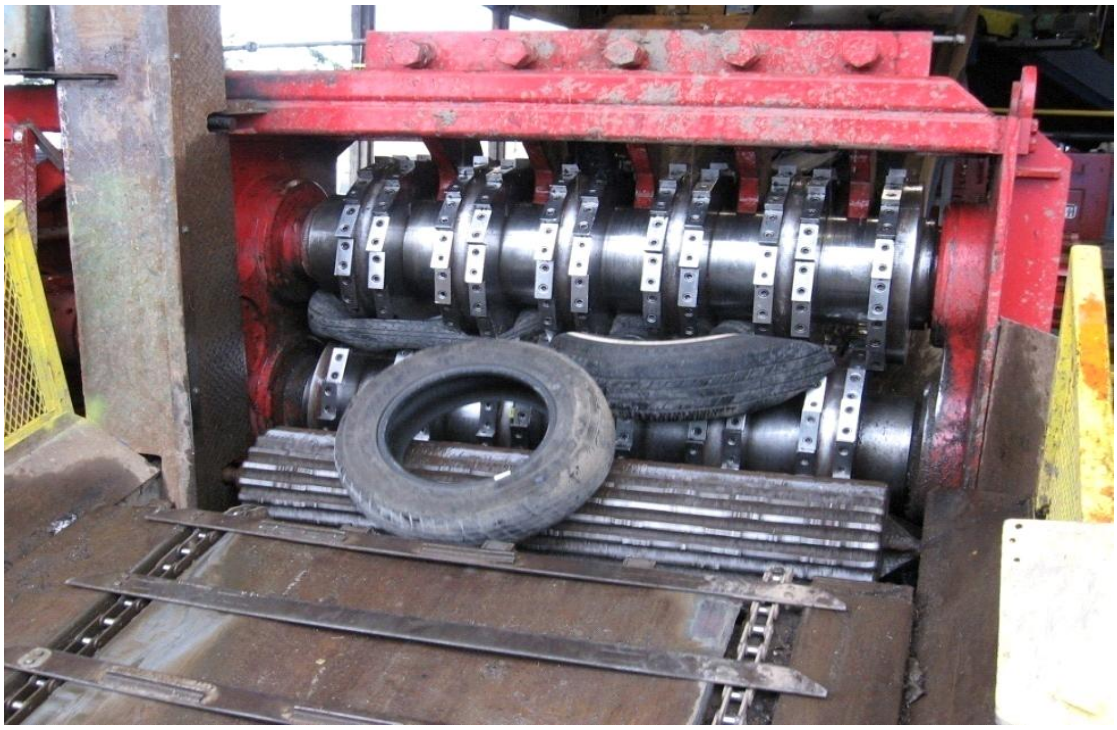

Figure 2.4 Typical Tire Shredding Machine (Terier Shredders 2011)

Figure 2.5 Tire Shredding Unit Set-Up (Terier Shredders 2011)

Figure 2.6 2010 Statistics of Tire Products Recycled in Saskatchewan (SSTC 2010)

2.4 Laboratory Characterization of Shredded Tire

Geotechnical laboratory characterization is a vital step in determining the engineering properties of shredded tires as a road construction material. Evaluation of test results gives an idea of material properties which can be correlated to their performance in the field. Material properties including gradation, shear strength and specific gravity of shredded tires were determined by past researchers (Humphrey et al 1993, Newcomb and Descher 1994).

The sizes of shredded tires are mostly larger than the maximum sizes of materials used in standard geotechnical testing, thus requiring test procedures and instrumentation modifications in order to obtain the actual material properties.

2.4.1 Gradation

The gradation test procedure is used to determine the particle size distribution of soils (ASTM 2006). Particle distribution of granular materials is determined using sieve analysis which involves passing a quantity of the granular material through a stack of sieves arranged in

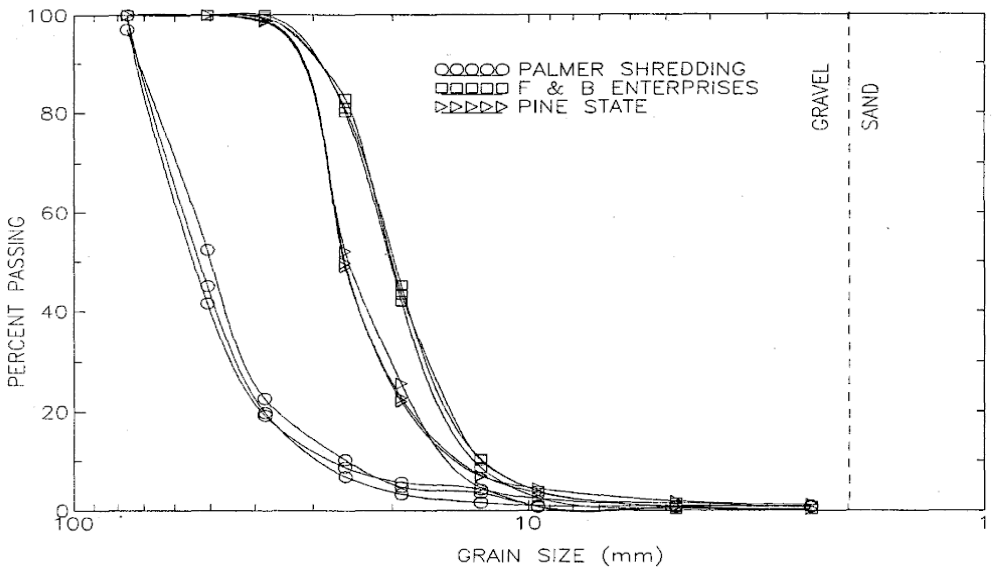

Figure 2.7 Gradation Results of Shredded Tire Samples (Humphrey et al 1993)

order of reducing aperture (ASTM 2006). A representative mass of the granular material is poured into the stack of sieves and the particle size distribution is ascertained by expressing the mass material passing each sieve as a percentage of the total mass of granular used. Sieve analysis test results are usually expressed in graphical or tabular form.

Humphrey et al (1993) conducted a gradation test on shredded tire samples obtained from three suppliers to determine the particle size distribution of these materials. The test procedure used was in accordance with ASTM T27-87 (1993). Results from this test indicated all samples from all three sources were uniformly graded. Particle sizes of samples mostly ranged between 10mm to 75mm as shown in Figure 2.7 with Palmer shredded tire samples being the coarsest of the three samples (Humphrey et al 1993).

2.4.2 Density

In order to determine the potential of using shredded tire materials as a lightweight fill material in road construction and other civil engineering projects, the
compacted density of shredded tire material have been characterized by numerous researchers (Newcomb and Descher 1994).

A laboratory investigation (Newcomb and Descher 1994) reported that shredded tires had an average bulk unit weight of 4.9kN/m^3. Humphrey et al characterized the compacted density of three groups of air dried samples of shredded tires using AASHTO T180-86 (1993). The samples were compacted in a mould 254mm in diameter and 254mm in height. The three samples of maximum sizes 38mm, 51mm and 76mm gave density readings of 618kg/m^3, 619kg/m^3 and 642kg/m^3, respectively under standard Proctor compaction. Consequently, conventional granular materials have bulk densities three times greater than that of shredded tire (Das 1995). Humphrey and Manion (1992) evaluated the effect of different compaction methods on the compacted density of shredded tire samples in Table 2.1. The method of compaction was found to have no significant influence on the compacted density of shredded tire material.

2.4.3 Thermal Conductivity

Freeze-thaw cycles are a main primary cause of pavement deterioration in cold climatic areas. Reducing the freezing effect in pavement structures helps inhibit the occurrence of freeze-thaw cycles thereby improving pavement performance (Humphrey et al 1993). Rubber used in the manufacturing of tires has been found to produce very low thermal conductivity sufficient to insulate pavements against freezing. Andersland and Ladanyi (1994) found the thermal conductivity of dry soil to be 1.1 W/m,K and that of shredded tires as 0.23W/m,K which is approximately 80% less than dry soil. The low thermal conductivity of shredded tires means that they can provide thermal insulation up to five times more than conventional aggregates if used as an insulating medium in roads.

Table 2.1 Effect of Different Compaction Methods on the Compacted Density of Shredded Tire (Humphrey and Manion 1992)

Proctor Compaction Energy	Energy per unit volume J/m^3	Blows per layer	Dry unit weight Kg/m^3
Modified	2.69	330	656
Standard	0.59	73	640

Numerous factors including size of shredded tire, degree of compaction and water content affect the thermal conductivity effect of shredded tires (Andersland and Ladanyi 1994). Thermal conductivity increases with increase in shredded tire particle size (Humphrey et al. 1993). Increase in thermal conductivity effect is due to the fact that the air voids between the tire shreds increase thereby increasing the effect of heat loss. The degree of compaction of shredded tires also affects the thermal conductivity effect generated due to its effect on the void content of the material. A higher state of compaction means low void content, thereby reducing air circulation and hence decreasing in thermal conductivity (higher thermal insulation). High water content or moisture in shredded tire materials increases the thermal conductivity and reduces the thermal insulation effect of the tire shreds (Guidance Manual 2008).

2.4.4 Compressibility Characterization

Compressibility is the measure of the rate of volume decrease of a material subjected to vertical loading (Sridharan and Gurtug 2005). In simple terms, a highly compressible material can be referred to as unstable. In order to improve the structural stability and performance of pavements, materials used for road construction should be able to withstand high magnitudes of loading with no significant change in volume.

Due to the high content of rubber in shredded tires, shredded tires exhibit high compression under mat loading as compared to conventional mineral aggregates. Edeskar and Westerberg (2006) characterized the compressibility, void ratio and porosity of a shredded tires specimen under the following compaction energies: loose fill, standard Proctor energy and modified Proctor energy so as to ascertain the effect of various compaction methods on shredded tire behaviour. Loose fill and compacted shredded tire specimen were tested in a custom-made Proctor apparatus of diameter 313mm and height 316mm. The apparatus containing the shredded tire specimen was placed in a load frame and subjected to confined compressive testing (as seen in Figure 2.8).

Loading was applied in a step function from 0.93kPa, 3.6kPa to 10kPa using load cells and was gradually increased up to 400kPa using a hydraulic load cell (Edeskar and Westerberg 2006). As shown in Figure 2.9, the stress strain response in the standard Proctor compacted

specimen was similar to that of the 60% standard Proctor specimen (Edeskar and Westerberg 2006).

There was significant variation between stress strain response of the loose fill material and the compacted samples. This variation indicates that shredded tires have the potential of undergoing high deformation when initially loaded in the loose state. The fact that there is insignificant variation in stress strain response between the compacted samples indicates that the shredded tires do not undergo high deformation after loading.

2.4.5 Void Ratio and Porosity

Void ratio of a soil mass is defined as the ratio of volume of voids in the soil to the volume of the soil particles. Voids in soils are normally filled with air, water or both. The three phase illustration of soil mass is shown in Figure 2.10. Void ratio can be represented mathematically as shown in equation 2.1 below.

$$e = \frac{V_v}{V_s} \qquad \textbf{2.1}$$

Where e = void ratio

V_v = volume of voids

V_s = volume of solids

Porosity is related to void ratio and is defined as the ratio of volume of voids to the total volume of the soil mass. It is represented mathematically as shown in equation 2.2.

$$n = \frac{V_v}{V_T} \qquad \textbf{2.2}$$

Where n = porosity

V_v = volume of voids

V_T = volume total

In general, the higher the void ratio of a soil mass, the higher the porosity of the soil.

Figure 2.8 Set-up for Compressive Test using Custom Made Cylinder (Edeskar and Westerberg 2006)

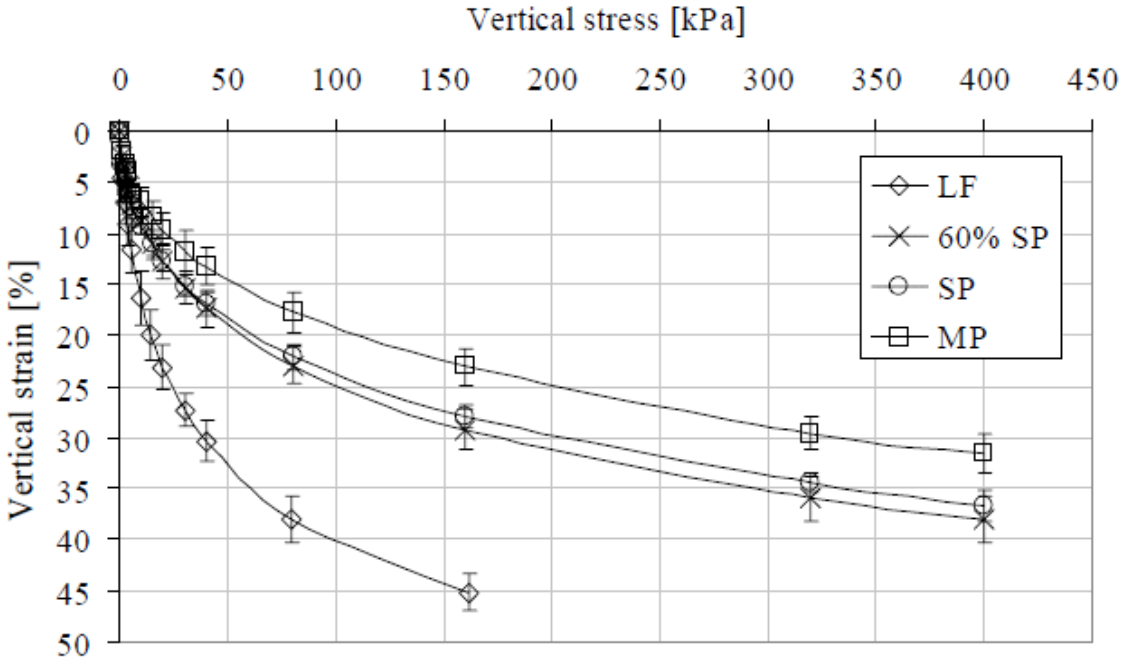

Figure 2.9 Stress Strain Curves for Compression Test (Edeskar and Westerberg 2006)

The porosity measurement was conducted in the second phase of the compression experiment [by Edeskar and Westerberg (2006) discussed above] as the apparatus was subjected to compressive loading. Initial loading was done at 0.94kPa and water was poured into the cylinder containing specimen.

Air bubbles were eliminated by tapping the cylinder and loading gradually increased as similar to the stress-strain response characterization process. Pore volume was measured at individual load steps as the volume of water was added. Figure 2.11 shows the relationship between the void ratio and vertical stress. The void ratio of the individual specimen decreased with increasing vertical stress.

2.4.6 Water Absorption Capacity

Water absorption capacity defines the amount of water retained on the surface of a soil particle after drainage. Water absorption capacity is the ratio of the amount of water retained by the soil to the weight of dry soil expressed as a percentage. Humphrey (2006) reported the water absorption capacity of tire shreds to range between 2 to 4%.

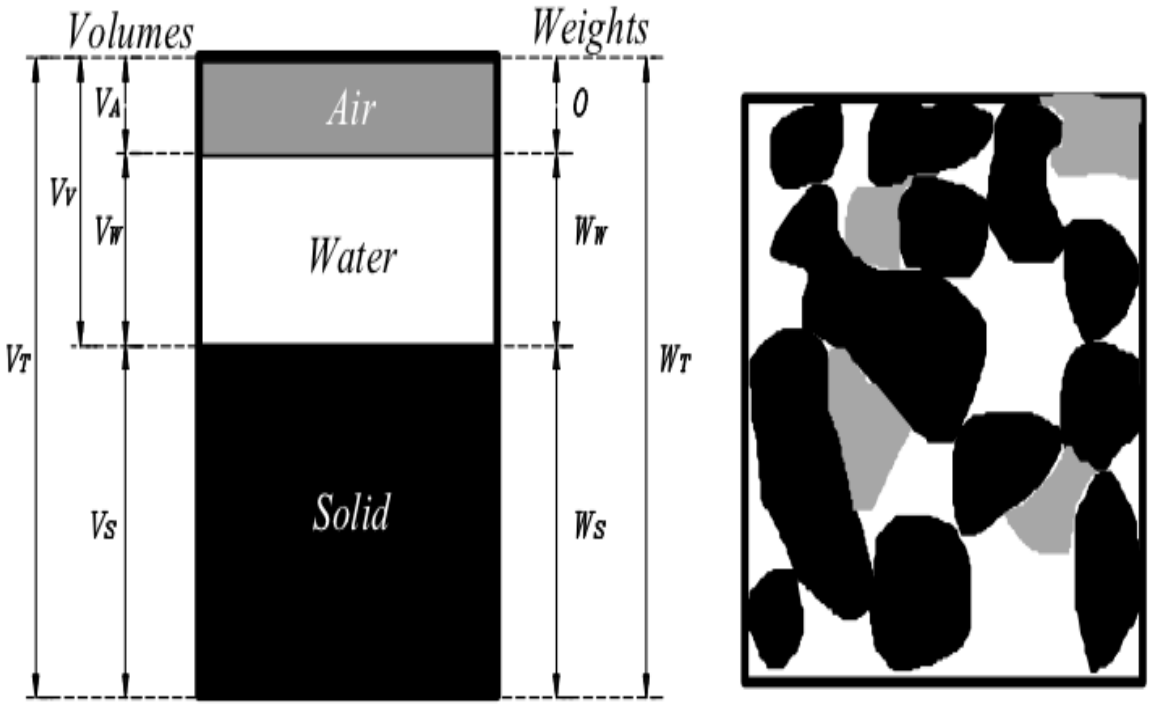

Figure 2.10. Three Phase Illustration of Soil Mass (Mecsi 2009)

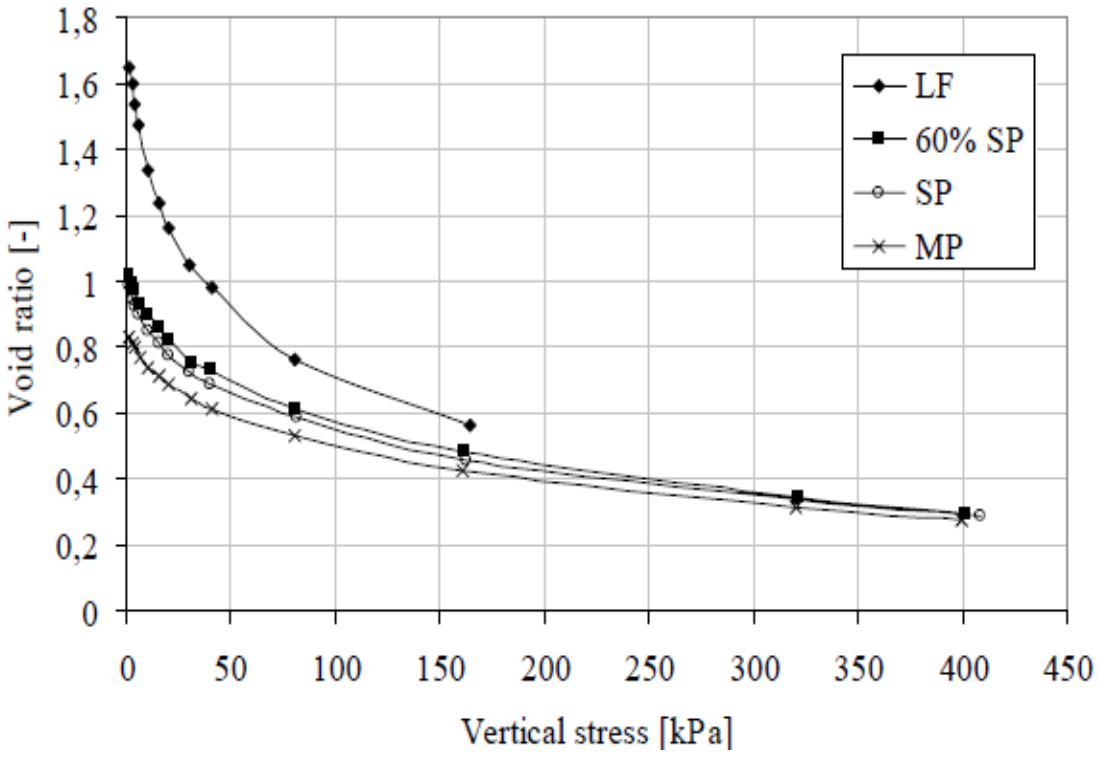

Figure 2.11 Void Ratio Characterization (Edeskar and Westerberg 2006)

2.5 Chemical Stability/ Leaching Properties of Shredded Tires

In order to determine the potential leaching effect of shredded tire materials on groundwater quality and human health, laboratory and field investigations were conducted to evaluate the amount of organic and inorganic substances released by these materials. Khan and Shalaby (2001) conducted the groundwater quality test on a shredded tire embankment in Manitoba between March and April of 2001. Table 2.2 compares the level of inorganic substances with Environmental Quality Guidelines (EQGs) recommended.

The shredded tire layer was 1500mm thick buried at 450mm below the road surface. Organic compounds were found to be in trace amounts in the groundwater as compared to Canadian Council of Ministers of the Environment (CCME) EQGs.

Table 2.2. Inorganic Test Results as Compared with Environmental Quality Guidelines (EQGs) Values (CCME 1999, Khan and Shalaby 2001)

Analyte	Detection Limit (mg/L)	Canadian Limit2 (mg/L)	March Results (mg/L)	Tested in April (mg/L)
Aluminum	0.009	0.2	1.53	0.055
Barium	0.0002	1	0.0780	0.0454
Calcium	0.2	1000	120	83.2
Chromium	0.0009	0.05	0.0024	<.0009
Iron	0.003	0.3	5.75	0.159
Magnesium	0.06	No Limit	54.7	31.3
Manganese	0.0002	0.05	0.714	0.033
Sodium	0.4	200	11.5	5.5
Zinc	0.0007	5	0.0868	0.0098

Aluminum, iron and manganese indicated high levels of concentration above EQGs, but was not regarded to pose great environmental impact since EQGs considers them as secondary parameters (Khan and Shalaby 2001).

2.6 Environmental Field State Conditions in Northern Climates

Environmental field state conditions have an effect on road pavement design and performance throughout their service lives. Canada and other countries in the northern climatic zone experience cold temperatures below freezing for half the year with the southern part of Canada experiencing hot temperatures during summer (Nix et al 1992).

Extreme variations in temperature and other environmental conditions in Canada cause up to 50% and 80% pavement deterioration on high and low-volume roads respectively (Nix et al 1992). Pavement deterioration in cold regions is mostly caused by freeze-thaw cycles and sub-structural moisture variations. Freeze-thaw cycles cause heaving of pavement substructure during winter and subsequent melting of ice lenses formed resulting in the release of moisture into the sub-structure (Dore and Zubeck 2008). Evidence points to the fact that pavement deterioration in cold regions is mostly initiated by frost thawing in spring when moisture is

released into the substructure. Reports from the AASHTO road test indicate that 60% of pavement deterioration that occurred was recorded in spring (White and Coree 1990).

2.7 Frost Action

Frost action in the context of this research refers to the freezing and thawing of road pavement substructure which causes a loss in the structural and functional integrity of the road. This condition occurs as a result of seasonal variation in temperatures between winter and spring in cold climates in frost susceptible soils (Dore and Zubeck 2008). Cold temperatures cause the freezing of roads and subsequently propagate downward into the subgrade layer. Upon thawing in spring, the release of moisture causes loss in bearing capacity in unbound pavement materials and subgrade soil (Dore and Zubeck 2008). Frost action occurs to some extent on most roads in northern climates but the magnitude of this effect depends on the prevailing climate, the type of soil and the amount of precipitation. Frost action causes the fatigue cracking in pavements in early spring and normally calls for the implementation of load restrictions on heavy traffic using most roads in these regions in order to reduce the magnitude of damage caused by excessive loading (Waalkes 2003).

The following three conditions or factors need to be present for frost action to take place (Dore and Zubeck 2008, Waalkes 2003):

- Sufficiently low soil temperature;
- Moisture availability; and
- Frost susceptible soil.

2.7.1 Sufficiently Low Soil Temperature

Ambient temperature should be below freezing for a significant number of days to cause moisture within soil pores in the upper layer of the substructure to get frozen (Waalkes 2003). The freezing rate and depth of frost formation is also affected by other factors including the thermal properties of the soil, wind, snow cover and solar radiation (Dore and Zubeck 2008).

2.7.2 Moisture Availability

Before frost action can take place in a frost susceptible area, moisture within the soil pores should be sufficient to freeze and form ice lenses (Boyd 1973). The fore stated phenomenon makes moisture another important factor necessary for frost action to take place. Moisture may be drawn up from underlying groundwater table, from soil pores, infiltration from surroundings or an aquifer. An area located on a higher groundwater-table zone will be much more prone to frost action since so much water will be available to flow up to the freezing zone within a short period of time (Boyd 1973). In a frost susceptible area where no adequate drainage systems are provided, moisture within this catchment area is drawn up into the freezing zone causing the formation of larger ice lenses than would have been formed for a well drained area (Dore and Zubeck 2008).

2.7.3 Frost Susceptible Soil

Frost susceptibility of saturated soils depends on the fines content, specific surface area of fines fraction and the ratio of the material's water content to its liquid limit (Konrad 1999). Most agencies define frost susceptible soils as soils containing more than 3% of grains passing a 0.02mm (No. 635) sieve or more than 10% of grains passing a 0.075mm (No. 200) sieve (Janoo 1997). Primary elements that control the magnitude of frost susceptibility of soils include grain size distribution (amount of fines) and the pore size distribution (Hoppe 1996). There is a relationship between the grain size and pore size distribution in soils and it is clearly evident in uniform soils where the pore size increases with grain sizes (Knutson, 1993). The extent of frost susceptibility in soils is, however, much more affected by the pore size than grain size distribution in non uniform soils. Pore size distribution in soils controls the rate of flow and amount of moisture drawn into the freezing zone by capillary action. The smaller and more interconnected the pores are, the more frost susceptible the soil is likely to be (Konrad 1999).

Moisture flow within soil pores is induced by two hydraulic properties of the soil: capillarity and permeability. While capillary moisture suction increases with decreasing grain or pore size distribution, permeability instead decreases. Konrad (1999) reported moisture suction in coarse grain soils to be relatively much slower and less intense than that of fine grained soils. Thus, coarse-grained soils such as coarse sand and gravels have very low moisture suction and

high permeability and are non frost-susceptible whereas silts, fine sands and clays are highly frost susceptible soils (Waalkes 2003).

2.8 Damaging Mechanisms of Frost Action

Frost action in roads occurs in two main stages namely:

- Frost heaving; and
- Thaw weakening.

2.8.1 Frost Heaving

Frost heave involves the accumulation of moisture resulting in the formation of ice lenses in the freezing plane in frost susceptible soils. The mechanism of frost heaving involves the interaction between frost susceptible soils and available moisture resulting in the formation of layers of frozen ice in freezing field state conditions (Konrad 1994). Low field state temperatures below freezing initiate freezing of moist fine grained soils. Water within the soil pores tends to solidify into ice leading to the formation of a freezing plane below the surface of ground/road (Horiguchi 1987; Hilf 1975). Formation of ice crystals below the surface of the soil is influenced by the intensity of the surrounding temperature and moisture available (Horiguchi 1987).

The presence of unfrozen moisture surrounding frozen particles creates a mechanical and thermal gradient across the warmer water molecules and ice (Dash 1989, Rempel et al. 2004). A state of thermal and mechanical gradient developed across the frozen and non frozen parts of the soil creates a pressure differential that induces the flow of moisture from unfrozen regions within the soil structure towards the frozen plane (Rempel et al 2004). This phenomenon is further explained in Figure 2.12. Moisture drawn from the unfrozen regions flows towards the freezing front (Miller 1977; Loch and Kay 1978) to feed the pore ice already formed and this accumulates with time and makes contact to form an ice lens (Sheng and Knutsson 1995). Pressure effects developed at water-ice interphase and energy generated from heat loss causes moisture suction (Horiguchi 1987). Ice lenses formed are oriented parallel to the surface and heaving in the direction of heat flow (Penner 1959).

Flow of moisture is enhanced by the efficiency of pore structure of the soil. The smaller the pores within the soil structure the higher the capillary action and cohesive force. Soils with

finer particles have smaller pores and generate higher capillary pull than coarser soils. Konrad (1994) reported that clay and silty soils tend to generate much more capillary action than gravels and are able to serve as an efficient transport medium of water to the freezing zone leading to an increase in rate of crystallization and development of bigger ice lenses. As water is drawn from the unfrozen zone, the water content of the soil within the freezing zone increases. Growth in the size of the ice lenses generates a heaving pressure (lifting thrust) that pushes overlaying soil upwards (Beskow 1991). This phenomenon is illustrated in Figure 2.13. This condition in pavement structures leads to the development of cracks and uneven driving surfaces on the road surface as shown in Figure 2.14 (Dore and Zubeck 2008). This phenomenon is called frost heaving and is mostly seen on road pavement in cold climates.

The degree of frost heaving is mostly affected by two factors: rate of cooling and water content and grain size distribution of soil

With regards to the first factor, increasing rates of freezing increases the mobility or absorption of unfrozen water. Total frost heave in a frost susceptible soil is a result of the freezing of the *in-situ* pore water and the water drawn from the unfrozen zone (Guthrie and Hermansson 2003). The amount of *in-situ* moisture in the soil plays a vital role in the initial crystallization process of frost heaving. Higher water content increases the potential of higher frost action occurring. An additional water supply source in the form of aquifers and water-table facilitates the formation of thicker ice layers, thereby pronouncing the effect of heaving (Waalkes 2003).

Depth of groundwater also affects the extent of heaving as it serves as an additional source of water supply needed to enhance ice segregation. Lowering the groundwater table according to Beskow (1935) tremendously reduces the amount of frost heaving in frost susceptible soils.

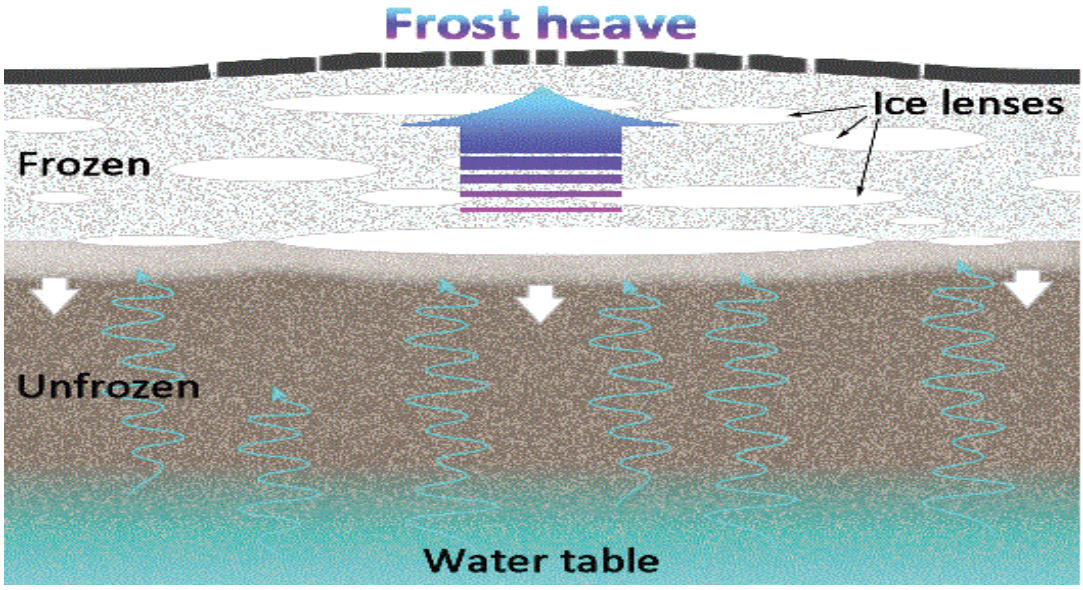

Figure 2.12 Propagation of Moisture to Freezing Plane
(Courtesy of Quebec Transport 2007)

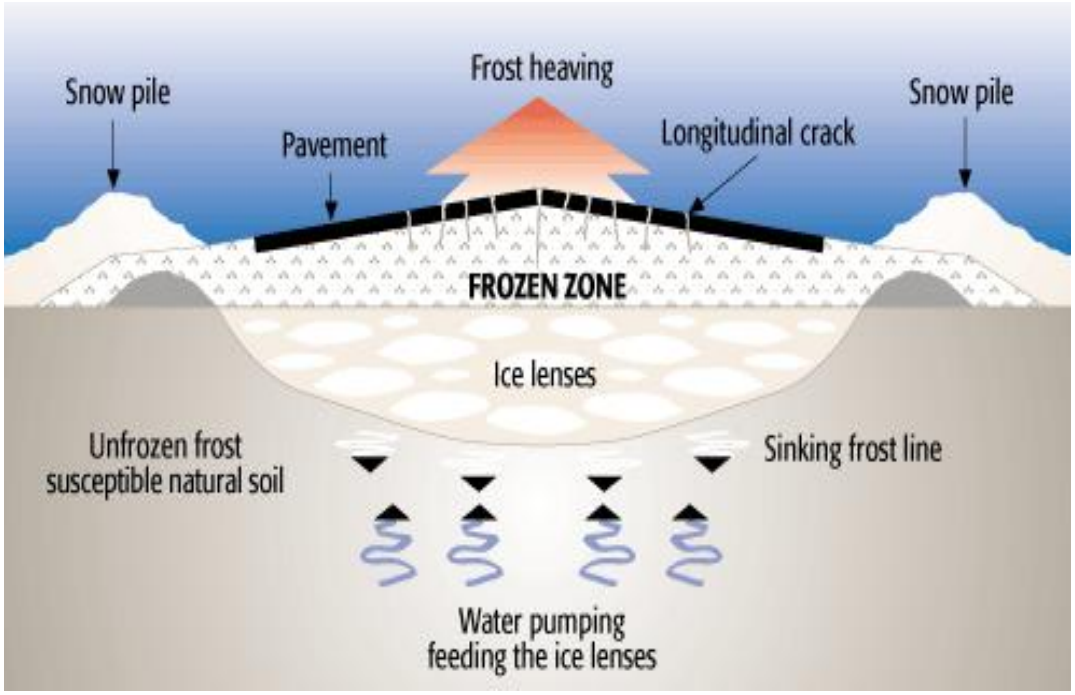

Figure 2.13 Frost Heaving Effect
(Courtesy of Quebec Transport 2007)

With regards to the second factor, grain size and grain-size distribution of soils have a significant influence on the intensity and nature of heaving (Penner 1976; Everett 1961; Everett and Haynes 1965). The height to which water can be drawn from the water-table or underground water supply source is dependent on the diameter and percentage of voids in the soils. In most cases, the height of the rise of water is inversely proportional to the diameter of the capillary voids (Penner 1976). Fine grain soils have narrower capillary pore diameters than coarse materials. Finer soils like clay, however, do not have extremely high hydraulic permeability to cause the flow of moisture from greater depths as much as silty soils due to the presence of high percentage of colloids (Penner and Ueda 1977). Clay under confined conditions is able to heave to a great extent but is generally considered as less frost susceptible than silty soils which are the most frost susceptible soils (Penner and Ueda 1977).

Generally, coarse grained soils like clean sands and gravels do not heave but the presence of small amounts of clay, silts or fine sands in these coarse materials may cause them to heave (Chamberlain 1981). Non frost susceptible soils with coarse grains and a large volume of voids do not heave due to their high permeability.

2.8.2 Thaw Weakening

During spring, ambient temperatures get warmer than in winter causing frozen ice layers formed under freezing field state temperatures to melt. Precipitation and melting snow also infiltrate underground generating excess undrained water in some cases (Dore and Zubeck 2008). Melting of frozen ice is initiated from the surface and progresses downwards.

Frozen layers of ice lying beneath melted water from the overlaying acts as an impervious medium thereby hindering downward percolation until a greater portion of frozen ice layers has eventually melted (Osler 1966). This manner of thawing reduces drainage performance drastically. Reduced rate of infiltration and inefficient substructure drainage results in the accumulation of excess undrained water in pavements.

Figure 2.14. Effect of Differential Frost Heaving
(Courtesy of Road Scanners 2010)

Undrained substructure condition reduces the bearing capacity of the granular material in pavements thereby leading to excessive pavement deterioration on loading (Nordal 1973). The drainage ability of pavement granular materials is mostly associated with the amount of fines contained in the granular material. The drainage performance of saturated base and subbase materials can be ascertained by determining the quantity of fines in the material (Chamberlain 1981). The presence of excess fines reduces the permeability and drainage performance of the granular material thereby increasing the thaw weakening effect which reduces bearing capacity. Reports from the Corps of Engineers' (COE) field test from the 1940s in the northern parts of the states indicate that base course materials with 10% fines passing a 0.075mm sieve showed significant thaw weakening reducing bearing capacity by up to 70% (Johnson 1974).

Melting of frozen ice and snow initiates near the surface of the pavement and progresses down the pavement substructure. Excess water generated from this thawing process creates an undrained condition within the base layer material causing a drastic reduction in the bearing

capacity (Nordal 1973). As a result of this effect, the structural support provided by this layer to the overlaying layer(s) is highly compromised leading to the propagation of fatigue cracks on the road surface (as shown in Figure 2.15). Fatigue cracks gradually become more pronounced with time due to the destructive effect of traffic loading and may manifest into alligator cracks (Waalkes 2003).

As thawing progresses through the substructural layers further to the subgrade, the quantity of undrained water increases as more frozen ice melts with no channel available to get rid of excess water (Dore and Zubeck 2008). Layers of frozen ice initially provide structural support, but melt with time, causing significant consolidation depending on the thickness of the ice layer. Thaw consolidation results in permanent deformation of pavement due to substructural collapse resulting in deep ruts formed on the road surface (Dore and Zubeck 2008), as illustrated in Figure 2.16.

Undrained water also reduces the bearing capacity of the substructural layers and subgrade material leading to a significant reduction in structural strength (Dore and Zubeck 2008). This effect results in accelerated pavement deterioration on loading. Fatigue cracks, potholes and alligator cracks become pronounced with deep ruts on the road surface, and in serious cases the road completely fails structurally.

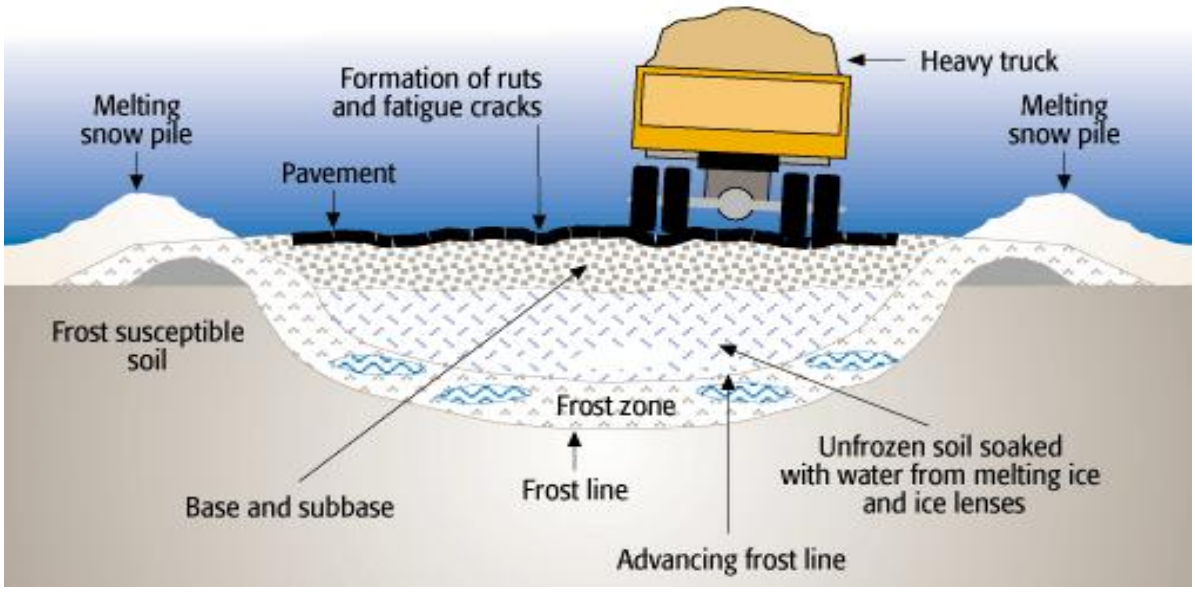

Figure 2.15 Illustration of Thaw Weakening
(Courtesy of Quebec Transport 2007)

Figure 2.16 Effect of Spring Thaw Weakening
(Courtesy of Road Scanners 2010)

The extent of pavement deterioration caused by thaw weakening is dependent on the amount of frost heave, rate of thawing and the rate of substructure consolidation on thawing (Waalkes 2003).

2.9 Mitigating Frost Action

Frost heaving and thaw weakening affect pavement performance in cold climates. In order to mitigate frost action, factors that cause frost heaving and thaw weakening should be eliminated.

Since not much can be done about the environment or climatic conditions of a particular locality, much attention is focused on *in situ* granular material properties and the moisture availability within or around the pavement structure.

2.9.1 Design and Rehabilitation Methods for Mitigating Frost Action

Frost susceptible soils are a major contributing factor causing frost heaving that needs to be eliminated in order to mitigate frost action. Road design and rehabilitation with the use of

low-fine granular materials helps reduce the potential of having a frost susceptible condition within the pavement structure (Chamberlain 1981, Dore and Zubeck 2009). Reducing the amount of fines in the granular materials eliminates moisture migration and ice segregation that causes heaving (Chamberlain 1981). Once significant heaving is eliminated, the effect of thaw weakening becomes extremely minimal as freezing and subsequent undrained condition is cut off. Rehabilitation carried out on roads with defects associated with frost action should also replace frost susceptible soils such as silts and clays (Jahren 2001).

Moisture within pavement structures can be controlled by providing efficient drainage. An efficient drainage system provided helps cut off moisture supply required for frost heaving and also provides an exit for excess water during thawing. Substructural drainage systems can be used to drain off excess water within the pavement structural layers during thawing. Aggregates used for construction should enhance infiltration (so as to eliminate excess water within pavement structure) and lateral drainage within the pavement structure. In some cases drainage layers are used within the base layer and on the surface of the subgrade to reduce pore pressure build up caused by excess water and rate of consolidation on thawing respectively (Kersler 1996, Dore and Zubeck 2009).

Cooling effects that cause the freezing of pavement structures can be reduced by the use of thermal insulation technologies. Thermal insulation provided within a certain depth from the road surface impedes heat flow towards the road surface and stops the freezing front from progressing down to the frost susceptible subgrade (Konrad et al 1996). This mechanism cuts off or reduces the depth of frost penetration and heaving of the road substructure. One common way is the use of a layer of materials (with thermal insulating properties) of a suitable thickness as a substructure layer within the zone of anticipated freezing. Saw dust, tire chips and polystyrene have been used as insulation materials in field experiments conducted in Quebec (Konrad et al 1996).

Shredded tire materials can be used in road construction and rehabilitation as a substructural insulation and drainage layer for the mitigation of frost action (Konrad et al 1996). The thermal insulation effect of shredded tires enables them to reduce heat loss, minimising freezing and prevents the penetration of frost into the frost susceptible subgrade during winter (Andersland and Ladanyi 1994). Shredded tire materials also act as a drainage layer (free

draining material) creating a channel of exit for melted water and preventing the subgrade from getting soaked.

2.9.2 Load Restrictions on Highways

Road agencies in some jurisdictions have implemented load restriction policies on roads during spring periods in order to minimise the effect of loading on the pavement since they are quite prone to failure at this period of the year (Van Deusen, 1998). Reducing the axle loading helps reduce the effect of thaw weakening by cutting down the rate of consolidation of substructure and also the loading to be supported by the pavement structure (Dore and Zubeck 2008). Although this approach is efficient to some extent, truck and trailer drivers tend to use alternative routes thereby increasing the extent of damage on them. Since load restriction policies are also imposed within a certain time period in the spring, it is a less effective method since damage may be much pronounced before or after the restriction period (Van Deusen, 1998).

This approach does not attempt to prevent frost action from occurring but only aims at reducing the extent of damage caused by traffic loading. There is the need to adopt more advanced engineering technological approaches to mitigating frost action.

2.10 Chapter Summary

Chapter Two presented a review of shredded tire material production and engineering properties. A review of frost action and mechanism of frost initiation and propagation were also discussed in this chapter. Test procedures to be used for characterizing shredded tire and shredded tire mixes were also reviewed. A summary of the findings from the literature review is presented as follows.

Scrap tire recycling in Canada is promoted in the various provinces by government funding through stewardship programmes. Recycling of scrap tire in Saskatchewan is managed by SSTC, which has recycled about 16 million tires since 2005. The sizes of shreds produced from scrap tires depend on the intended use and can range from 100mm to 450mm in length. Shredded tires can be further processed into other products such as ground rubber and crumb rubber for making crumb-rubberised asphalt.

Previous laboratory characterization of shredded tire adopted modified test procedures and instrumentation to enhance the acquisition of accurate results since these materials differ in sizes and other physical properties than granular materials. Shredded tires were found to mostly have uniform gradation from production to supply. Size distribution analysis for shredded tires obtained from three manufacturers all showed uniform gradation. Proctor compaction results showed shredded tires had an average dry density about three folds lighter than conventional granular materials. The lightweight property enhances their application as backfill material on soft subgrades. Shredded tire was also found to provide thermal insulation about five times more than conventional granular aggregates. Under high compressive stress state, shredded tires were still found to have permeability values that are comparatively higher than permeability for granular materials. Laboratory characterization to determine the effect of shredded tire leaching on groundwater quality concluded that organic and inorganic compounds released from shredded tires are of negligible amounts to affect groundwater quality.

Frost action in roads in northern climates is caused by the presence of three conditions: moisture, low temperature below freezing and frost susceptible soils. The intensity of frost action occurring depends on the duration and extent of freezing of moisture within the soil. Grain size distribution of soils influences the suction of moisture in ice lenses' formation and crystallization during frost heaving. Fine grained soils induce much greater moisture suction and therefore heave much more than coarse grained soils. Melting of ice lenses occurs during spring when temperatures no longer support freezing. This condition leads to the release of moisture which reduces the bearing capacity of the substructure thereby resulting in pavement structure failure during loading.

Frost action can be mitigated provided one of the above mentioned conditions is eliminated. Road construction projects adopt the use granular materials with little or no fines for construction of structural layers so as to prevent frost action. Efficient substructure drainage and use of aggregates that facilitate infiltration and lateral drainage is another vital step taken by engineers to control frost in roads. Shredded tires have been found to provide thermal insulation; they also provide higher infiltration and drainage than conventional granular materials.

CHAPTER 3 LABORATORY CHARACTERIZATION

This research employs the use of standard and mechanistic laboratory test procedures to characterize the physical and mechanical properties of shredded tires and shredded tire/sand mixes. This section uses laboratory testing to evaluate the feasibility of improving the structural performance of shredded tires using clean sand and also investigating the effect of the quantity of sand added to the drainage performance of shredded tire materials. Shredded tire and shredded tire/sand material properties were compared to City of Saskatoon subbase materials: Saskatchewan Ministry of Highways (SMHI) Type 6 subbase, crushed rock and granular base.

This chapter documents shredded tire material sampling and the various test procedures used in the characterization process and results obtained from the tests conducted. Laboratory tests used in the research include:

- Grain size distribution;
- California Bearing Ratio (CBR);
- Confined frequency sweep characterization;
- Confined compressive strength/stiffness, and;
- Permeability test.

3.1 Material Sampling

Shredded tire materials used for the laboratory characterization were obtained from Shercom industry in Saskatoon (Figures 3.1 and 3.2). Shredded tires in their raw state were mostly of sizes ranging from 50mm to 300mm in length as shown in Figure 3.3. Steel fibres used in the tire remained embedded in them.

Clean sand was also obtained for the laboratory characterization process (Figure 3.4). Sand was mixed with shredded tires in various mix ratios in order to compare the effect of the amount of sand on the structural as well as drainage performance of the mix.

Figure 3.1 Shercom Shredding Plant

Figure 3.2 Shredded Tires Produced at Shercom

Figure 3.3 Shredded Tire Sample

Figure 3.4 Clean Sand Sample

3.2 Prepared Samples

Full scale testing of shredded tires was not available for this research, so the research materials were reduced to smaller sizes with nominal sizes ranging between 12.5mm to 25mm. The modification of tire shred sizes was done in order that the testing processes conformed to the principles of continuum testing and sample size ratio limitation. Sample size ratio is the diameter of the specimen divided by the maximum particle size. The effect of the sample size ratio on the material properties being characterised becomes negligible as the sample size ratio approaches 6:1 (Head 1982, Marachi et al 1972). This is the rationale behind reduction of the shredded tire sizes to smaller pieces for the laboratory characterization process. It is, however, important to note that the smaller size tire shreds will have smaller amount of voids in their loose state but (an almost) similar amount of voids in the compacted state relative to the normal sized shredded tires.

3.3 Specimen Material Description

Laboratory characterization was performed on shredded tire materials and shredded tire/sand blends and compared to City of Saskatoon subbase materials. Shredded tires together with four shredded tire/sand blends of different mix ratios as well as City of Saskatoon materials considered include:

- 100% shredded tire;
- Sand;
- 1Tire:1Sand;
- 1Tire:2Sand;
- 1Tire:3Sand;
- SMHI Type 6 subbase;
- Granular base; and
- Crushed rock.

The amount of material used for laboratory tests was measured by mass of material during the specimen preparation and then converted to volume using mass-volume relationship. Figure 3.5 shows a 1Tire:3Sand blend.

Figure 3.5 1Tire:1Sand Mix

3.4 Grain Size Distribution

Mechanical sieve analysis was used to determine the grain size distribution of shredded tires, clean sand and shredded tire/sand blends. Table 3.1 shows the grain size distribution of shredded tire, shredded tire/sand blends in mix ratios 1:1, 1:2 and 1:3 as well as sand. Figure 3.6 shows the gradation curve for the various mixes and City of Saskatoon subbase materials.

As illustrated in Figure 3.6, the shredded tire materials used in this test could be deemed as uniformly graded with a greater percentage of individual grains ranging between 12.5mm to 25mm in size. Sand had a gradation with particle sizes larger than 0.071mm. Sand used in this research as shown in the grain size distribution contained no fines and could be considered as clean sand. Shredded tire/sand mixes of 1Tire:1Sand, 1Tire:2Sand and 1Tire:3Sand could be described to have gap gradations. As the quantity of sand in the shredded tire/sand mixes increased the amount of course materials in each mix decreased. A denser gradation was obtained in the 1Tire:3Sand as compared to the 1Tire:1Sand mix. Higher amounts of voids were observed in the mixes with a small amount of sand but this was found to decrease as the quantity of sand increased.

Table 3.1 Grain Size Distribution of Shredded Tire/Sand Mixes and COS Subbase Materials

Sieve (mm)	Shredded Tire	Tire:Sand 1:1	Tire:Sand 1:2	Tire:Sand 1:3	Sand	SHMI Type 6	Granular Base	Crushed Rock
50.0	100	100	100	100	100	100	100	100.0
31.5	100	100	100	100	100	100	100	68.5
25.0	99	99	99	99	100	100	100	20.8
20.0	96	96	96	98	100	92.6	100	5.7
18.0	55	79	90	89	100	90.2	100	5.1
16.0	18	68	83	85	100	87.4	100	4.8
12.5	6	59	78	81	100	81.4	100	4.6
9.0	2	57	76	80	100	72.5	100	4.4
5.0	0	56	75	79	99	57.3	91.5	4.3
2.0	0	48	65	70	87	40.5	73.2	4.0
0.9	0	32	40	41	54	30.5	53.3	3.6
0.4	0	3	4	5	7	22.5	39.5	3.2
0.16	0	1	1	2	1	15.6	2.3	2.6
0.071	0	0	0	0	0	9.9	16.3	1.7
Pan	0	0	0	0	0	-	-	-

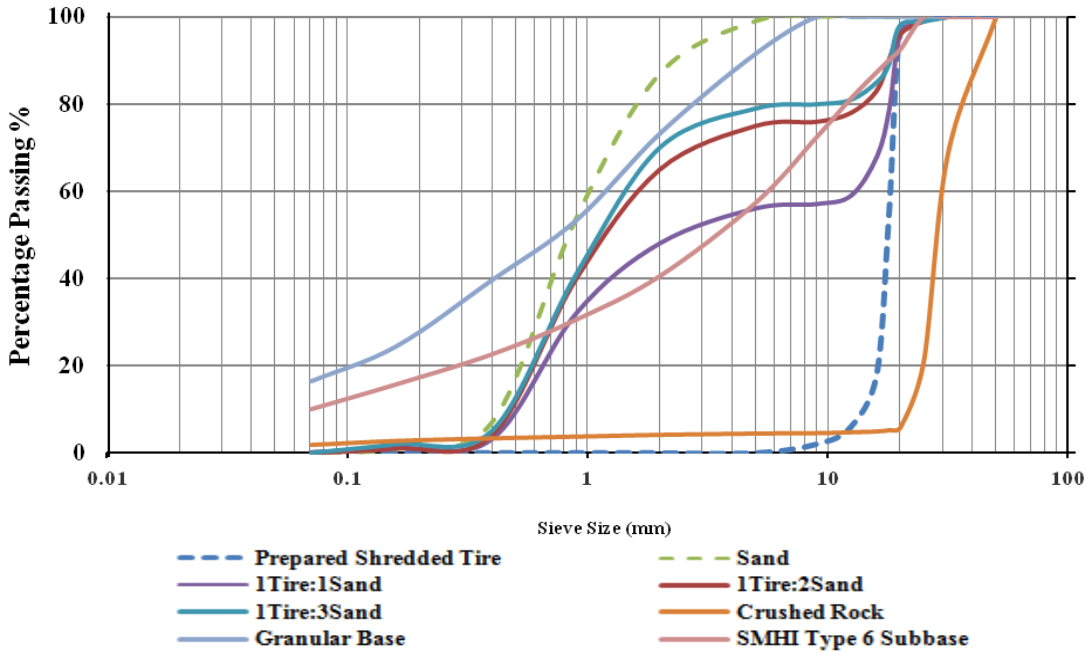

Figure 3.6. Grain Size Distribution Curves

Crushed rock materials were openly graded with small amount of fine particles. Crushed rock had coarser particles than the prepared shredded tire materials and all mixes. Granular base contained more fines than all other materials with about 20% of individual particles finer than 0.1mm. SMHI Type 6 subbase contained more fines than the shredded tire/sand mixes but were generally coarser than the granular base materials. Granular base and SMHI Type 6 could be deemed as densely graded but was denser in the granular base than all other materials considered. The granular base material could be deemed to contain the least amount of voids.

3.5 Standard Proctor Compaction

Standard Proctor compaction was used to prepare samples for CBR, confined compressive test, confined frequency sweep and permeability tests. Figure 3.7 illustrates shredded tire compaction using an automated hammer.

Figure 3.7 Compaction of Shredded Tire Samples

Compaction for shredded tires and shredded tire/sand mixes was performed at a moisture content of 2% by dry weight of sample for the shredded tire and sand mixes. Higher rebound was observed when compacting 100% shredded tire. The mixes containing higher amounts of sand retained more compaction than 1Tire:1Sand and 100% Shredded tire. Maximum standard dry density for the shredded tire and shredded tire samples are tabulated in Table 3.2. Figure 3.8 shows the Proctor curves for SMHI Type 6 subbase and granular base.

Table 3.2 Standard Proctor Characterization of Samples

Sample	Maximum Dry Density (Kg/m^3)	Opt. Moisture (%)
Shredded Tire	990	*
Sand	2180	*
1Tire:1Sand	1470	*
1Tire:2Sand	1680	*
1Tire:3Sand	1840	*
SMHI Type 6	2023	9.3
Granular Base	2177	7.2
Crushed Rock	1987	*

* Materials have greater percentage of coarse particles and therefore drain moisture; hence, 2% moisture was used in compaction for all shredded tire and sand mixes.

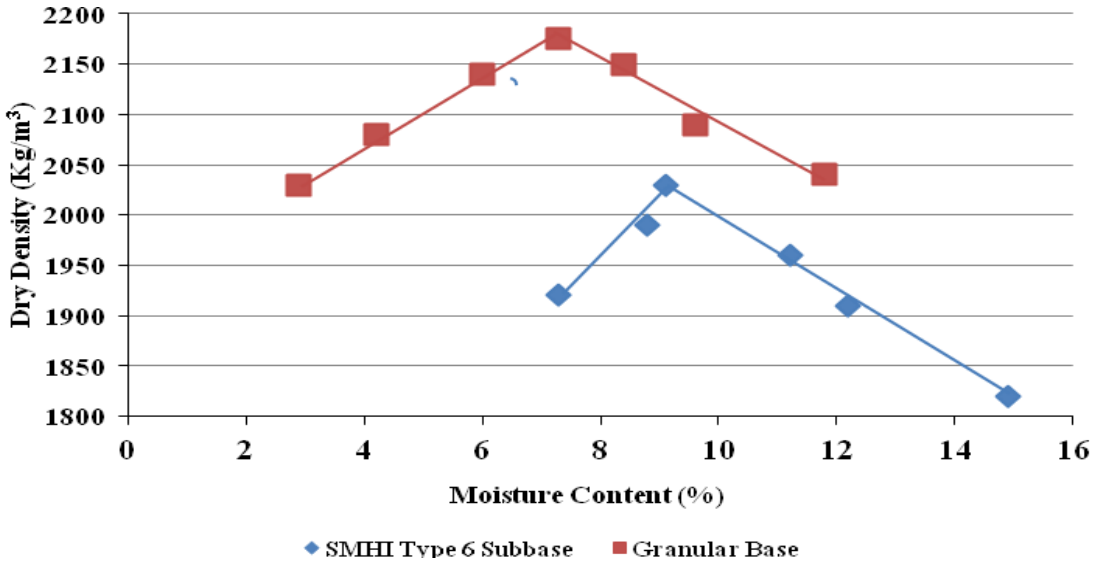

Figure 3.8 Proctor Compaction Curves for SMHI Type 6 Subbase and Granular Base

3.6 California Bearing Ratio Test

The California Bearing Ratio (CBR) test is used to determine the strength of granular materials and *in situ* subgrades of roads. CBR compares the bearing capacity of a material to that of crushed rock. This empirical method of road design was initially designed by the California State Highway Department in the 1930s for the sole purpose of assessing the subgrade strength of existing pavement (Muench 2004, ASTM 2007).

CBR test involves applying a load to a small penetration piston of diameter 49.6mm at a rate of 1.25mm/min and recording the total load at penetrations ranging from 0.64mm to 7.62mm. The CBR is then determined by measuring the pressure required to penetrate the material relative to the pressure required to penetrate standard crushed rock material. This relation can be represented as shown in equation 3.1.

$$\text{CBR } (\%) = (x/y) \times 100 \qquad \textbf{3.1}$$

Where:

x = Unit load on the piston for 2.54mm (or 5.08mm) of penetration

y = Unit load on piston for well graded crushed stone

The CBR test is described in AASHTO T193, ASTM Standards D1883and D4429 (2007).

Unsoaked CBR strength characterization was performed on 100% shredded tire and shredded tire/sand mixes as specified in ASTM 1883. Six repeat samples were tested for each material sand tabulated in Appendix C. Results of this test are shown in Table 3.3 and Figure 3.8 below. The CBR strength of typical subbase materials used in the City of Saskatoon are shown in Table 3.3 and Figure 3.9 below.

As shown in Table 3.3, the mean CBR values recorded for 100% shredded tire, 1Tire:1Sand, 1Tire:2Sand, 1Tire:3Sand are 1.3%, 2.9%, 6.7% and 9.6%, respectively.

Table 3.3 Peak CBR Readings CBR of Samples

Sample	Mean CBR Strength	Minimum	Maximum	Coefficient of Variance (%)
100% Shredded Tire	1.3	1.0	1.7	15.8
Sand	7.8	6.9	8.9	9.0
1Tire:1Sand	2.9	2.5	3.6	16.3
1Tire:2Sand	6.7	6.0	7.3	7.3
1Tire:3Sand	9.6	9.2	10.3	4.4
SMHI Type 6	45.0			
Granular Base	77.0			
Crushed Rock	100.0			

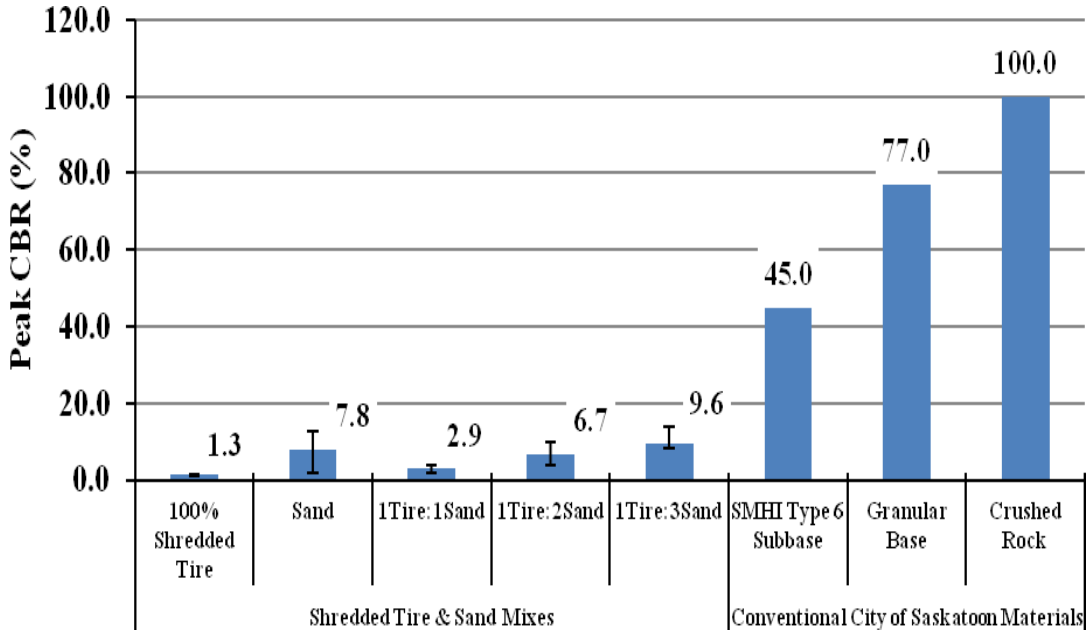

Figure 3.9 Mean Unsoaked CBR of Shredded Tire, Shredded Tires/Sand Mixes and COS Subbase Materials

These values are generally low as compared to the CBR readings of conventional City of Saskatoon materials and could be associated with the low stiffness of rubber material in the tire shreds. Shredded tire sample recorded the lowest average CBR and this was observed to increase as the quantity of sand in the mix was increased.

This progressive increase in the CBR reading was a result of the fact that the sand material occupied the voids between the shredded tire materials thereby serving as reinforcement for the material. Shredded tire/sand mix in the ratio of 1:3 had the highest CBR of 9.6%, which is about a 634% increase in strength as compared to 100% shredded tire. CBR of 1Tire:3Sand was also 23% higher than that of sand which indicates a mutual improvement in strength for both shredded tire and sand.

Conventional City of Saskatoon subbase materials were found to have CBR values much higher than the shredded tire mixes. SMHI Type 6 subbase recorded a CBR of 45% while crushed rock and granular base were measured at 100% and 77% respectively. The CBR of 1Tire:3Sand is approximately 4.5 times less than that of the SMHI Type 6 subbase and about 10 times less than that of crushed rock.

3.7 Confined Compression Strength/Stiffness Characterization

Shredded tire and shredded tire/sand mixes were also tested in an axial loading device to determine their confined compressive strength and stiffness. Compacted samples were subjected to vertical confined compressive loading confined in a mould. The walls of the mould provided lateral pressure thereby putting the sample in a confined compressive stress state as shown in Figure 3.10. A dial gauge was incorporated in the set up to measure the displacement as the material underwent compression due to loading. The strength of the material tested was measured as the highest modulus reading at which failure occurred. Six repeat samples were tested for each material. Table 3.4, Table 3.5, Figure 3.11, and Figure 3.12 show the confined compressive strength/stiffness results.

Average confined compressive strength yielded by 100% shredded tire, 1Tire:1Sand, 1Tire:2Sand and 1Tire:3Sand are 0.6kPa, 8.4kPa, 20.6kPa, 42.9kPa and 65.9 kPa, respectively. The sand sample had a confined compressive strength of 55.9kPa which represents a 15% decrease in strength as compared to the 1Tire:3Sand.

Figure 3.10. Confined Compression Strength/Stiffness Characterization Test Apparatus

The shredded tire materials failed at 0.6kPa due to their high elasticity behaviour under loading. The elastic effect of shredded tire was observed to be reduced by the added sand and was observed to progressively improve the strength behaviour of the material as the quantity of sand increased. The highest strength value of 65.9kPa was recorded by shredded tire/sand in the mix ratio of 1:3. The high value recorded by this mix could be attributed to the fact that the high amount of sand acted as a reinforcing medium in the mix, occupying voids and reducing the creep effect of the rubber. The confined compressive strength of the 100% shredded tire was increased by a 1300% as compared to the 1Tire:1Sand mix.

City of Saskatoon materials were generally found to have confined compressive strength values higher than shredded tire and shredded tire/sand mixes. Crushed rock had strength about 580% higher than 1Tire:3Sand.

Quantified stiffness of the shredded tire and shredded tire/sand mixes are shown in Table 3.5 and Figure 3.12.

Table 3.4 Mean Confined Compressive Strength for Shredded Tire and Shredded Tires/Sand Mixes

Sample	Mean Compressive Strength (kPa)	Minimum	Maximum	Coefficient of Variance (%)
100% Shredded Tire	0.6	0.5	0.7	11.4
Sand	55.9	49.9	60.8	8.4
1Tire:1Sand	8.4	7.2	9.3	9.3
1Tire:2Sand	42.9	40.1	46.0	5.0
1Tire:3Sand	65.9	64.7	70.2	5.5
SMHI Type 6	103			
Granular Base	218			
Crushed Rock	447			

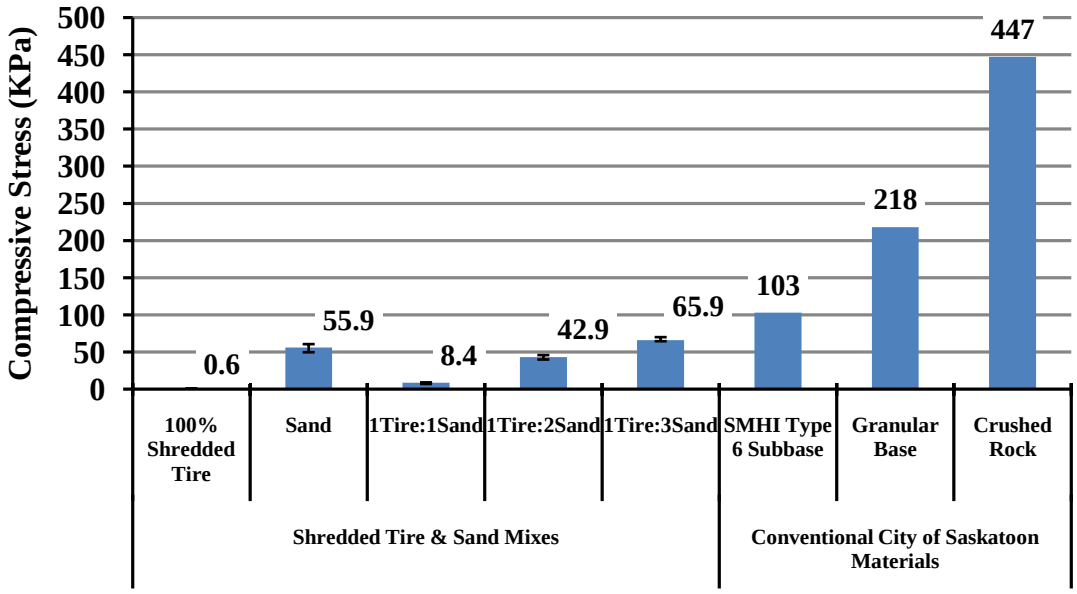

Figure 3.11 Mean Confined Compressive Strength Results

Table 3.5 Calculated Confined Compressive Stiffness for Shredded Tire and Shredded Tire/Sand Mixes

Sample	Stiffness (MPa)
100% Shredded Tire	0.01
Sand	1.90
1Tire:1Sand	0.28
1Tire:2Sand	1.62
1Tire:3Sand	2.21

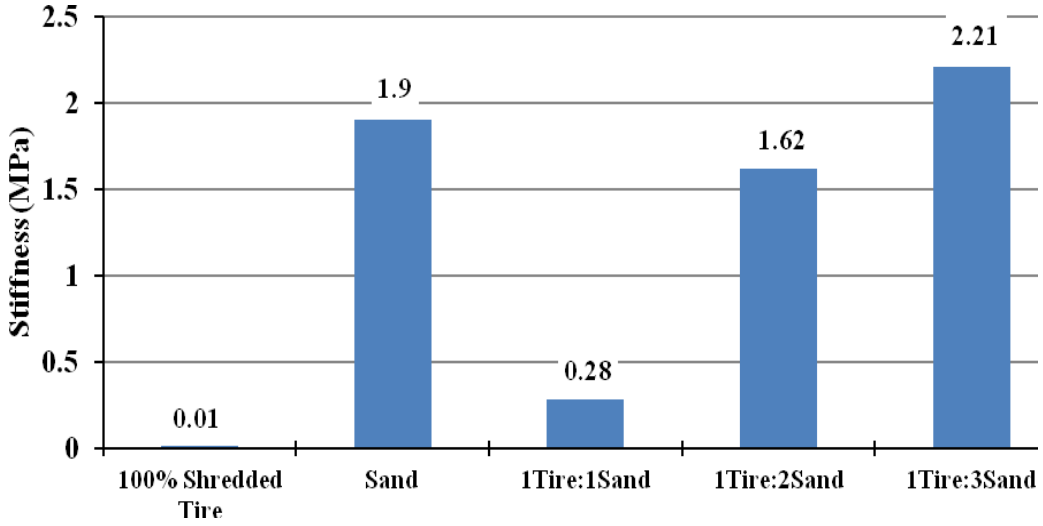

Figure 3.12 Mean Confined Compressive Stiffness Results for Shredded Tire and Shredded Tires/Sand Mixes

A similar trend in behavior was also observed in the stiffness readings. The 100% shredded tire sample recorded the least stiffness of 0.01MPa which increased through the mixes to 1.79MPa in the 1Tire:3Sand mix representing a high increment. Confined compressive stiffness measured in the 1Tire:3Sand was 36.4% and 16.3% higher than the stiffness of 1Tire:2Sand and Sand, respectively.

3.8 Confined Frequency Sweep Characterization

The rapid triaxial frequency sweep test (RaTT) determines the material stiffness properties of bulk soils and asphaltic concrete materials. The RaTT cell apparatus (Figure 3.13) is used for mechanistic design and was first used in 1996 for Strategic Pavement Research

Programme (SHRP) Specific Pavement Studies 9A (SPS-9A) test section in Saskatchewan (Berthelot et al. 1997, Berthelot 1999, Berthelot and Widger 2004). This device subjects the sample to sinusoidal axial stress and confined pressure state at multiple frequencies and stress states so as to quantify the time-dependent and stress dependent response of the specimen. In order to simulate field state loading, the RaTT cell applies dynamic sinusoidal stresses to the specimen in the radial/horizontal direction (Widger 2004).

The RaTT cell consists of a temperature controlled chamber which houses the specimen to be characterized. This machine is equipped with a rubber membrane that holds the specimen in a pneumatic confining chamber. Confining pressure is applied to the specimen through the rubber membrane while axial sinusoidal loading is applied by a hydraulic test frame. Vertical and horizontal displacements of the specimen are measured by two vertical LVDTs and four radially mounted LVDTs respectively (Berthelot 1999).

The RaTT cell apparatus through the use of a computer automated system is capable of controlling the applied vertical loading, confining pressure, test temperature and other applied stresses thus making the system user defined (Anthony and Berthelot 2004). The RaTT is designed to simulate various field state loading conditions in the process of material characterization. The vertical sinusoidal loading applied to the specimen simulates various wheel-loading conditions whereas varied sinusoidal load frequencies simulate the various traffic speed levels experienced on the field (Anthony and Berthelot 2004). The RaTT cell is also capable of performing material characterization at various test temperatures enabling characterization across a wide-ranging field service temperature spectrum.

Material properties characterized by RaTT cell in this research include:

- Dynamic Modulus; and
- Phase Angle.

RaTT cell has many advantages over other conventional test protocols which among others include the ability to simulate field state conditions (such as traffic loading) and the fact that material characterization can be performed at different temperature states. This apparatus also accomplishes material characterization within a short time frame and is also cost effective (Anthony and Berthelot 2004).

3.8.1 Modified Test Procedure Description

Dynamic modulus and phase angle of 100% shredded tire and shredded tire/sand mixes were quantified using RaTT cell. Other material properties such as Poisson's ratio could not be measured in this research. This was because the 100% shredded tire, shredded tire/sand mixes and sand specimen that were to be tested could not be moulded (specimen breaks apart when extruded from mould as shown in Figure 3.14). The specimens were therefore tested in CBR moulds placed in the RaTT chamber. The rubber membrane of RaTT cell was removed from chamber (to avoid being punctured) thereby eliminating the effect of pneumatic radial confinement. The samples were subjected to sinusoidal axial loading contained in the CBR mould.

Compacted samples of shredded tire material, shredded tire/sand blends and sand were tested at 5Hz frequency and under 50kPa static and 25kPa dynamic loading state to determine the material stiffness properties. Three repeat samples were tested for each material at room temperature.

Figure 3.13 RaTT Cell University of Saskatchewan

Figure 3.14 Gyratory Compacted Specimen Fails on Extruding from Mould

3.8.2 Dynamic Modulus Characterization

The dynamic modulus material was characterized using RaTT cell. Dynamic modulus is a measure of the stiffness of a material under dynamic loading. The dynamic moduli values of the shredded tire/sand materials were compared to those of SMHI Type 6 subbase, crushed rock and granular base materials. Results of the test are shown in Table 3.6 and Figure 3.15.

Table 3.6 Confined Dynamic Modulus Results at 50 kPa Static and 25 kPa Dynamic Stress Loading States

Sample Name	Freq (Hz)	Dyn. Mod. E_d (MPa)	Minimum	Maximum
Shredded Tire	5	5	4	7
Sand	5	126	116	128
1Tire:1Sand	5	30	26	36
1Tire:2Sand	5	110	102	121
1Tire:3Sand	5	158	139	164
SMHI Type 6	5	94		
Granular Base	5	174		
Crushed Rock	5	471		

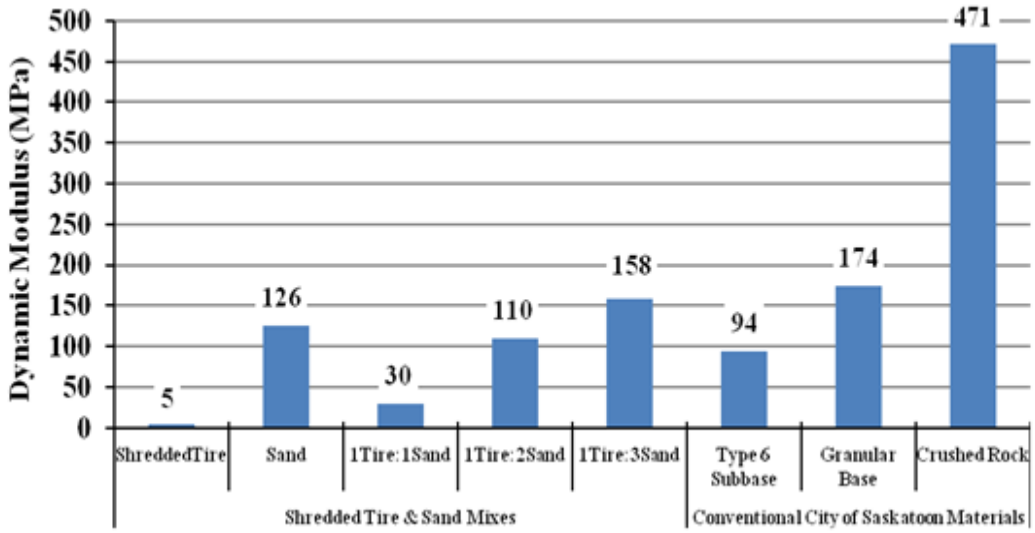

Figure 3.15 Confined Dynamic Modulus Results at 50 kPa Static and 25 kPa Dynamic Stress Loading States

As illustrated in the Figure 3.15, the 100% shredded tire and shredded tire/sand blends showed low dynamic modulus (stiffness) readings under varied loading conditions. Dynamic modulus value for 1Tire:1Sand sample was observed to be higher than that of 100% shredded tire by 500%. The dynamic modulus readings were observed to increase with increase in quantity of sand. 1Tire:2Sand and 1Tire:3Sand had dynamic modulli values about 267% and 427% higher than 1Tire:1Sand, respectively. The stiffness of the shredded tire/sand mixes was higher than the shredded tire material due to the presence of sand. The increase in stiffness behavior of the mixes measured by the RaTT cell is an indication that the mixes that contain more sand will provide more structural support. Adding up to three parts of sand provided mutual improvement in stiffness for both the shredded tire and sand; hence,1Tire:3Sand was observed to have a higher stiffness than Sand.

SMHI Type 6 subbase, crushed rock and granular base were found to have average dynamic moduli values of 94MPa, 471MPa, and 174MPa, respectively. The dynamic moduli values of crushed rock and granular base are approximately 200% and 10% higher than 1Tire:3Sand, respectively. SMHI Type 6 subbase had a dynamic modulus of about 40% less than 1Tire:3Sand. The stiffness measured in the 1Tire:2Sand sample was also observed to be 17% higher than the stiffness of SMHI Type 6 subbase.

Crushed rock was deemed to have the highest stiffness as compared to all materials characterized. Granular base was also quantified to have a higher stiffness than the 100% shredded tire, shredded tire/sand mixes and SMHI Type 6 subbase. The high stiffness behavior of the crushed rock and granular base is an indication of the structural support these materials have in a pavement structure. Shredded tire/sand mixes of 1Tire:2Sand and 1Tire:3Sand were observed to have higher stiffness than SMHI Type 6.

3.8.3 Phase Angle Characterization

Phase angle is a mechanistic material property that measures viscoelasticity (Xu 2008). It is defined as the lag in strain response caused by an applied traction state. Phase angle measurement for materials usually range between 0 to 90 degrees. A phase angle value of 0 means that material is purely elastic where as 90 degrees means purely viscous (Xu 2008). Results for the test are shown in Tables 3.7 and shown in Figure 3.16.

Phase angle values for the shredded tire/sand mixes was found to decrease with increase in quantity of sand in the mixes. Phase angle of 31.6 degrees was measured in the 100% shredded tire and was observed to decrease through to 7.6 degrees in 1Tire:3Sand. The decrease in phase angle measured in the mixes indicates a decrease in energy absorption (hence a decrease in deformation) with increase in quantity of sand in the mixes.

Table 3.7 Confined Phase Angle Results at 50 kPa Static and 25 kPa Dynamic Stress Loading States

Sample Name	Freq (Hz)	Phase Angle (^{o})	Minimum	Maximum
Shredded Tire	5	31.6	28.4	36.7
Sand	5	14.3	13.6	15.1
1Tire:1Sand	5	16.3	14.3	18.7
1Tire:2Sand	5	15.8	13.9	16.4
1Tire:3Sand	5	12.6	11.4	14.8
SMHI Type 6	5	14.9		
Granular Base	5	15.5		
Crushed Rock	5	9.5		

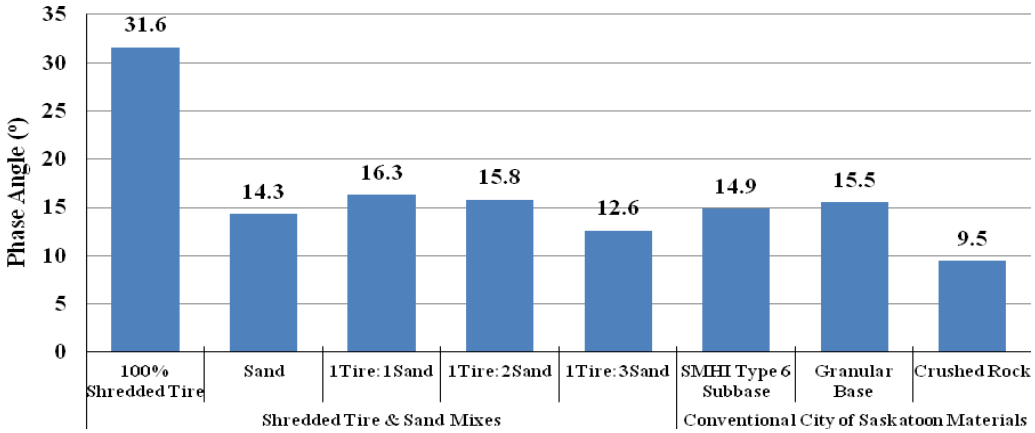

Figure 3.16 Confined Phase Angle Results at 50 KPa Static and 25 KPa Dynamic Stress Loading States

RaTT characterization identified 100% shredded tire to exhibit higher energy absorption and dissipation than the shredded tire/sand mixes. SMHI Type 6 subbase, crushed rock and granular base tested yielded phase angle values of 14.9 degrees, 9.5 degrees and 15.5 degrees respectively. Phase angle measured in the City of Saskatoon subbase materials were observed to exhibit lower energy absorption and dissipation behavior as compared to the 100% shredded tire, 1Tire:1Sand and 1Tire:2Sand.

3.9 Permeability Characterization

The free drainage test was used to determine and compare the relative permeability of the research material prepared by standard proctor compaction. An amount of water was poured into the compacted samples and the time required for the water to percolate through the surface of the specimen was measured as shown in the Figure 3.17 below. Six repeat samples were tested for each sample.

Permeability of the material tested was calculated as the depth of penetration per unit second. Table 3.8 gives the mean permeability readings of the samples tested. Permeability readings for the various materials tested are shown in Table 3.8 and Figure 3.18.

As illustrated in Table 3.8, 100% shredded tire yielded an average permeability of 1.42cm/s. Permeability was seen to decrease through 0.0115, 0.0032 to 0.0026cm/s recorded by 1Tire:1Sand, 1Tire:2Sand and 1Tire:3Sand shredded tire/sand mixes, respectively. Permeability values were shown to decrease as the quantity of sand was increased in the mixes.

Figure 3.17 Free Drainage Test

To illustrate, permeability of 1Tire:1Sand was measured at an average value of 0.0013cm/s which represents a 99% decrease in permeability as compared to the 100% shredded tire material.

The permeability of sand was measured at 0.0013cm/s which is 50% less than the permeability of 1Tire:3Sand. The difference in permeability between the sand and 1Tire:3Sand shows the higher free draining properties of the shredded tire and shredded tire/sand mixes than conventional aggregates.

As illustrated in Table 3.8, 100% shredded tire recorded the highest value due to the high amount of voids. As the amount of sand was increased, the amount of voids decreased drastically between shredded tire and 1Tire:1Sand mix, hence the higher variation in permeability reading between the two samples. Variation in permeability readings decreased progressively between shredded tire/sand mixes with the lowest permeability reading of 0.0026cm/s recorded by 1Tire:3Sand sample.

SMHI Type 6 subbase has permeability comparatively lower than those of the mixes while the granular base materials could be described as insignificantly permeable relative to the mixes. The poor drainage behavior of granular base could be attributed to the fact that the material is densely graded with the least amount of voids.

Table 3.8 Mean Permeability Readings for Shredded Tire and Shredded Tires/Sand Mixes

Sample	Mean Permeability (cm/s)	Minimum (cm/s)	Maximum (cm/s)	Coefficient of Variance (%)
100% Shredded Tire	1.4200	1.0962	1.8271	23.3
Sand	0.0013	0.0012	0.0013	3.9
1Tire:1Sand	0.0115	0.0107	0.0122	5.2
1Tire:2Sand	0.0032	0.0030	0.0034	4.4
1Tire:3Sand	0.0026	0.0024	0.0029	5.8
SMHI Type 6 *	0.001800			
Granular Base *	0.000025			
Crushed Rock *	1.12			

* Referenced permeability of granular subbase and base materials of similar specifications to City of Saskatoon subbase materials (Theyse 2002).

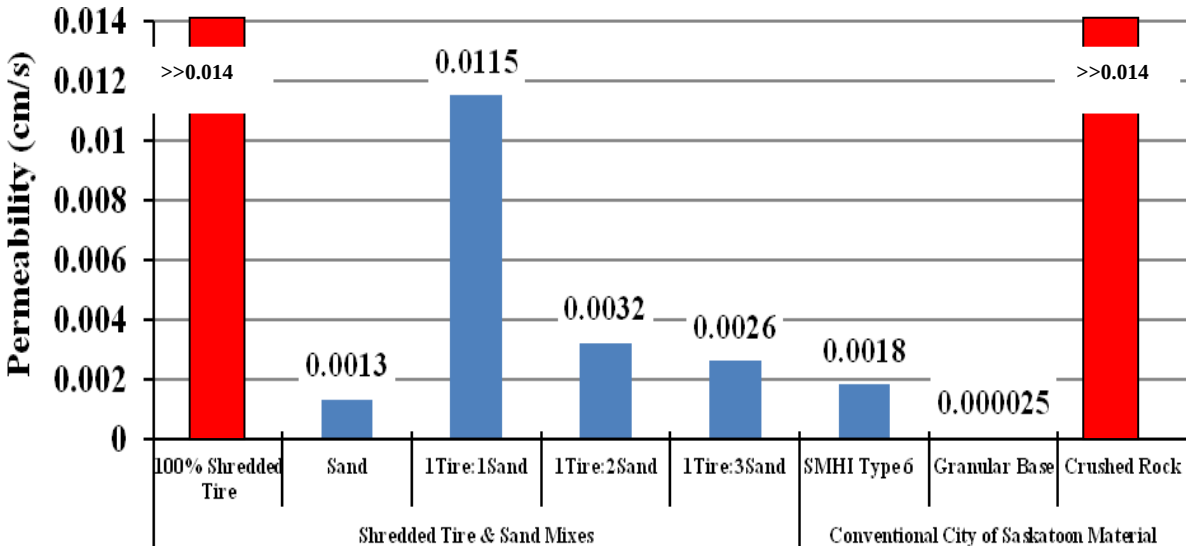

Figure 3.18 Mean Permeability Readings for Shredded Tire and Shredded Tires-Sand Mixes

The permeability of granular base is about 100 folds lower than that of 1Tire:3Sand. Crushed rock is deemed to have a permeability of 1.12cm/s which is 27% less than the permeability of 100% shredded tire materials and much higher than the shredded tire/sand mixes. Granular base is deemed as the least permeable among all materials considered in this research. The low permeability behavior of granular base could be associated with low amount of voids in the material due to its dense gradation. Granular base material can therefore be considered as not suitable for used as drainage layer material.

3.10 Chapter Summary

Chapter 3 provides laboratory characterization results for shredded tire and shredded tire/sand blends. Five samples (100% shredded tire and shredded tire/sand mixes in the mix ratio of 1Tire:1Sand, 1Tire:2Sand, 1Tire:3Sand and sand) were characterized using grain size distribution, CBR, vertical confined compressive strength, confined frequency sweep test, and permeability tests. Characterized material properties were compared to those of SMHI Type 6 subbase, crushed rock, and granular base materials.

Shredded tires used in this research were obtained from Shercom Industries in Saskatoon, Saskatchewan. Shredded tires obtained were mostly 150mm long with embedded metal fibres. Shredded tires were cut into smaller chips for the laboratory characterization process since full scale testing of shreds was not available.

The grain size distribution test showed uniform gradation for the shredded tire materials used in this research. Sand material tested contained no fines. Increasing the quantity of sand in the tire/sand mixes made them more densely graded compared to the gradation of shredded tire. City of Saskatoon crushed rock contained more coarse individual particles than there were in the prepared shredded tire sample and shredded tire/sand mixes and were deemed to have gap gradation. Granular base was densely graded with high amount of fine particles.

CBR strength characterization showed shredded tire to be low in mechanical stiffness with an average CBR of 1.3%. The CBR values for the mixes were observed to increase as the quantity of sand in the mix increased. However, CBR value for the sand samples was found to be lesser than 1Tire:3Sand mix. SMHI Type 6 subbase, crushed rock and granular base materials

were all found to have a CBR higher than all the mixes yielding CBR values of 45%, 100% and 77%, respectively.

The vertical confined compressive strength test characterized 100% shredded tire as a material with the highest compressibility. Compressibility was observed to decrease with increase in the quantity of sand in the mix. The trend in behavior could be associated with voids in the shredded tire. Increasing the quantity of sand in the mixes improved the compressive strength by filling up the voids.

Dynamic modulus and phase angle mechanistic properties of samples were determined using confined frequency sweep testing in the RaTT cell. The 100% shredded tire and 1Tire:1Sand yielded confined dynamic modulus values less than City of Saskatoon Subbase materials. 1Tire:2Sand and 1Tire:3Sand yielded confined dynamic modulus values 17% and 68% higher than SMHI Type 6 subbase. Crushed rock and granular base were characterized to have a higher stiffness than all shredded tire and shredded tire/sand mixes. Confined dynamic modulus characterization results also validated the mechanical support behavior of sand in the mixes.

Permeability characterization of 100% shredded tire and shredded tire/sand mixes was performed using a simple free drainage test. Samples of 100% shredded tire were found to be free draining at 1.42cm/s. Increasing the quantity of sand in the mixes reduced the permeability by a small margin as compared to the shredded tire to 1Tire:1Sand relation. Permeability of SMHI Type 6 subbase and granular base were significantly less than that of clean sand and all shredded tire/sand mixes while the permeability of crushed rock was deemed as free draining similar to 100% shredded tire.

CHAPTER 4 FINITE ELEMENT STRUCTURAL MODELING

The structural behavior of shredded tire road systems and typical City of Saskatoon local road structures were evaluated using a 3D structural computational modeling software, PSIPave3D^{TM}. In order to directly compare the structural behaviour of shredded tire and shredded tire/sand mixes with City of Saskatoon subbase materials, a typical baseline road structure (City of Saskatoon local road design) was used with varying subbase layer materials for each respective road model. Primary deflection responses and 3D-strain behaviour of the two categories of road structures were quantified using the modeling framework under single axle dual tire loading (Berthelot et al. 2012).

The modeling software is a 3D non-linear orthotropic road model used to predict peak surface deflection and three dimensional strain behaviour of road structures by incorporating field state conditions such as road geometry, load spectra, climatic conditions and material constitutive properties into the design (Berthelot 2011, Berthelot et al. 2012, Soares et al. 2012).

City of Saskatoon currently uses an empirically based road design method known as the Saskatchewan Highways' modified California Bearing Ratio (CBR) Shell Design Curves (SMHI 2009). This design method determines road structure geometry based on *in situ* subgrade conditions under the assumption that structural layers are of high quality material (Berthelot 2009, AASHTO 2002). Contrary to the software, the Shell Curve design method fails to account for the current field state conditions (complex road structure geometry, climatic and load spectra) experienced in Saskatchewan and pavement rehabilitation and construction using recycled materials (Berthelot et al. 2012).

PSIPave3D^{TM} model consists of a user-friendly software package which incorporates input variables to generate deflection and 3D-strain responses used in predicting and verifying field performances (Berthelot et al. 2011). Input variables include:

- Road structure geometry;
- Design load; and,
- Mechanistic material properties.

A study conducted previously to evaluate the structural performance of City of Saskatoon drainage layers validated the predicted peak surface deflection results of the PSIPave3D™ using field deflection data measured with heavy weight deflectometer across typical City of Saskatoon streets (Berthelot et al. 2012, Berthelot et al. 2011). Figure 4.1 shows the PSIPave3D™ input tool structure.

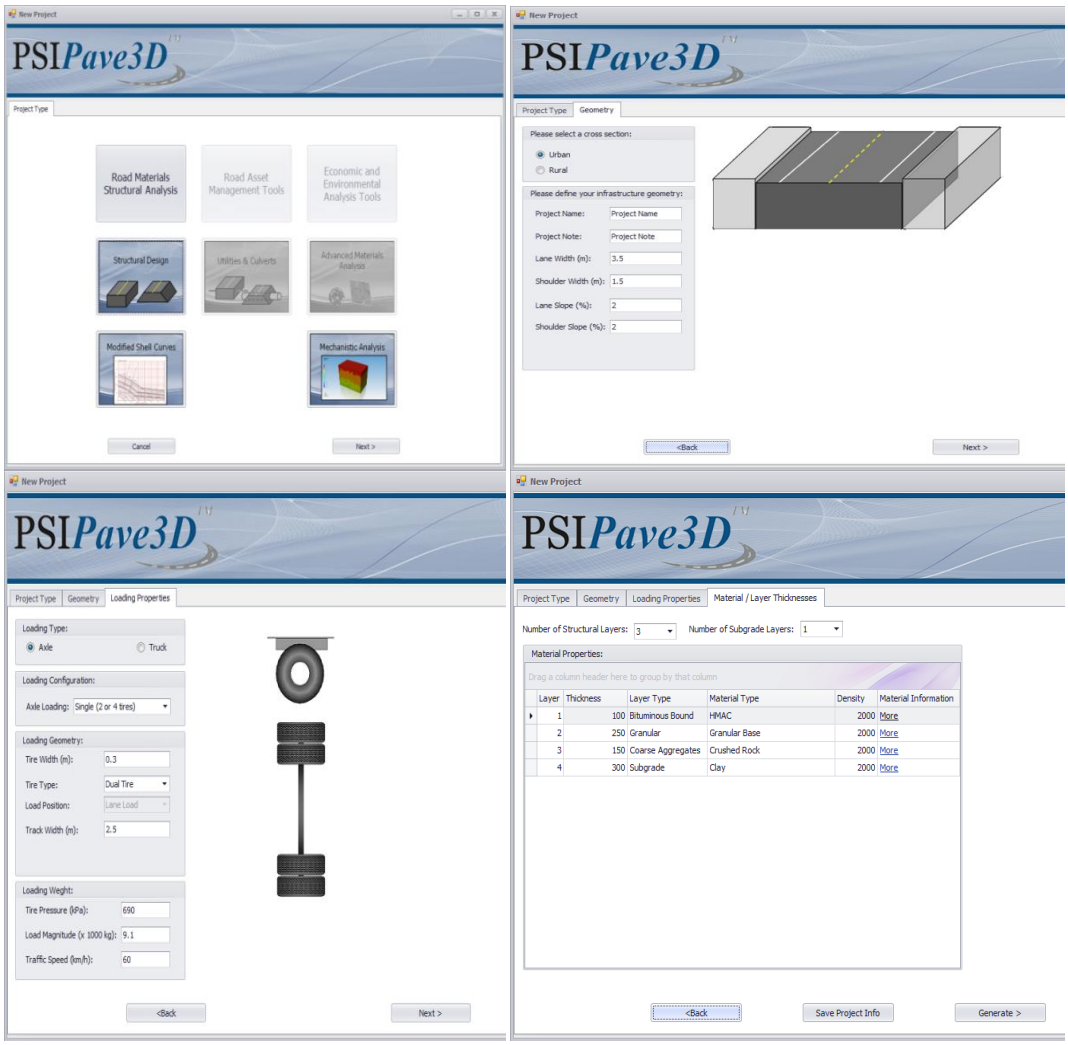

Figure 4.1 PSIPave3D™ Input Screens for Model (PSIPave3D™ 2013)

4.1 Model Input Data

4.1.1 Road Structure Geometry

Shredded tire and shredded tire/sand road sections were modeled and compared to typical City of Saskatoon local road structures. For the purpose of this study, a typical design structure with the same pavement layer thicknesses and materials was assumed for all roads with varying subbase material so as to directly compare the structural behaviour of subbase materials. The modeled roads were labelled by the name of the subbase layer material used: 100% shredded tire, 1Tire:1Sand, 1Tire:2Sand, 1Tire:3Sand, sand, SMHI Type 6 subbase, crushed rock and granular base roads. Table 4.1 shows the layer thicknesses for the modeled roads. Cross section of the typical City of Saskatoon road structure used for this study is shown in Figure 4.2. Detailed design of all road sections are shown in Appendix G.

Table 4.1 Modeled Cross Sections

Road Name	Subbase (mm)	Granular Base (mm)	AC (mm)
100% Shredded Tire	225	120	50
1Tire:1Sand	225	120	50
1Tire:2Sand	225	120	50
1Tire:3Sand	225	120	50
Sand	225	120	50
SMHI Type 6 Subbase	225	120	50
Granular Base	225	120	50
Crushed Rock	225	120	50

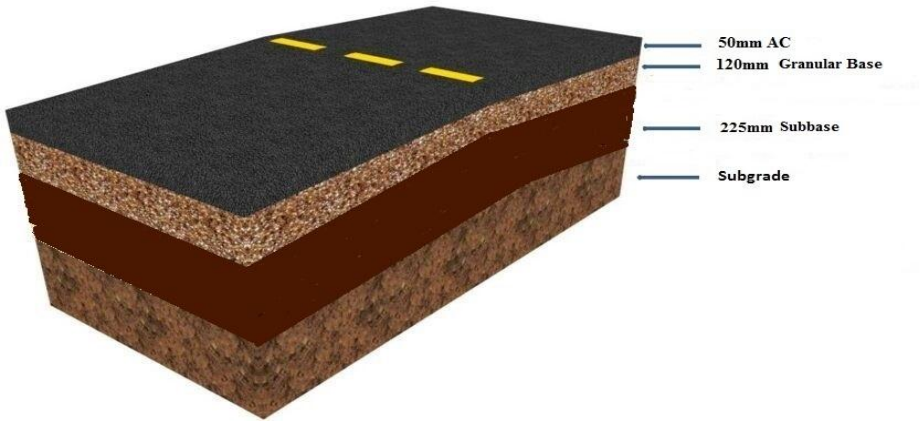

Figure 4.2 Typical City of Saskatoon Cross Section

4.1.2 Design Load

Loading criteria incorporated in the PSIPave3D™ tool was based on the design loads used by the City of Saskatoon for local roads (Berthelot et al 2012). Single dual tire axle loading under Saskatchewan's highway primary weight limit category was used as the design load for modeling. The magnitude of loading induced by the City of Saskatoon transit bus (Figure 4.3) and garbage trucks are examples of field state simulation of the design load incorporated in the models (Berthelot et al. 2012). A single dual tire axle induces a loading of weight 89kN (Figure 4.4) (Berthelot et al 2012).

4.1.3 Mechanistic Material Properties

Mechanistic properties of structural layer materials needed as input variables for modelling were determined in the laboratory characterization chapter of this document. A dry clay subgrade of poor structure was assumed for all roads considered in this research. The subgrade condition was chosen based on the fact that most frost susceptible areas have poor clayey subgrades.

Figure 4.3 City of Saskatoon Transit Bus

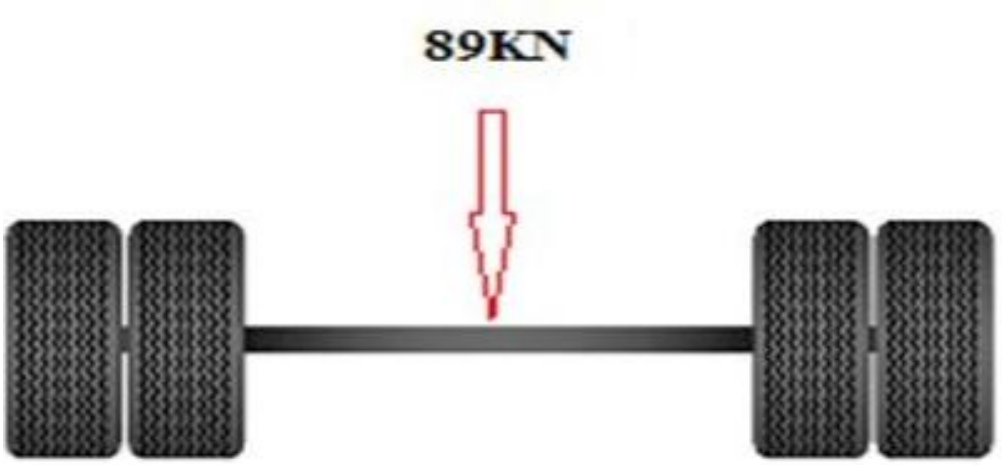

Figure 4.4 Single Dual Tire Axle Load

4.2 PSIPave3D™ Predicted Results

4.2.1 Peak Surface Deflection

Peak surface deflection measures the ability of a pavement structure to withstand loading (Berthelot et al. 2012). The structural integrity of an existing road structure can be determined by measuring the peak surface deflection under specified loading using a heavy weight deflectometer (HWD). The City of Saskatoon employs the use of HWD non-destructive test equipment as a tool for assessing and verifying the structural integrity of road assets at the project level (Berthelot et al. 2011). A road structure that attains a higher peak surface deflection value is classified as poor. The City of Saskatoon established deflection threshold for local roads which rates peak surface deflection of 0 to 1.0mm as good, 1.0mm to 1.5mm as fair and peak surface deflections above 1.5mm as poor (Berthelot et al. 2011).

Peak surface deflection was modeled for the shredded tire/sand roads and City of Saskatoon local roads. Table 4.2 and Figure 4.5 show the peak surface deflection results generated.

Table 4.2 Model Predicted Peak Surface Deflections at Primary Weight Limits

Road Name	Predicted Peak Surface Deflections (mm)
100% Shredded Tire	2.19
1Tire:1Sand	1.48
1Tire:2Sand	1.01
1Tire:3Sand	0.96
Sand	1.00
SMHI Type 6 Subbase	1.14
Crushed Rock	0.73
Granular Base	0.89

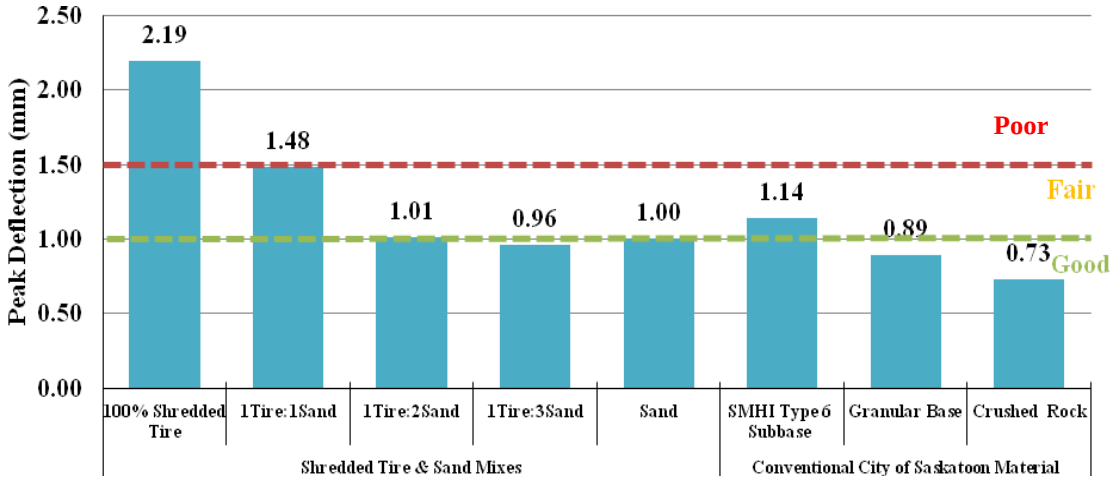

Figure 4.5 Model Predicted Peak Surface Deflections (mm) at Primary Weight Limits

The 100% shredded tire road recorded the highest peak surface deflection value of 2.19mm, which falls within the poor deflection threshold. Mixing the shredded tire with sand improved the structural integrity by reducing the peak surface deflection. For instance, 1Tire:1Sand recorded a fair peak deflection of 1.48mm, which is a 32% reduction in the magnitude of deflection as compared to that of the 100% shredded tire road. Both 1Tire:2Sand and 1Tire:3Sand road models yielded good levels of peak deflection measured at 1.01mm and 0.96mm, respectively. The sand road also had a good peak surface deflection of 1.00 mm.

The structure with the crushed rock subbase layer exhibited tremendous structural performance with peak surface deflection value of 0.73mm. Granular base road also recorded a good peak deflection of 0.89mm which is also much more efficient in structural performance

than the shredded tire/sand roads. Crushed rock and granular base peak surface deflections represent 31.5% and 7.9% improvement in structural performance, respectively, relative to 1Tire:3Sand. SMHI Type 6 subbase road was deemed to perform fairly with an average deflection of 1.14mm, which represents 18% higher deflection than the 1Tire:3Sand road and 13% higher than 1Tire:2Sand road. These results indicate that the 1Tire:2Sand and 1Tire:3Sand roads performed better structural wise than SMHI Type 6 subbase in terms of providing structural stability.

The peak surface deflection results illustrate the structural enhancement capabilities of mixing sand with shredded tires.

4.2.2 Horizontal Tensile Strain

Fatigue cracking in pavement structures is generally considered to be caused by the horizontal tensile strains at the bottom of the HMAC (Hu et al. 2008). Fatigue cracks on the surface of a road can be statistically correlated to failure tensile strains under the bottom of HMAC layer. Model predicted horizontal tensile strain values measured under the bottom of the HMAC of the roads are shown in Table 4.3 and Figure 4.6.

The highest predicted horizontal tensile strain value of 410με was measured at the bottom of the HMAC of the 100% shredded tire road. Increasing the quantity of sand reduced the horizontal tensile strain at the bottom of HMAC of the mixes as seen in Figure 4.6. For instance, the horizontal tensile strain was reduced by 15% in the 1Tire:1Sand, 37% in the 1Tire:2Sand and 42% in the 1Tire:3Sand structures as compared to the 100% shredded tire road. Using sand as the subbase material showed a predicted horizontal tensile stain value of 257με which falls in between the values recorded by 1Tire:2Sand and 1Tire:3Sand.

City of Saskatoon crushed rock road had the least horizontal tensile strain value of 189με under the HMAC layer, which is 54% lower than that of 100% shredded tire road. The crushed rock road could therefore be considered as the least prone to fatigue cracking. SMHI Type 6 subbase and granular base roads also recorded horizontal tensile strain values of 275με and 209με, respectively. SMHI Type 6 subbase horizontal tensile strains represent 6% and 15% increments in magnitude as compared to the tensile strains measured under the HMAC of 1Tire:2Sand and 1Tire:3Sand, respectively.

Table 4.3 Model Predicted Horizontal Tensile Strain at Bottom of HMAC

Road Name	Horizontal Tensile Strain (με)
100% Shredded Tire	410
1Tire:1Sand	349
1Tire:2Sand	260
1Tire:3Sand	238
Sand	257
SMHI Type 6 Subbase	275
Granular Base	209
Crushed Rock	189

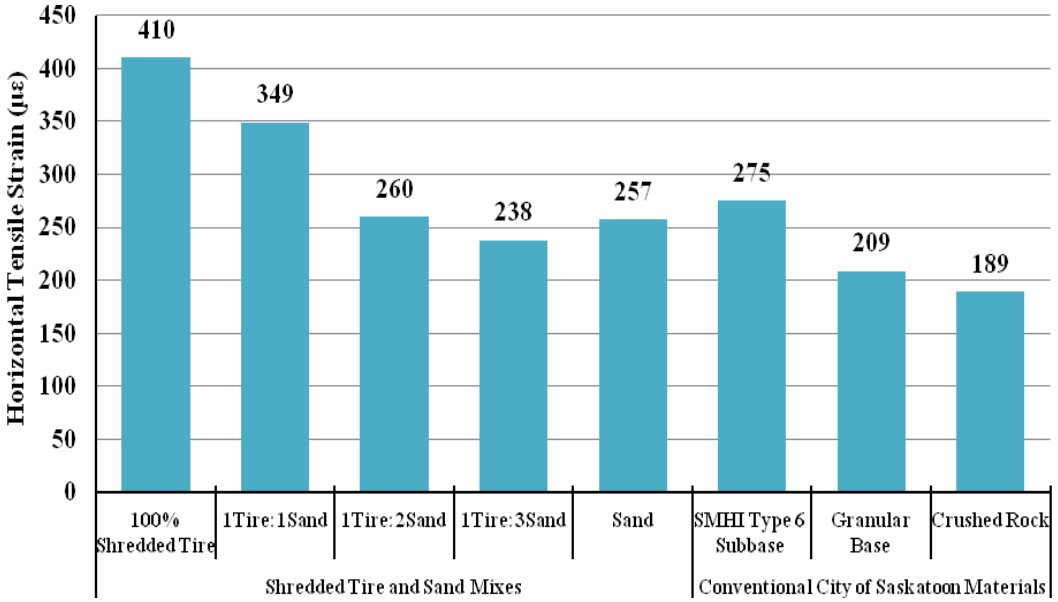

Figure 4.6 Model Predicted Horizontal Tensile Strains at Bottom of HMAC

Both 1Tire:2Sand and 1Tire:3Sand roads will therefore be less likely to undergo failure due to fatigue cracking than the SMHI Type 6 subbase.

Figure 4.7 to 4.14 show the horizontal strain profiles measured on all roads modeled. The red spots on the road profile shows the locations of high-induced strains and are the most prone to failure. The 100% shredded tire road could be observed to be most prone to failure with respect to the color pattern on its profile. The crushed rock road shows the least failure spots as compared to all other roads.

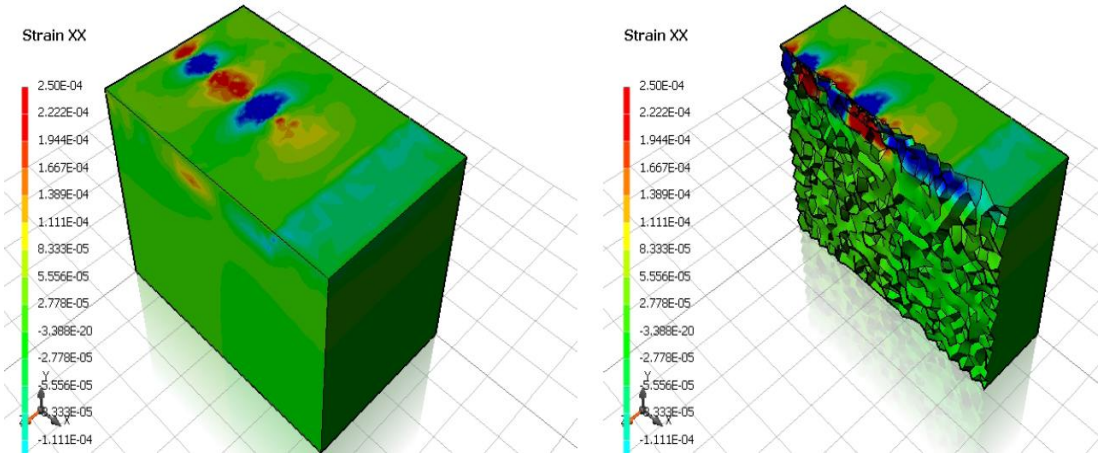

Figure 4.7 Horizontal Strain (Transverse) Profile for 100% Shredded Tire

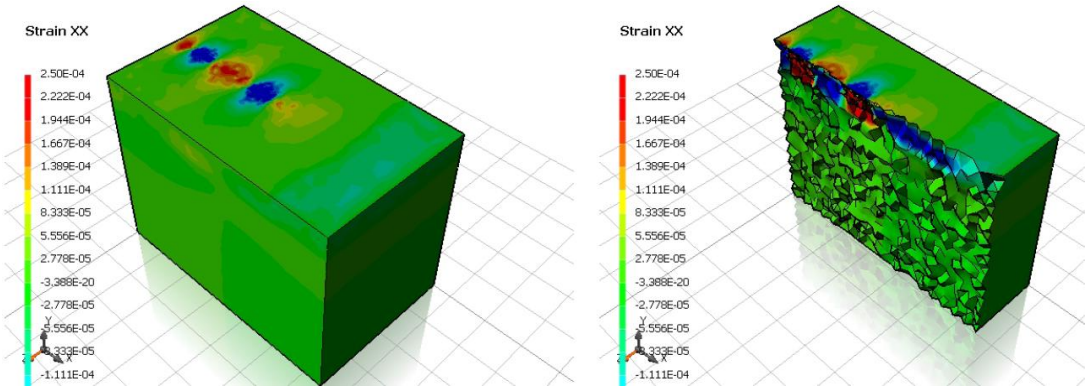

Figure 4.8 Horizontal Strain (Transverse) Profile for 1Tire:1Sand

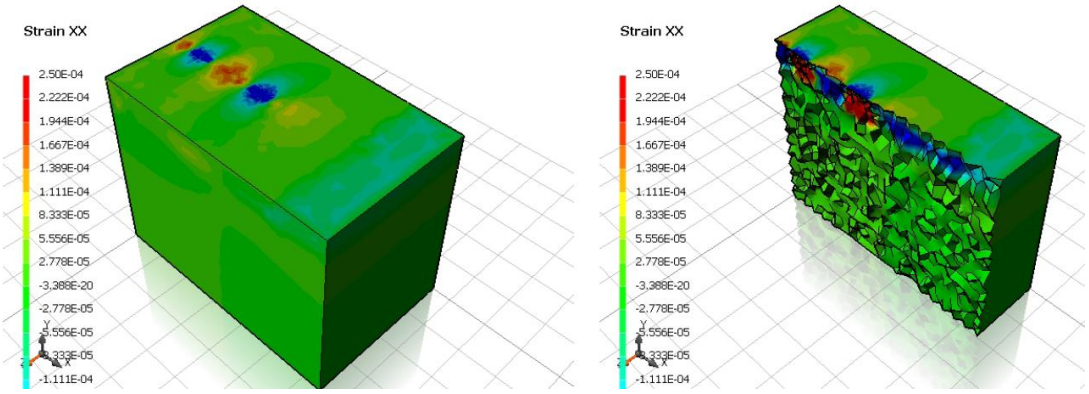

Figure 4.9 Horizontal Strain (Transverse) Profile for 1Tire:2Sand

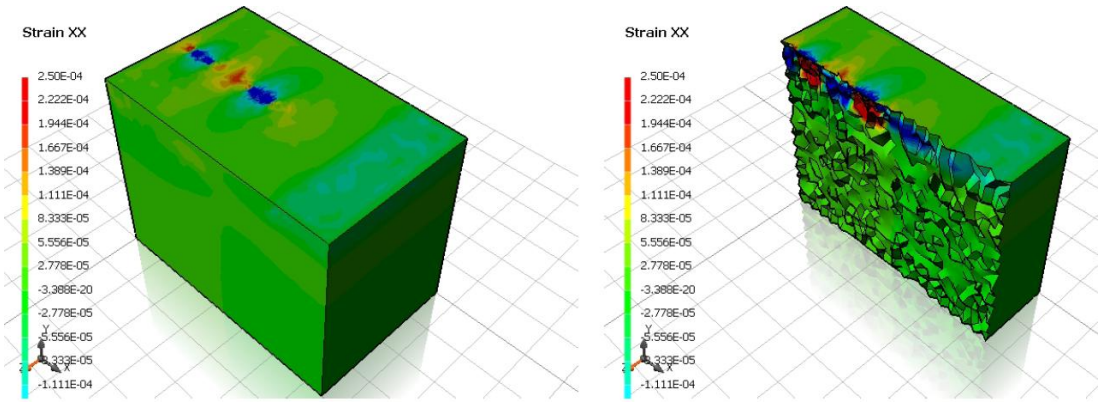

Figure 4.10 Horizontal Strain (Transverse) Profile for 1Tire:3Sand

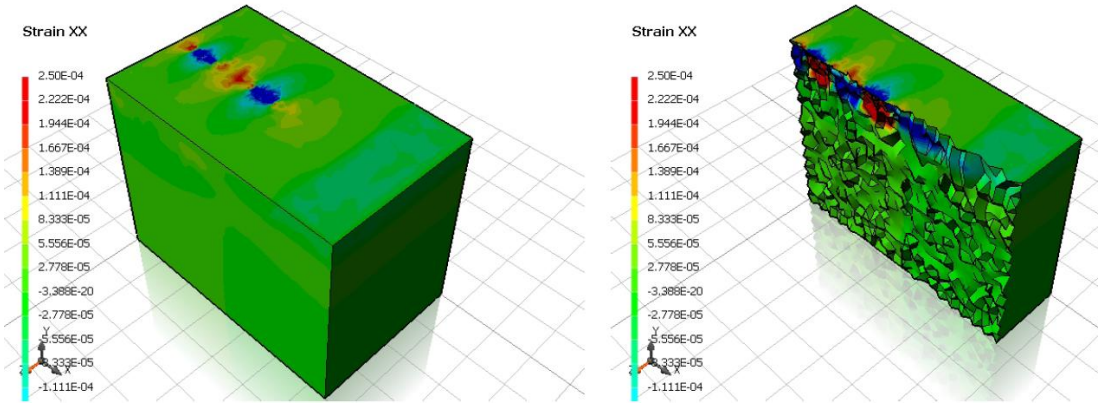

Figure 4.11. Horizontal Strain (Transverse) Profile for Sand

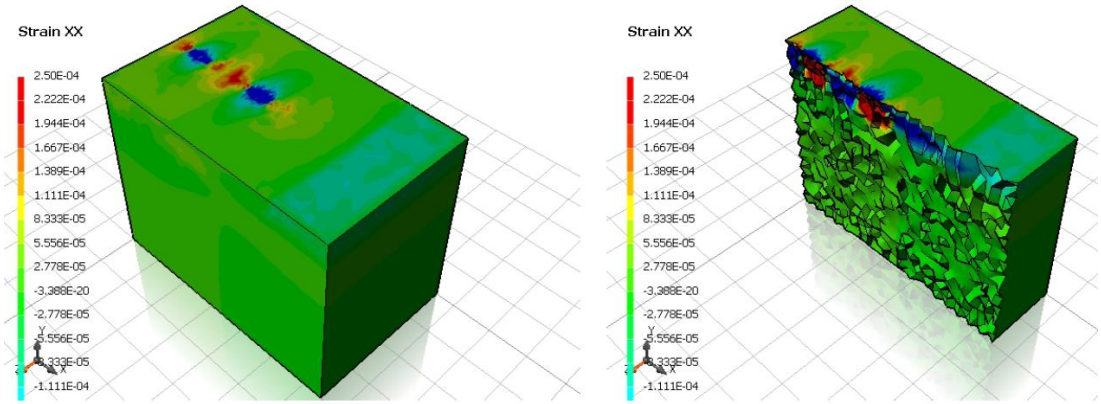

Figure 4.12. Horizontal Strain (Transverse) Profile for SMHI Type 6

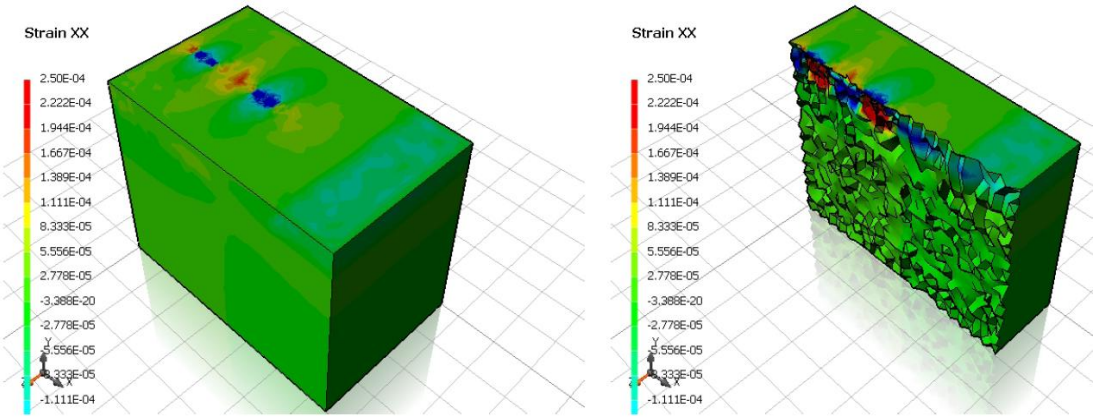

Figure 4.13 Horizontal Strain (Transverse) Profile for Granular Base Tire

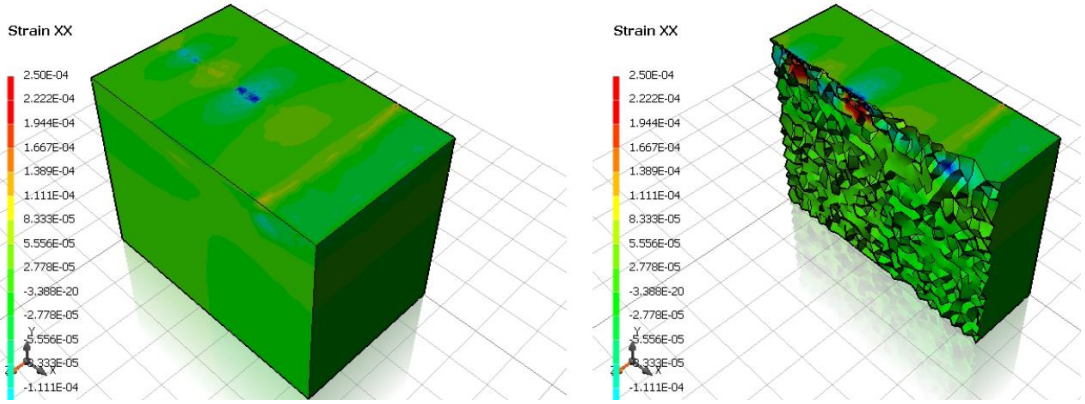

Figure 4.14 Horizontal Strain (Transverse) Profile for Crushed Rock

4.2.3 Vertical Compressive Strains on Top of Subgrade

Pavement design engineers correlate vertical compressive strains on the top of the subgrade to rutting on the field (Roberto et al. 2012). The extent to which rutting occurs on a pavement structure is highly dependent on the magnitude of compressive strains acting on the subgrade of the structure.

Table 4.4 and Figure 4.15 illustrate the predicted vertical strain values measured on the top subgrade of the subgrade of all modeled roads. The highest vertical compressive strain of 29400με was recorded on the subgrade of the 100% shredded tire road. Similar to the trend in peak surface deflection analysis, the compressive strains measured on the top of the subgrade for each road were significantly reduced as the quantity of sand in the mix increased. A significant reduction of up to 45% was obtained in 1Tire:1Sand and 68% in the 1Tire:3Sand structures as

compared to that of 100% shredded tire road model. The crushed rock road recorded the least vertical compressive strain value of 6118με.

The poor structural performance behaviour of the 100% shredded tire road could be associated with the high compressibility behaviour within the shredded tire layer. SMHI Type 6 subbase and granular base roads recorded vertical compressive strains of magnitude 11634με and 9326με, respectively. Both 1Tire:2Sand and 1Tire:3Sand yielded compressive strains about 8.6% and 20% lower than the vertical compressive strains measured on the subgrade of the SMHI Type 6, respectively.

Table 4.4 Model Predicted Peak Vertical Compressive Strain on Top of Subgrade at Primary Weight Limits

Road Name	Vertical Compressive Strain (με)
100% Shredded Tire	29400
1Tire:1Sand	16321
1Tire:2Sand	10630
1Tire:3Sand	9302
Sand	10007
SMHI Type 6 Subbase	11634
Granular Base	8359
Crushed Rock	6118

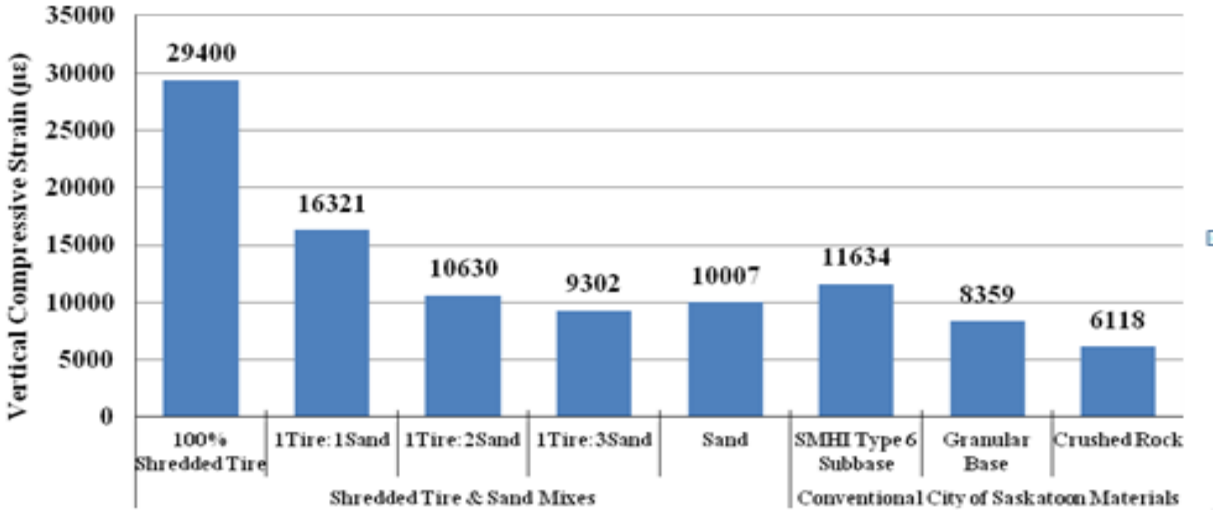

Figure 4.15 Model Predicted Peak Vertical Compressive Strain on Top of Subgrade at Primary Weight Limits

The high vertical compressive strain measured on the subgrade of the SMHI Type 6 subbase demonstrates the possibility of this road structure undergoing more failure due to rutting as compared to 1Tire:2Sand and 1Tire:3Sand roads.

Model predicted vertical compressive strain profiles for all road structures are shown in Figures 4.16 to 4.23. The models show the magnitude and strain contours that the road structure will experience under primary weight loading. Each figure shows a structure on the left and a sliced section (shows contours within road structure) on the right. Two red locations shown on the surface of models simulate induced strains at the point of contact between the vehicle tires and the road surface.

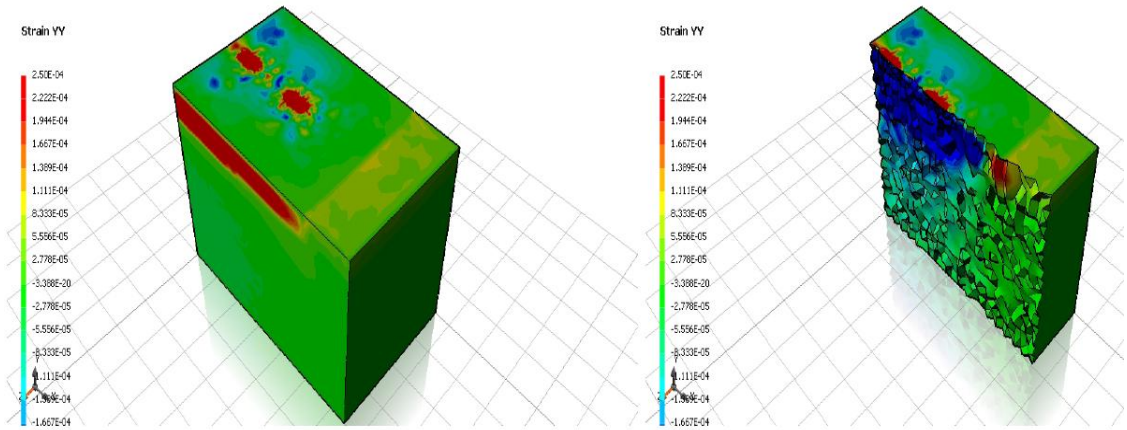

Figure 4.16 Vertical Strain Profile for 100% Shredded Tire

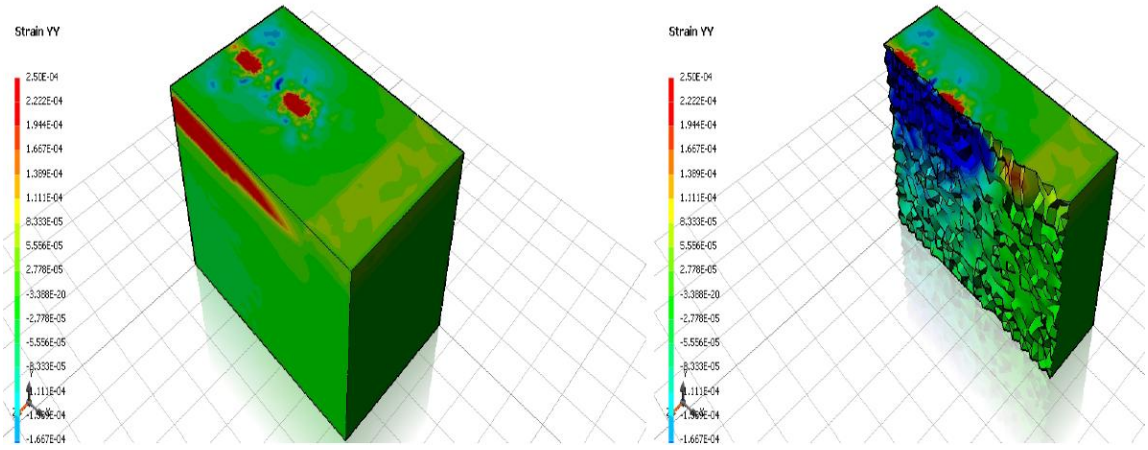

Figure 4.17. Vertical Strain Profile for 1Tire:1Sand

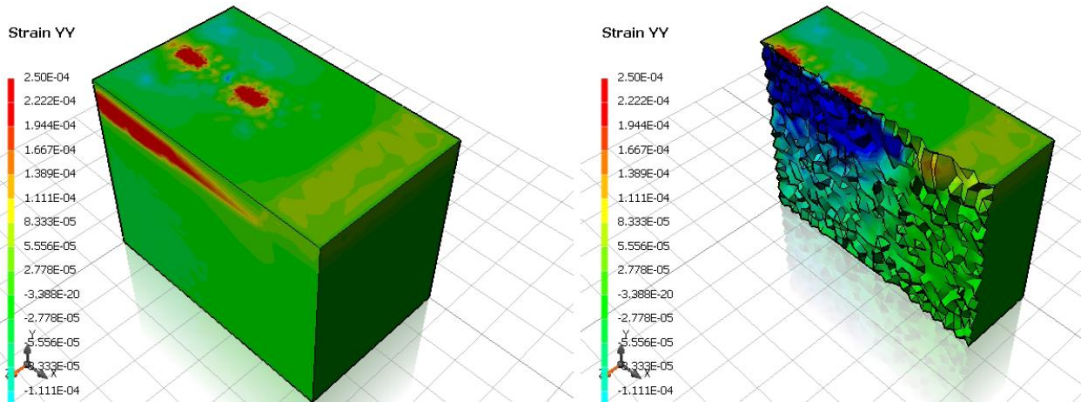

Figure 4.18 Vertical Strain Profile for 1Tire:2Sand

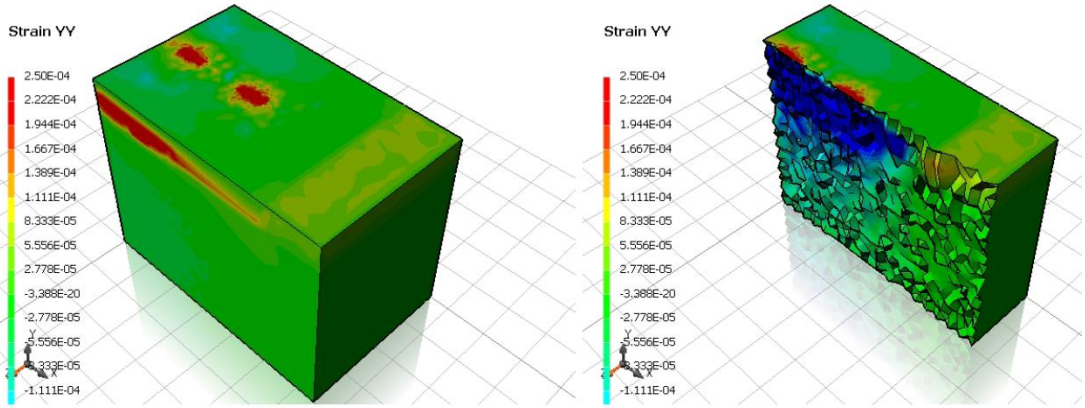

Figure 4.19. Vertical Strain Profile for 1Tire:3Sand

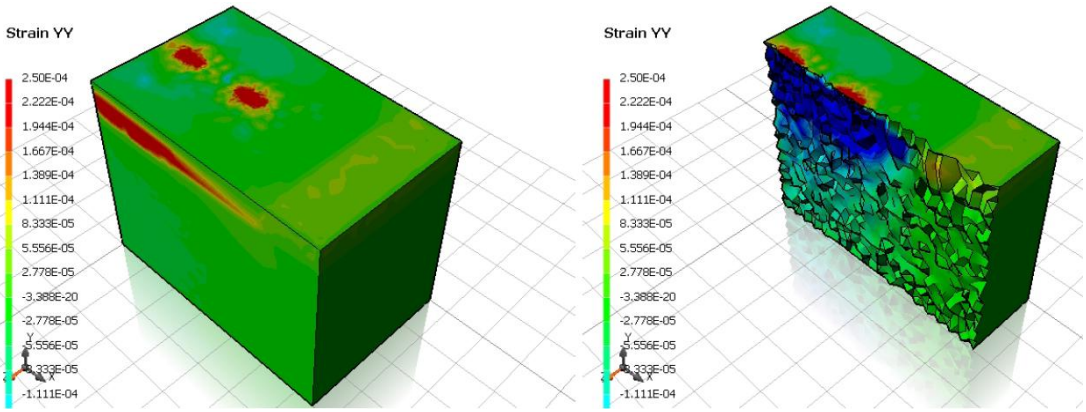

Figure 4.20. Vertical Strain Profile for Sand

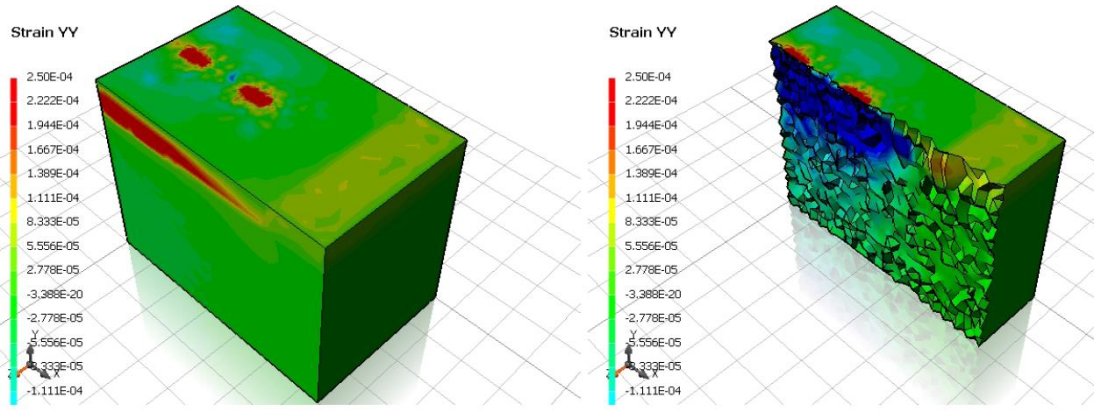

Figure 4.21. Vertical Strain Profile for SMHI Type 6 Subbase

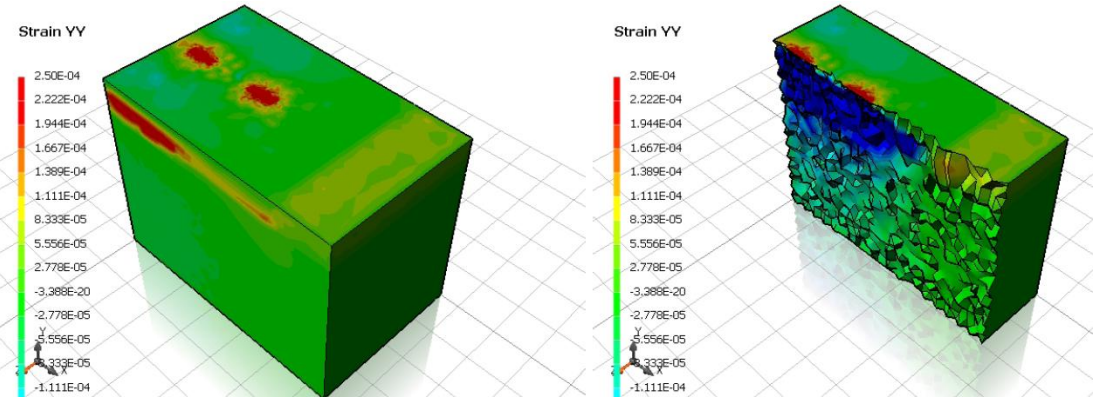

Figure 4.22. Vertical Strain Profile for Granular Base

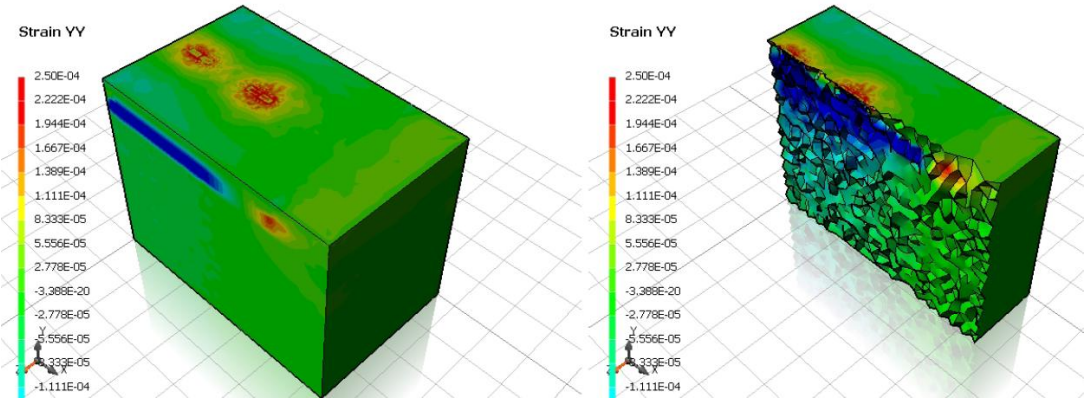

Figure 4.23. Vertical Strain Profile for Crushed Rock

As shown in the profiles, the highest extent of vertical strain failure was recorded within the 100% shredded tire structure. The depth of penetration of strains was also more pronounced in this structure as compared to the rest. However, the intensity and depth of profiles decreased as the quantity of sand increased in the mix used within the subbase of structures. Sand road profile showed a poor performance as compared to 1Tire:3Sand. Crushed rock road profile showed the least amount of strains within the structure. Detailed 3D strain profiles for all roads are shown in Appendix G.

4.2.4 Shear Strain Analysis

Measuring shear strain in the structural layers is considered vital in this research since most roads in Saskatchewan fail in shear due to high traffic loading. Table 4.5 and Figure 4.24 illustrate the model predicted shear strains within the structural layers of the roads under primary weight limits.

Shear strain results showed a general trend similar to the peak surface deflection and vertical compressive strain results. The highest overall strain responses were recorded within the layers of the 100% shredded tire road. The model predicted shear strain was greatest within the subbase of the 100% shredded tire at 3029με as compared to the other road structures. Overall shear strain behaviour was observed to decrease as the quantity of sand in the mixes increased. For instance, the shear strains measured in the subbase layer were reduced by 26.6% in 1Tire:1Sand and 64.3% in subbase of 1Tire:3Sand relative to 100% shredded tire road subbase. The crushed rock road exhibited the best performance as it recorded the least shear strain values in each layer. The least shear strain value was recorded in the subbase layer of the crushed rock road which showed a tremendous performance at 509με.

Considering the shear strain under the bottom of the HMAC layers for all structures, 100% shredded tire had the highest strain value of 694με which is significantly higher than those of HMAC strain values for the other roads.

Table 4.5 Model Predicted Shear Strains on All Layers at Primary Weight Limits

Road Name	Maximum Shear Strain by Layer (με)			
	HMAC	Base	Subbase	Subgrade
100% Shredded Tire	1181	2358	3029	2118
1Tire:1Sand	965	1998	2222	2016
1Tire:2Sand	759	1651	1323	1523
1Tire:3Sand	721	1540	1081	1363
Sand	724	1515	1099	1324
SMHI Type 6 Subbase	781	1700	1422	1575
Crushed Rock	636	1221	509	923
Granular Base	671	1364	851	1189

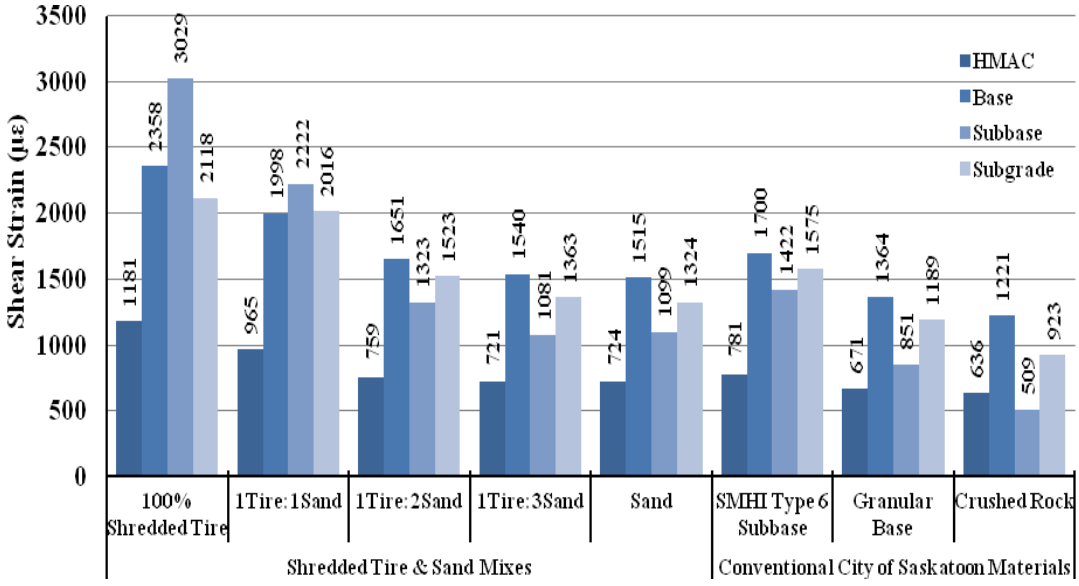

Figure 4.24 Model Predicted Shear Strain at Primary Weight Limits

The 100% shredded tire road, as predicted by the model, will have the greatest tendency of failing in shear in Saskatchewan field state conditions. Both 1Tire:2Sand and 1Tire:3Sand roads will perform much better in terms of withstanding shear failure in the field than SMHI Type 6 subbase road since they yielded lower shear strain values in all layers than the SMHI Type 6.

4.3 Chapter Summary

Structural performance modeling was used to evaluate and compare the structural performances of shredded tire systems with typical City of Saskatoon local roads. Input variables for the 3D computation modeling included road geometry, layer mechanistic material properties and design loading. Design loading used was single axle dual tire loading which simulates Saskatoon transit bus loading.

Modeled results showed the 100% Shredded tire road to have poor peak surface deflection value of 2.19mm. As the quantity of sand increased in the subbase of structures the deflection measured was observed to decrease significantly to the good threshold in 1Tire:3Sand. City of Saskatoon crushed rock road recorded the lowest deflection of 0.73mm while sand had a peak surface deflection less than that of 1Tire:3Sand road. Peak surface deflection on the granular base local road measured at 0.89mm, which was less than those of 1Tire:2Sand and 1Tire:3Sand. SMHI Type 6 subbase road was deemed to perform less efficiently than 1Tire:2Sand and 1Tire:3Sand roads in terms of structural performance.

Horizontal tensile strain results showed improved structural performance as the quantity of sand was increased in the subbase mix. For example, the horizontal tensile strain value predicted to develop in the HMAC layer of the 100% shredded tire road was 410με while 349με, 260με, 238με and 257με were predicted to develop in those of 1Tire:1Sand, 1Tire:2Sand, 1Tire:3Sand and sand roads, respectively. Since horizontal tensile strain could be correlated to fatigue cracking in the field, 100% shredded tire road section may sustain the most fatigue cracks under similar loading conditions than any other road modeled in this research. Crushed rock road provided the most structural integrity with the least horizontal tensile strain value of 189με. SMHI Type 6 subbase road performed less efficiently than 1Tire:2Sand and 1Tire:3Sand roads while the horizontal tensile strain in the granular base road was less than those measured for all shredded tire/sand roads.

The highest magnitude of vertical compressive strains were recorded on the subgrade of the 100% shredded tire road. The high magnitude of compression recorded could be attributed to the creep behaviour of the rubber. Vertical compressive strain values decreased with an increase in the amount of sand. These results indicate that 100% shredded tire road will be more prone to

deep ruts under similar field state conditions. Both 1Tire:2Sand and 1Tire:3Sand roads will perform much more efficiently in terms of structural support than SMHI Type 6 subbase roads in Saskatchewan field state conditions

Stress strain response measured across all layers of the modeled roads exhibited a similar trend in behaviour as the peak surface deflection, horizontal tensile strain and vertical compressive strain results.

CHAPTER 5 – FIELD TEST SECTION TRIAL CONSTRUCTION

This chapter describes field observations made while using shredded tire in a field section constructed in Saskatoon, Saskatchewan. The purpose of the experiment was to determine the feasibility of constructing shredded tire roads and to evaluate the structural performance of shredded tires as a pavement substructural layer compared to typically used aggregates. Design for the test section was based on City of Saskatoon local road design criteria. Final structural designs used for the test sections were selected by the City of Saskatoon.

5.1 Road Test Section Description

The test section used in this study is Adolph Way. Adolph Way is located in Sutherland, about 4.5 kilometres drive northeast of the University of Saskatchewan. Figure 5.1 shows the location of the test section. A 100 meter length of the residential road section was allocated for this experiment. Two sections consisting of a test section with shredded tires as subbase layer material and a control section using crushed rock were to be constructed on each half of the road section as shown in Figure 5.2.

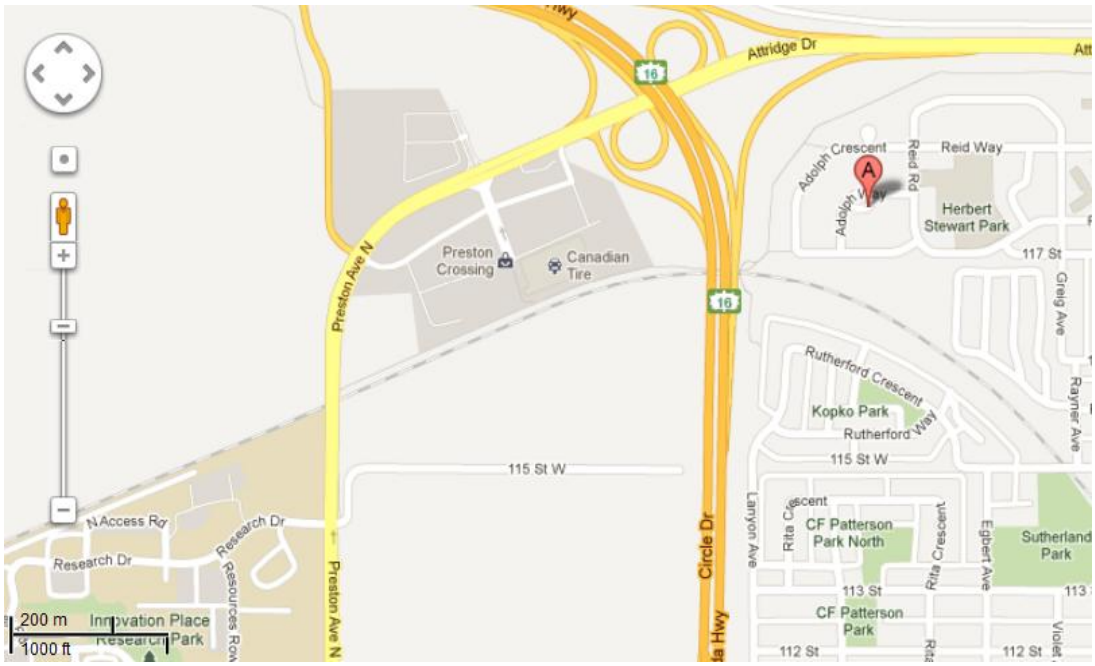

Figure 5.1 Location of Adolph Way in Saskatoon (Google Maps 2010)

5.2 *A priori* Test Section Assessments

Pre construction visual site survey showed pronounced alligator cracks on the road section. Fatigue cracks were also present along wheel paths with ruts along the entire length of the section as seen in Figure 5.3. The extent of damage could also be seen to be severe at the side of the roadway as permanent deformation in the form of deep ruts and undulating road surfaces were found at various spots along both sides of the road. Pavement structure failure could be associated with inefficient drainage provided and the effect of loading from vehicles parked along these parts of the roadway. Pavement deterioration covered more than 75% of the entire road surface and could be attributed to substructural moisture problems.

Pre construction non-destructive heavy weight deflectometer (HWD) test measured a high peak surface deflection of 3.38mm (Guenther 2013).

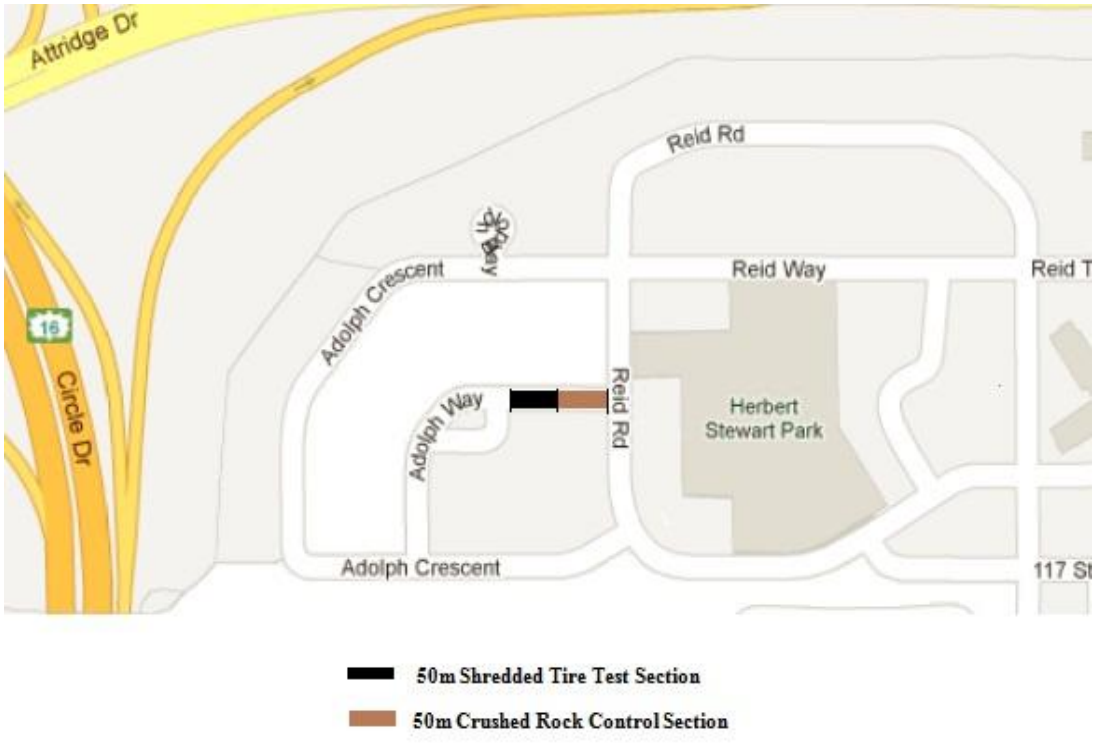

Figure 5.2 Test Section and Control Section Locations (Google Maps 2010)

Figure 5.3 Extent of Pavement Deterioration on Adolph Way

5.3 Test Section Design

Based on the results obtained from the laboratory characterization and review of reports from previous research and designs, shredded tires are deemed as a material of low stiffness but high permeability even under compressive stress loading. The extent of stability of the shredded tire layer will also depend on the reinforcement provided and the depth of placement of the reinforcement. These guidance principles used together with design specifications of City of Saskatoon were used to determine the pavement structure design of shredded tire section and control sections respectively. Figure 5.4 shows the cross section of the design for the two sections selected by the City of Saskatoon.

As indicated in the design, the subbase (drainage) layers of the two sections to be built with shredded tire and crushed rock are to be covered top and bottom with a woven geotextile fabric to prevent the clogging of the subbase material by finer soils from the base and subgrade layers. Woven geotextile fabric was specified for this project. In order to ensure effective spread of geotextile fabric, a one meter of overlap is to be used at all edges.

Structural reinforcement was provided in the design for the subbase layer. Both shredded tire and crushed rock sections were reinforced with Tensar BX1200 geogrid material placed mid section and on top of upper geotextile across the full length and width of each section as shown in the cross section diagrams.

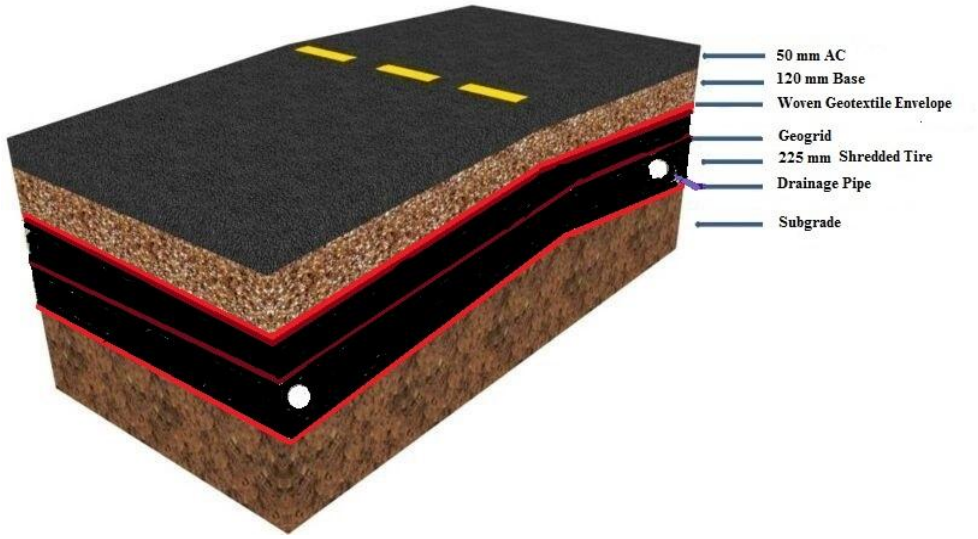

Figure 5.4 Design Cross Section of Shredded Tire Test Section

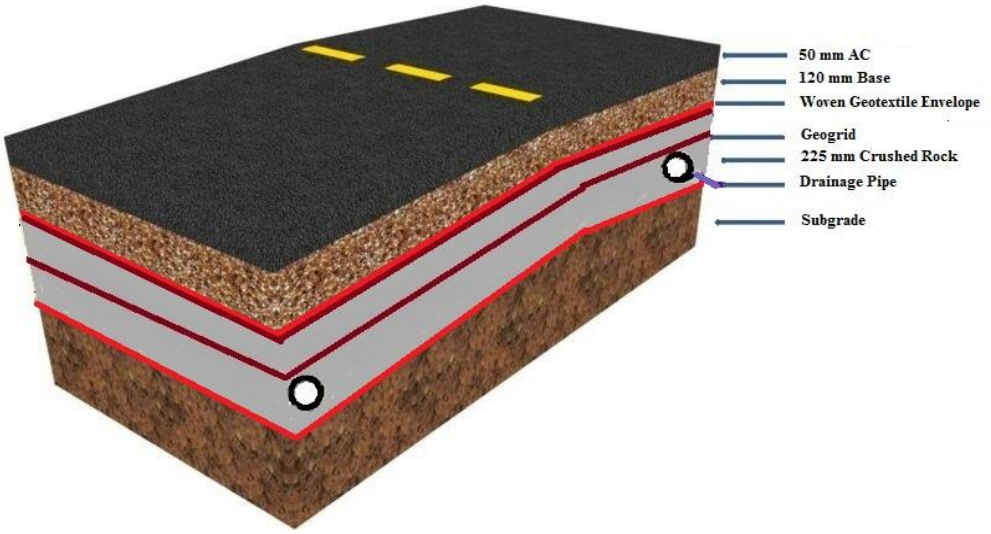

Figure 5.5 Design Cross Section of Crushed Rock Control Section

Drainage pipes also known as weeping tiles (100mm diameter) were installed and wrapped in woven geotextiles to prevent clogging. The weeping tiles had perforations along their entire length to enhance water percolation through them. Weeping tiles were laid along each side throughout the entire length of the road section. Design subgrade slope of five percent allows maximum drainage into the weeping tiles. All weeping tiles were drained into catch basins.

The existing road pavement was to be recycled and used as base material for the entire section. A hot mix asphalt concrete lift of 50mm was used as the wearing course for the entire section. Both the base and wearing course layers were cumbered at a slope of two percent to enhance surface water drainage of the roadway.

5.4 Construction Material Description

Shredded tires used in this experiment were obtained from Shercom Industries in Saskatoon. Shreds were of sizes ranging from 50mm to 150mm with metal fibres attached. These materials were free of deleterious materials such as wood, dirt, etc.

Crushed rock used for the control section subbase layer was mostly of 25mm diameter as specified by the City of Saskatoon. These aggregates were free of wood metals and deleterious materials.

5.5 Construction Process

The construction process involved initial partial reclamation of the existing road. *In situ* HMAC and granular material was milled to a depth of about 250mm using a rotary miller. About 150m^3 of this material was to be reused as base material for the entire section. Reclaimed material to be reused was made free of fines. The entire section was further excavated to a depth of about 400mm.

The *in situ* subgrade was shaped at a grade of about 5% towards the curb lines of the street from the centre line as indicated in the design to enhance drainage into the weeping tiles. The top layer of the subgrade was compacted with about three passes of a pneumatic tire roller. Woven geotextile material was spread on top of the subgrade across the entire width and length of the road section with overlap of at least 0.5m at sides (Figure 5.6). Weeping tiles were along

the edges of the trench as shown in the design and wrapped with a woven geotextile to prevent clogging.

Shredded tire materials were spread covering a length of 50m and the full width of the trench over the woven geotextile in two lifts and compacted to a thickness of about 120mm. Compaction was carried out using static loading on the shredded tire section since vibratory compaction had no effect on the density of the shredded tire. Shredded tires were seen to compact by a small extent as compared to compactions normally seen for granular materials.

Crushed rock aggregates were also spread on the remaining half of the trench and compacted in two lifts to a thickness of 120mm. Shredded tire and crushed rock material placement were done at the same time for both sections as shown in Figure 5.7. The layer of shredded tire on the test section and crushed rock on the other half formed the lower subbase layers for the two sections. Efficient compaction was ensured before the placement of the geogrid layer across the full length and width of both sections. The upper subbase layer for both sections were placed right on top of the geogrid in their respective sections and compacted to a total thickness of 225mm for each section and geogrid sandwiched mid depth as indicated in the design (Figure 5.8). Another geogrid was then placed over the subbase layers and covered with a woven geotextile as shown in Figure 5.9. The main purpose of incorporating the geogrid is to provide structural stability within the layers whereas the woven geotextile served as a material separator.

Base material in the form of reclaimed pavement from the old pavement was spread and compacted to a thickness of 120mm across the whole section. Compaction was done in six passes using a vibratory steel wheel roller. The base layer was shaped to a grade of two percent from the centreline of the road towards the curb. Figure 5.10 shows the road section constructed to the base level and ready for proof rolling.

Figure 5.6 Woven Geotextile Placed On Subgrade

Figure 5.7 Shredded Tire Subbase and Crushed Rock Layer

Figure 5.8 Geogrid Layer Placed Mid-Depth of Entire Subbase

Figure 5.9 Geogrid and Woven Geotextile Placed Before Base Material

Figure 5.10 Base Material Placed and Compacted

5.6 Preliminary Structural Evaluation and Observations

In order to ensure paving on a structurally stable pavement substructure, there is the need to conduct a preliminary structural evaluation. A simple and efficient method used in most jurisdictions is proof rolling. Proof rolling is performed by eyeballing the extent of deflection of a pavement structure under a tire of a heavy field equipment equivalent to anticipated traffic loading. The rule of thumb is no deflection at all under the tires of the vehicle used. The type of equipment or vehicle used is mostly from the discretion of the engineer and could be a water truck, loader etc. Proof rolling was carried out on the entire road section using a water truck (filled with water).

Deflection was noticed to have occurred on a number of spots on both the shredded tire section and the crushed rock control section. The extent of deflection could be seen to be the same. Since the control section consisting of crushed rock also deflected, the poor structural performance observed was attributed to factors other than the new structure built. The same could be attributed to the shredded tire section since the extent of deflection was found to be the same.

The site was further investigated to determine the cause of the poor structural performance. The constructed section was excavated to the *in situ* subgrade level to study the

nature of the subgrade material a few centimetres from the surface of the subgrade. Upon excavation the top layer of the subgrade was found to have been flooded by water from underground as shown in Figures 5.11 and 5.12. The subgrade was found to be mostly soft clay; hence, much consolidation and loss in bearing capacity had occurred within that short time span which resulted in the deflection of the constructed section. Another contributing factor is the fact that the design selected by the City composed of thin structural support layers especially for the shredded tire section since the shredded tire materials were deemed weak.

Figure 5.11 Re-Excavation of Adolph Way

Figure 5.12 Wet Subgrade – Adolph Way

The soft subgrade was treated by mixing the top 120mm with clean sand (free of fines) in order to reduce the fines content of the subgrade (Figure 5.13).

Figure 5.13 Adolph Way Subgrade Treatment – Adolph Way

Figure 5.14 Adolph Way Surface Paving

The whole section of road was reconstructed using only the design for the control section. The entire section was reconstructed using the design for the control section (50mm AC, 120mm base and 225mm crushed rock subbase). On completion of the road, proof rolling indicated no deflection at all throughout the entire road section. The road section was later paved with COS Type A2 HMAC.

The Adolph Way field experimentation did prove that shredded tire roads can be effectively constructed in Saskatchewan.

5.7 Modeling of Constructed Adolph Way Sections

Structural support behaviour of shredded tire test section and City of Saskatoon crushed rock section constructed at Adolph Way were further evaluated using computational modeling. Primary deflection responses and 3D-strain behaviour of the road structures were quantified using the modeling framework under single axle dual tire loading - primary weight limit (Berthelot et al. 2012). The test sections were modeled on two categories of subgrade conditions:

- Untreated Subgrade (Wet Clay Subgrade – Adolph Way *In situ* Subgrade); and
- Treated Subgrade (Dry Subgrade – Adolph Way Subgrade blended with sand)

Shredded tire mixes of 1Tire:1Sand, 1Tire:2Sand and 1Tire:3Sand were also incorporated in selected City of Saskatoon local road design (the baseline structure) and modeled together with the Adolph sections. Table 5.1 below shows the modeled cross-sections. Pavement structure geometry used for the shredded tire test section and crushed rock sections are shown in Figures 5.13 and 5.14 below.

Following the observations made on the field experimentation at Adolph Way, an improved shredded tire road structure referred to in this research as 100% shredded tire (double base) was designed and evaluated together with the test and control sections. Figure 5.17 shows the structure of the 100% shredded tire (double base) road. The geometry of the 100% shredded tire (double base) road was obtained following the evaluation of modeled results for different shredded tire subbase and RAP base layer thickness combinations that generated a peak surface deflection of one millimeter which is the least acceptable according to the City of Saskatoon urban road standards.

Single axle dual tire loading simulative of City of Saskatoon transit bus loading was used as design load for modeling. Peak surface deflection and strain response behaviors of road models are shown in Figures 5.18 to Figure 5.19.

Table 5.1 Modeled Cross Sections

	Road Name	Subbase (mm)	RAP Base (mm)	AC (mm)
Untreated Subgrade	100% Shredded Tire	225	120	50
	Crushed Rock	225	120	50
Treated Subgrade	100% Shredded Tire	225	120	50
	Crushed Rock	225	120	50
	1Tire:1Sand	225	120	50
	1Tire:2Sand	225	120	50
	1Tire:3Sand	225	120	50
	100% Shredded Tire (Double Base)	225	225	50

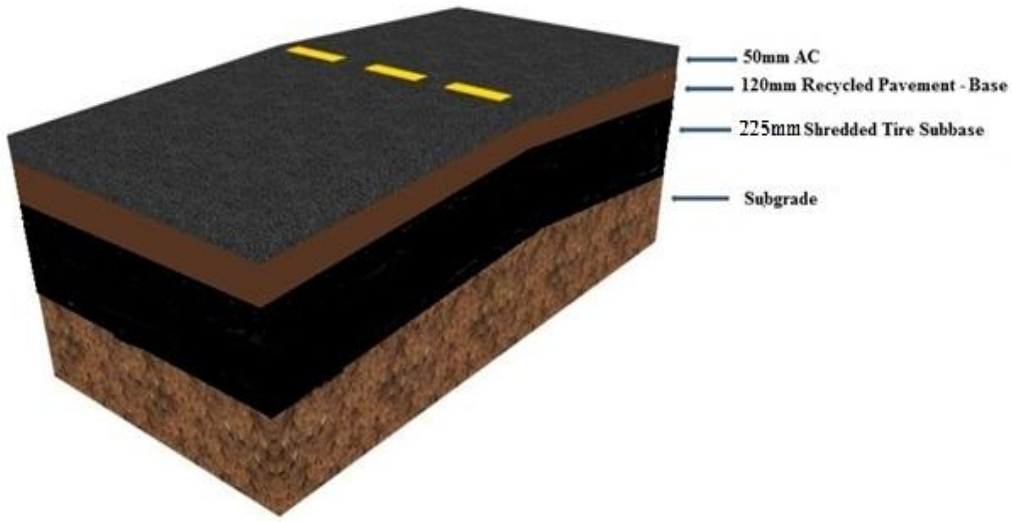

Figure 5.15 Shredded Tire Test Section (Adolph Way)

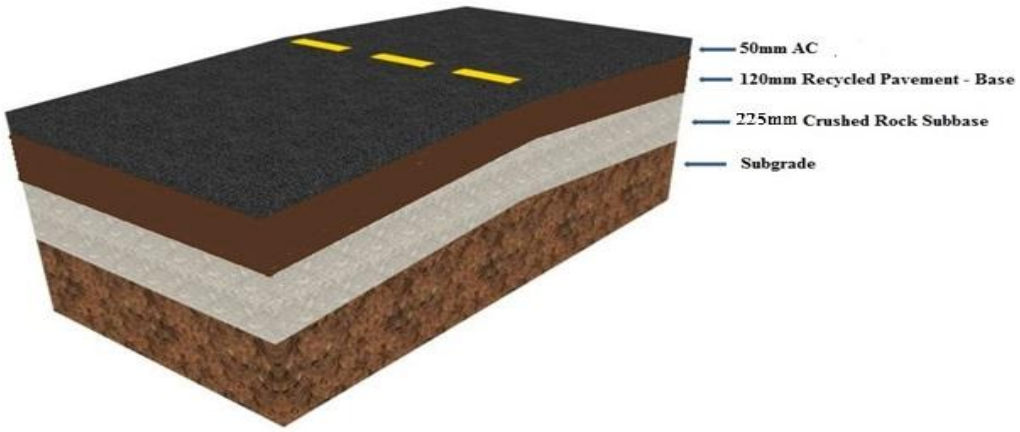

Figure 5.16 Crushed Rock Section (Adolph Way)

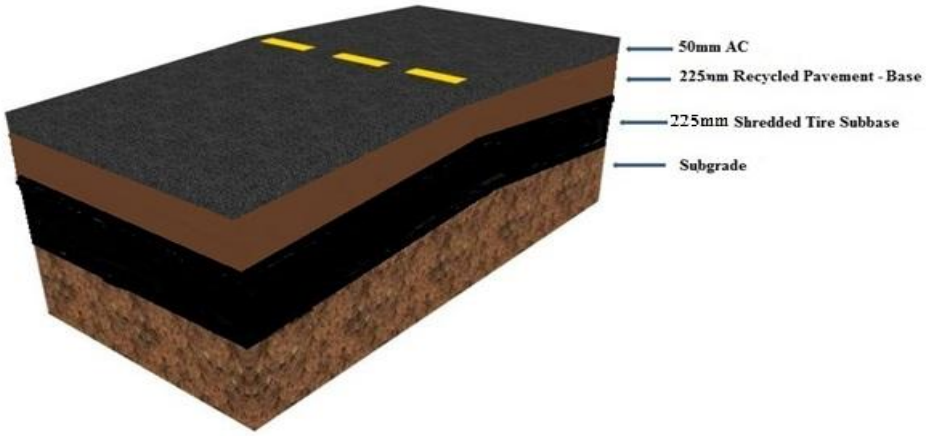

Figure 5.17 100% Shredded Tire (Double Base) Road

5.7.1 Peak Surface Deflection

Modeled peak surface deflection results shown in Table 5.2 and Figure 5.18 were sensitive to subgrade condition. The untreated subgrade condition as experienced at Adolph Way yielded higher deflection values for both 100% shredded tire and crushed rock roads than in the treated (dry condition) subgrade. Deflection in the 100% shredded tire and crushed rock were reduced by 30% and 59%, respectively, in the treated subgrade.

Table 5.2 Model Predicted Peak Surface Deflections (mm) at Primary Weight Limits

	Road Name	Predicted Peak Surface Deflections (mm)
Untreated Subgrade	100% Shredded Tire (Adolph Way)	2.79
	Crushed Rock (Adolph Way)	1.41
Treated Subgrade	100% Shredded Tire	1.64
	Crushed Rock	0.58
	1Tire:1Sand	1.15
	1Tire:2Sand	0.90
	1Tire:3Sand	0.83
	Improved Shredded Tire (D.B)	1.00

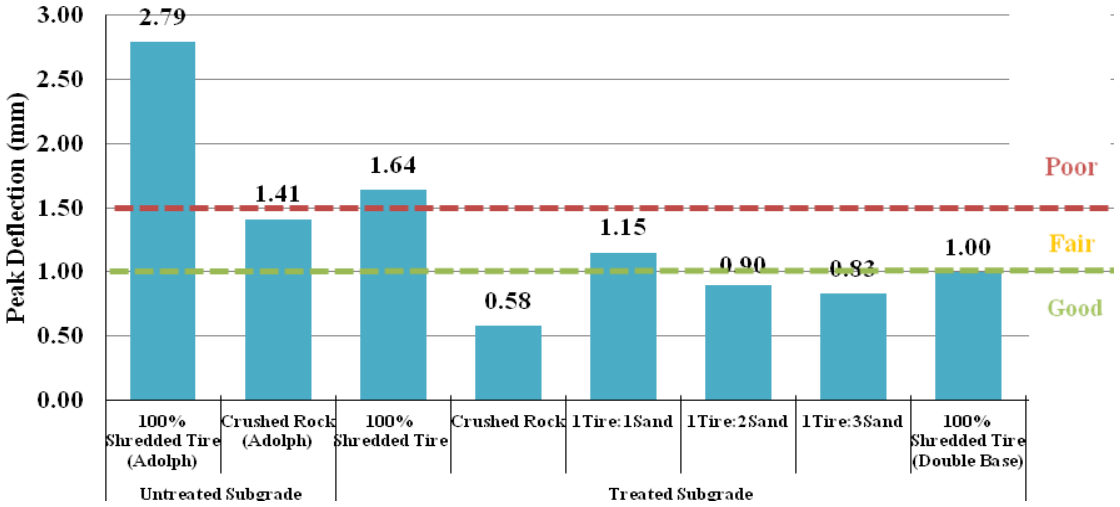

Figure 5.18 Model Predicted Peak Surface Deflection for Field Experimented Results

The 100% shredded tire road structure modeled on the treated subgrade condition showed a peak surface deflection of 1.64mm which falls within the poor deflection threshold. The poor deflection measured is an indication that the shredded tire section constructed at Adolph Way would have still deflected above acceptable standards even if the subgrade were dry and structurally stable. The control structure constructed with crushed rock recorded a deflection of 0.58mm (on the treated subgrade) which falls within the good deflection threshold. Peak surface deflection was found to decrease across the shredded tire/sand mixes as the quantity of sand in the mix increased.

As compared to the 100% shredded tire road constructed on the treated subgrade, peak surface deflection was reduced by 30%, 45% and 49% in 1Tire:1Sand, 1Tire:2Sand and 1Tire:3Sand, respectively.

The 100% shredded tire (double base) road was modeled such that its measured peak surface deflection was 1mm. Since the RAP base layer thickness was doubled (225 mm) to achieve the desired deflection, the structural behavior of the shredded tire road could be considered as sensitive to the base layer thickness.

5.7.2 Horizontal Tensile Strain at Bottom of HMAC

Horizontal tensile strains measured under the HMAC layer were highly sensitive to changes in subgrade condition. Higher magnitudes of tensile strains were measured under the HMAC of roads modeled on the untreated subgrade than on the treated subgrade. The higher tensile strains is an indication that the roads designed on the untreated subgrade would be more prone to undergoing fatigue cracking than those on treated subgrade. Horizontal tensile strains measured are shown in Table 5.3 and Figure 5.19.

Comparing horizontal tensile strains within the treated subgrade category, the highest predicted horizontal tensile strain value of 235με was measured at the bottom HMAC of the 100% shredded tire structure. The crushed rock road recorded a horizontal tensile strain value of 152με which is a 35% decrease in magnitude of strains. Measured horizontal tensile strains were observed to decrease in magnitude as the quantity of sand in the subbase of the shredded tire/sand mix roads increased. The 100% shredded tire (double base) road model recorded the least horizontal strain value of 136με. The thicker base layer of the 100% shredded tire (double base) structure accounts for the lower horizontal tensile strains under the bottom of HMAC layer. The horizontal tensile strain measured was 10.5% lower in the 100% shredded tire (double base) as compared to the crushed rock. The inference drawn from the results is that the 100% shredded tire (double base) road model would be less prone to fatigue failure as compared to all other roads modeled.

Table 5.3 Model Predicted Horizontal Tensile Strain (με) at Primary Weight Limits

	Road Name	Horizontal Tensile Strain (με)
Untreated Subgrade	100% Shredded Tire (Adolph Way)	319
	Crushed Rock (Adolph)	263
Treated Subgrade	100% Shredded Tire	235
	Crushed Rock	152
	1Tire:1Sand	217
	1Tire:2Sand	204
	1Tire:3Sand	181
	100% Shredded Tire (D.B)	136

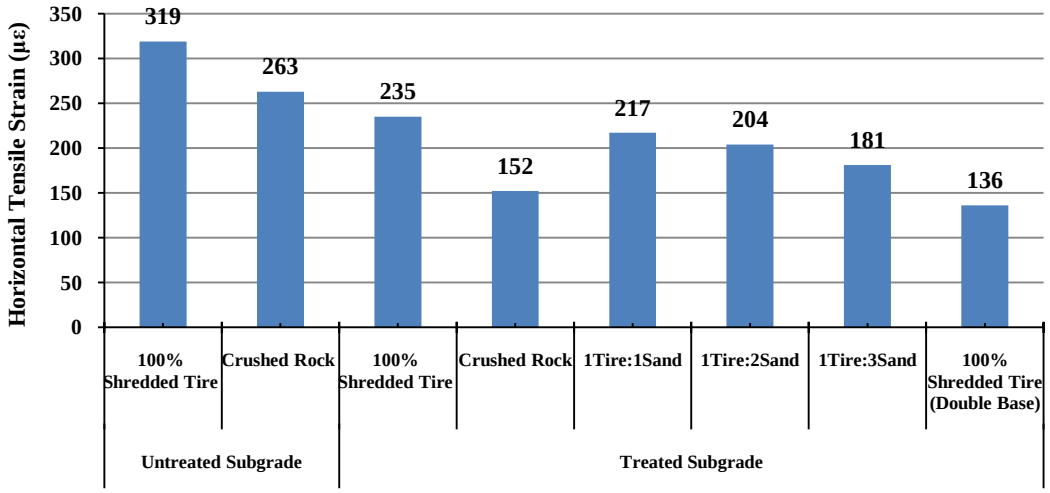

Figure 5.19 Model Predicted Horizontal Tensile Strains at Bottom of HMAC

Horizontal strain profiles for the roads modeled are shown in Figures 5.20 to 5.27. Horizontal strain profiles as shown below indicate higher strains denoted by red spots in the untreated subgrade category than there are in the treated subgrade roads. 100% shredded tire yielded the most high tensile strain spots as compared to all other roads for each category.

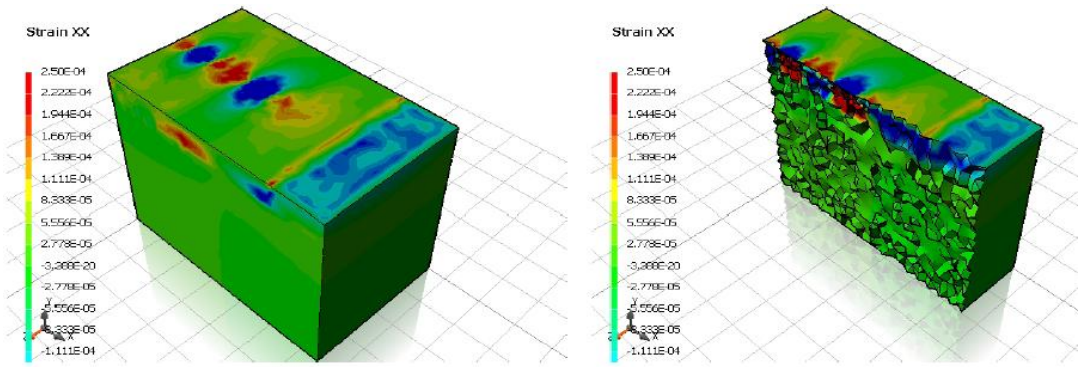

Figure 5.20 Horizontal Strain (Transverse) Profile for 100% Shredded Tire Section - Untreated Subgrade

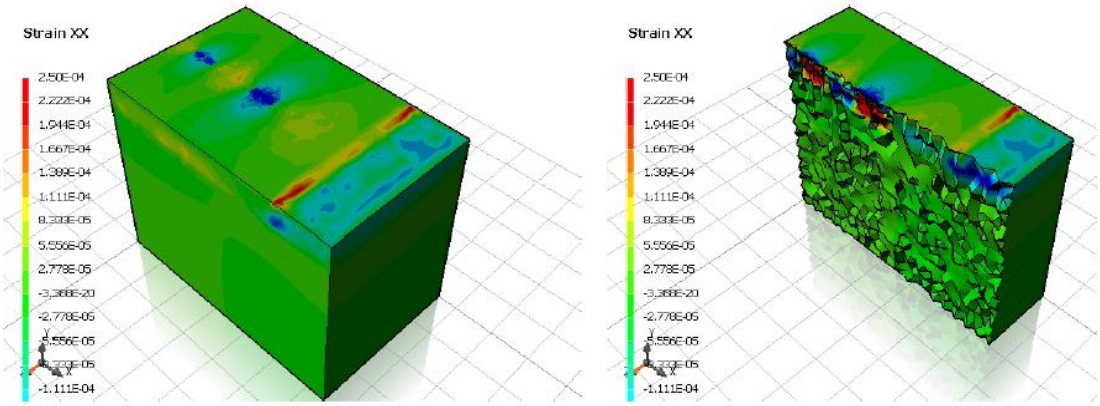

Figure 5.21 Horizontal Strain (Transverse) Profile for Crushed Rock Road - Untreated Subgrade

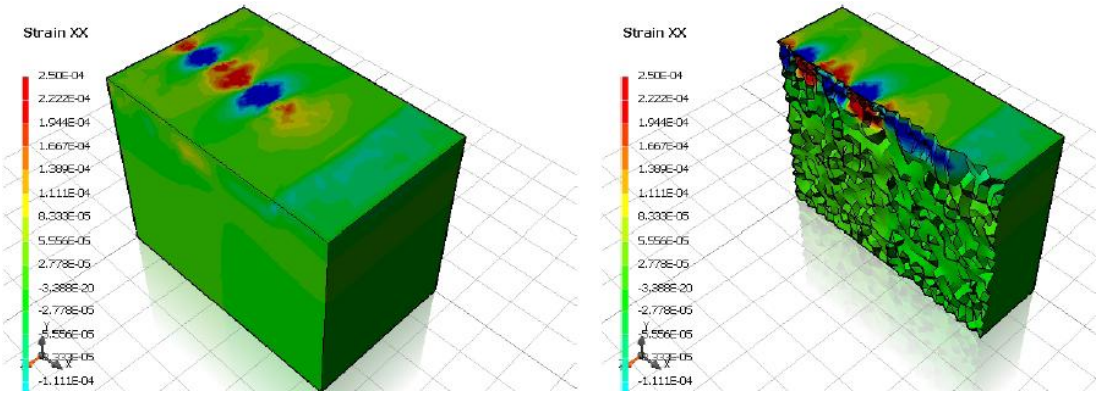

Figure 5.22 Horizontal Strain (Transverse) Profile for 100% Shredded Tire Section - Treated Subgrade

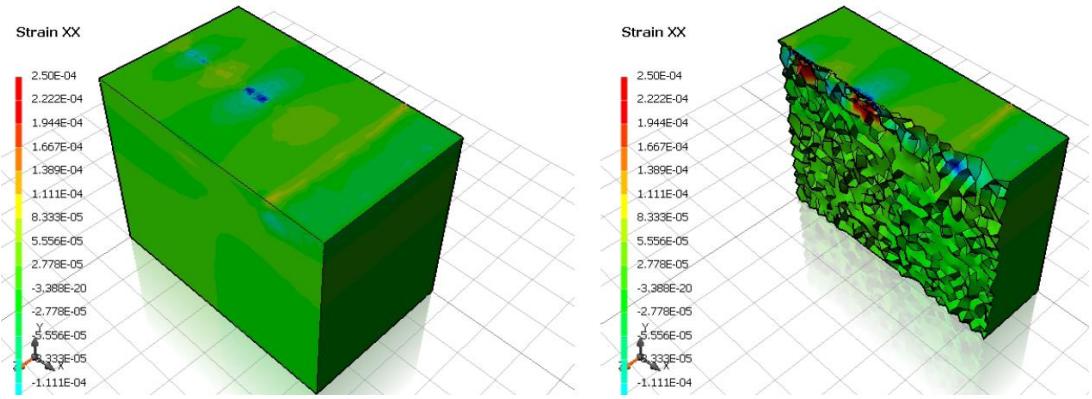

Figure 5.23 Horizontal Strain (Transverse) Profile for Crushed Rock Road - Treated Subgrade

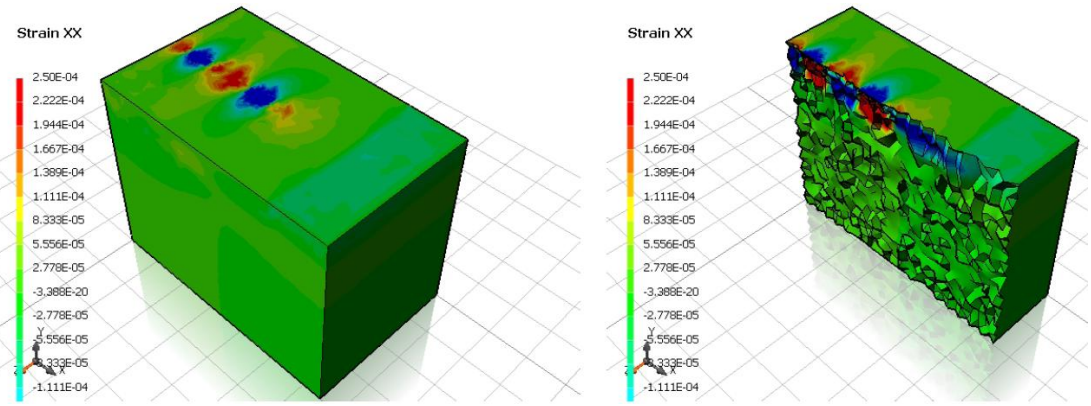

Figure 5.24 Horizontal Strain (Transverse) Profile for ITire:1Sand - Treated Subgrade

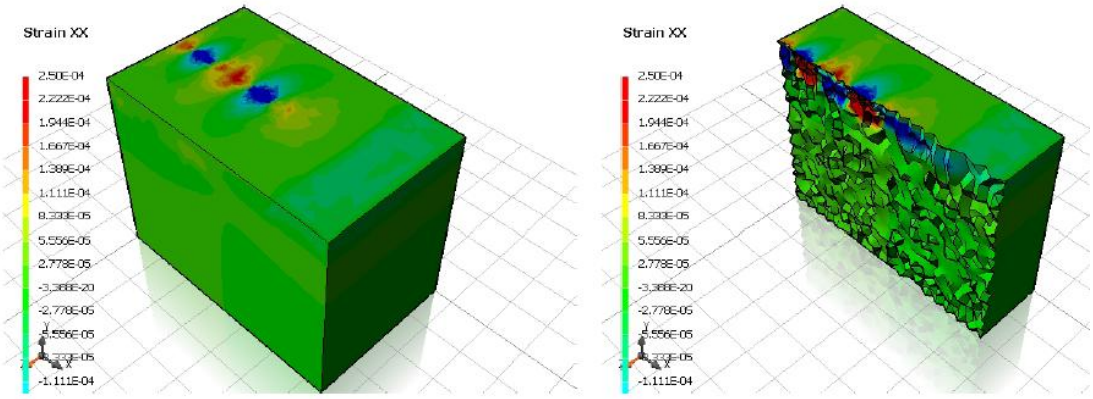

Figure 5.25 Horizontal Strain (Transverse) Profile for 1Tire:2Sand - Treated Subgrade

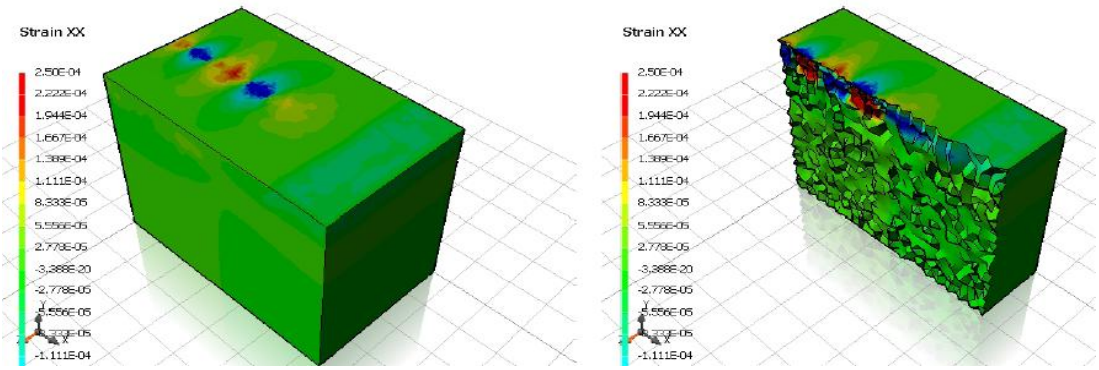

Figure 5.26 Horizontal Strain (Transverse) Profile for 1Tire:3Sand - Treated Subgrade

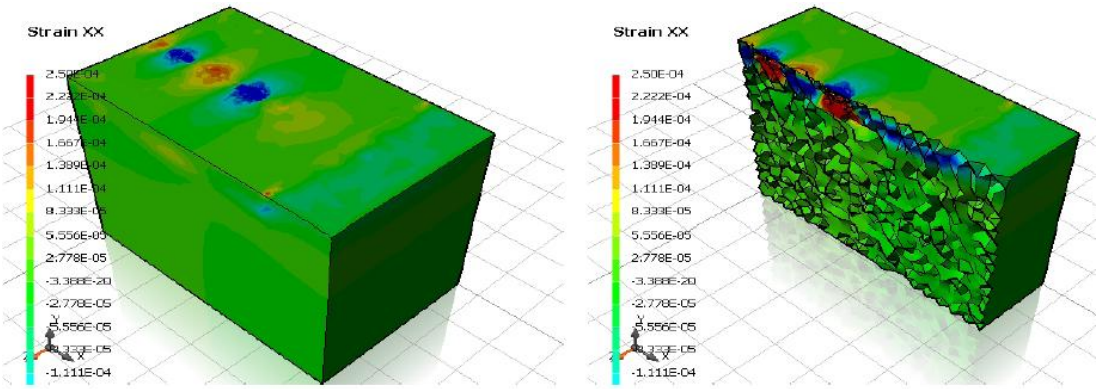

Figure 5.27 Horizontal Strain (Transverse) Profile for 100% Shredded Tire (Double Base) - Treated Subgrade

5.7.3 Vertical Compressive Strain on Top of Subgrade

Vertical compressive strains measured for both crushed rock and 100% shredded tire road models were sensitive to subgrade condition. Higher compressive strains were measured at the top of the subgrade for both crushed rock and 100% shredded tire roads for the untreated subgrade than for the treated subgrade. Up to 116% reduction in vertical compressive strains was achieved in the crushed rock road modeled for the treated subgrade as compared to the same road with a treated subgrade. For the treated subgrade condition, 100% shredded tire recorded the highest compressive stain value of 22075με at the top of subgrade. The compressive strains measured were observed to decrease with an increase in the quantity of sand in the mix. 1Tire:1Sand, 1Tire:2Sand and 1Tire:3Sand reduced the vertical compressive strains by 75%, 150% and 180%, respectively as compared to 100% shredded tire on treated subgrade condition.

Table 5.4 Model Predicted Vertical Compressive Strain on Top of Subgrade at Primary Weight Limits

	Road Name	Vertical Compressive Strain (με)
Untreated Subgrade	100% Shredded Tire (Adolph Way)	31752
	Crushed Rock (Adolph)	12097
Treated Subgrade	100% Shredded Tire	22075
	Crushed Rock	5601
	1Tire:1Sand	12726
	1Tire:2Sand	8829
	1Tire:3Sand	7845
	100% Shredded Tire (D.B)	9896

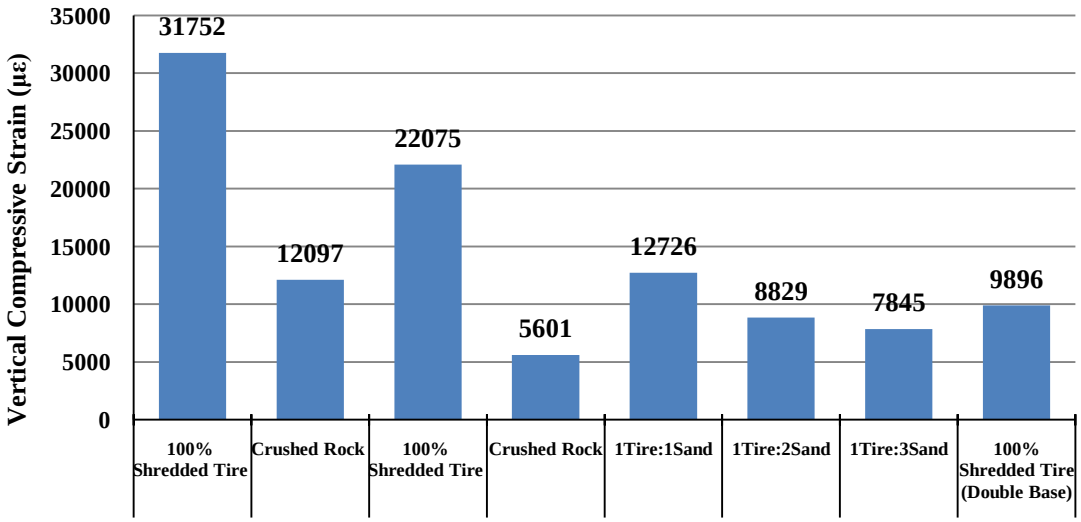

Figure 5.28 Model Predicted Vertical Compressive Strains on Top of Subgrade

The crushed rock road model recorded the least compressive strain value of 5601με. Strain of 12985με was measured on top of the 100% shredded tire (double base) subgrade representing a 123 percent reduction in strain magnitude as compared to 100% shredded tire. Figure 5.29 shows the model predicted vertical compressive strain results for the road sections. The results indicate that the 100% shredded tire section constructed on the untreated subgrade (similar to Adolph Way subgrade) is more prone to undergoing failure due to rutting caused by creep on the top of subgrade.

Vertical strain profiles for road models are shown in Figures 5.29 to 5.36.

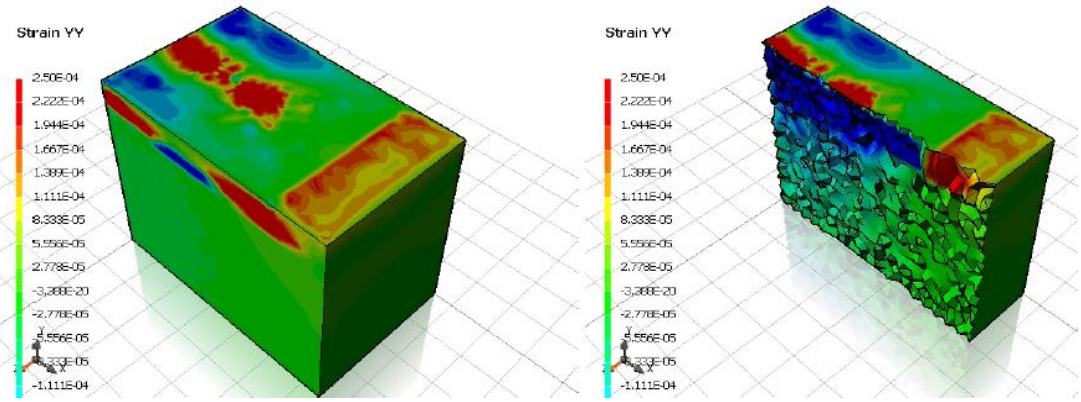

Figure 5.29 Vertical Strain Profile for 100% Shredded Tire – Untreated Subgrade

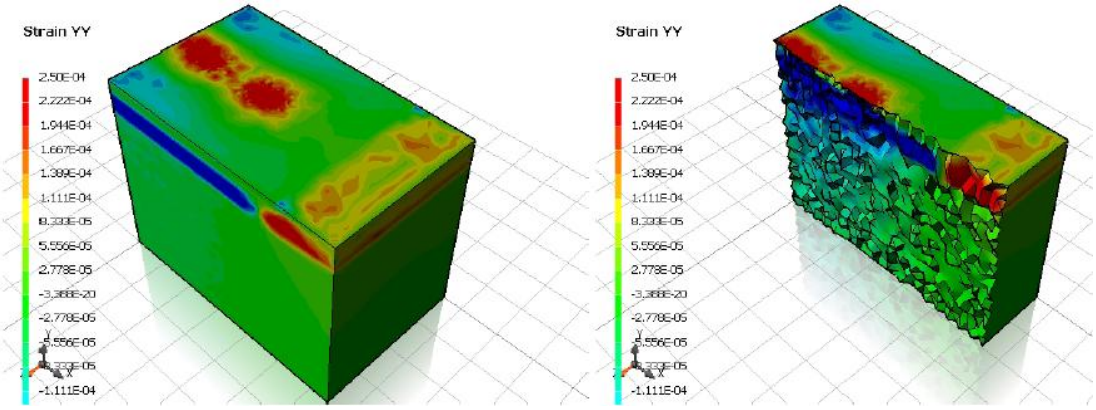

Figure 5.30 Vertical Strain Profile for Crushed Rock Road - Untreated Subgrade

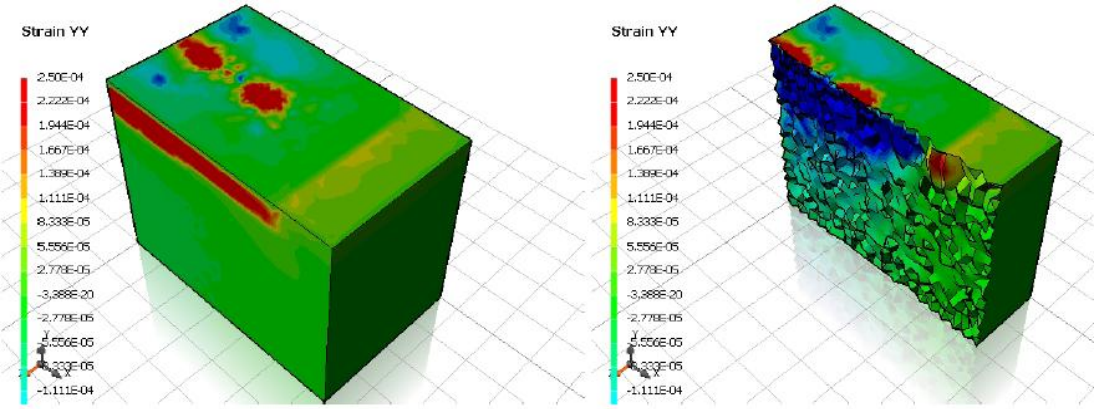

Figure 5.31 Vertical Strain Profile for 100% Shredded Tire Section - Treated Subgrade

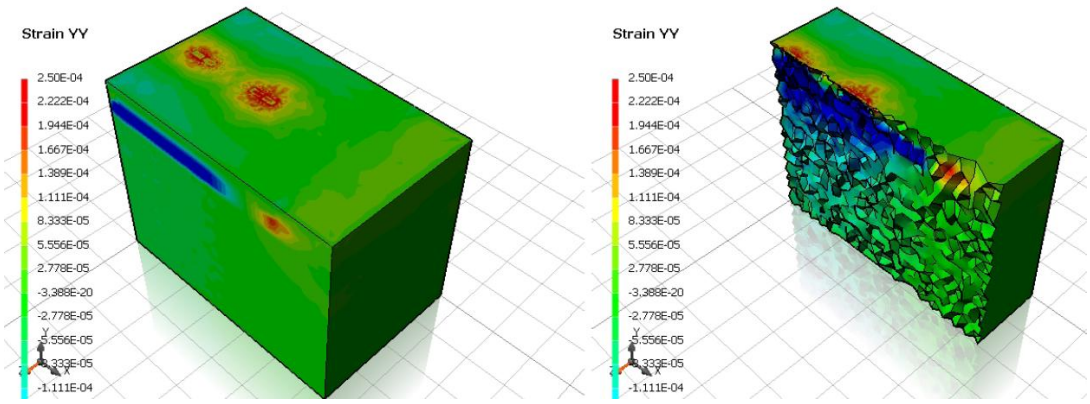

Figure 5.32 Vertical Strain Profile for Crushed Rock - Treated Subgrade

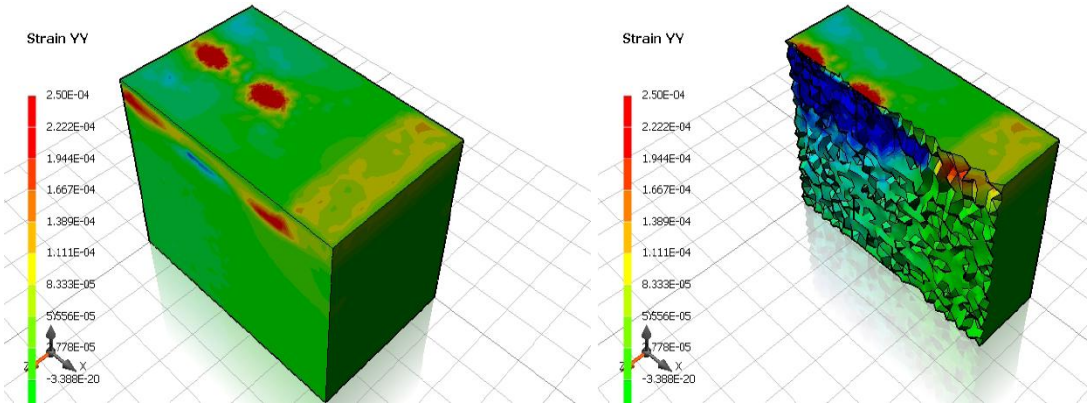

Figure 5.33 Vertical Strain Profile for ITire:1Sand - Treated Subgrade

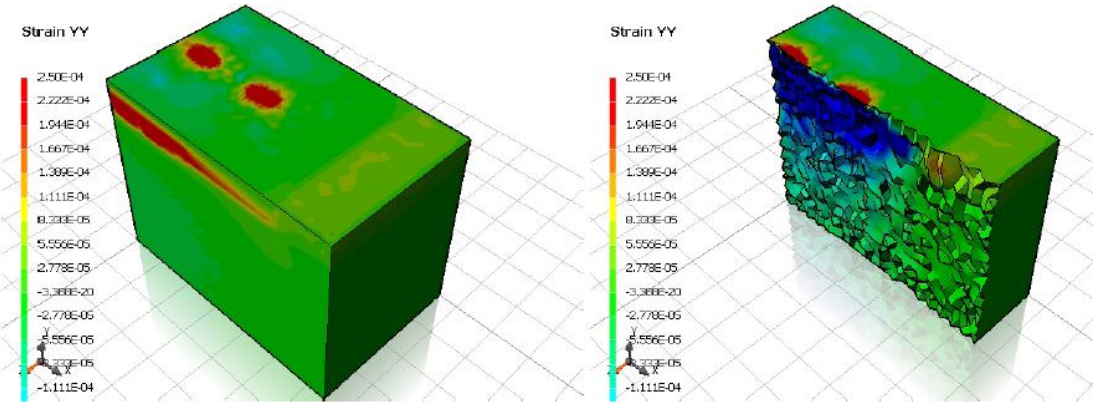

Figure 5.34 Vertical Strain Profile for 1Tire:2Sand - Treated Subgrade

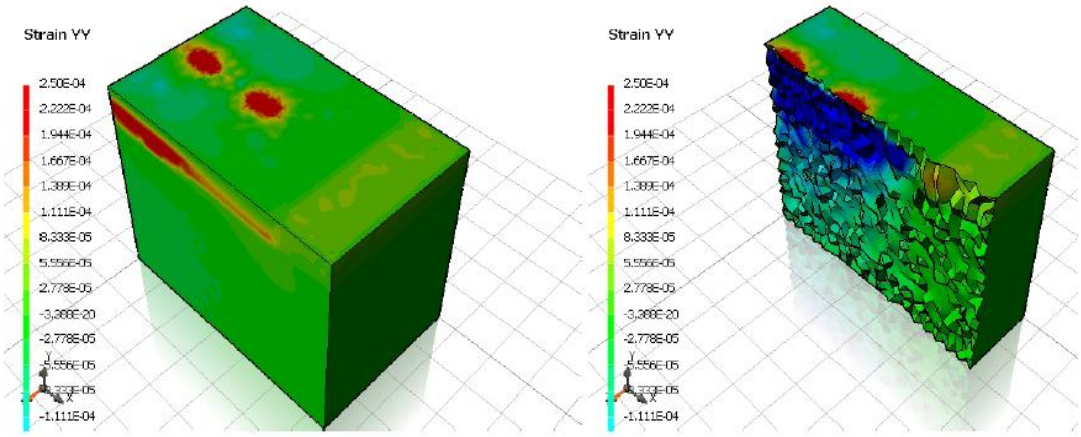

Figure 5.35 Vertical Strain Profile for 1Tire:3Sand Treated Subgrade

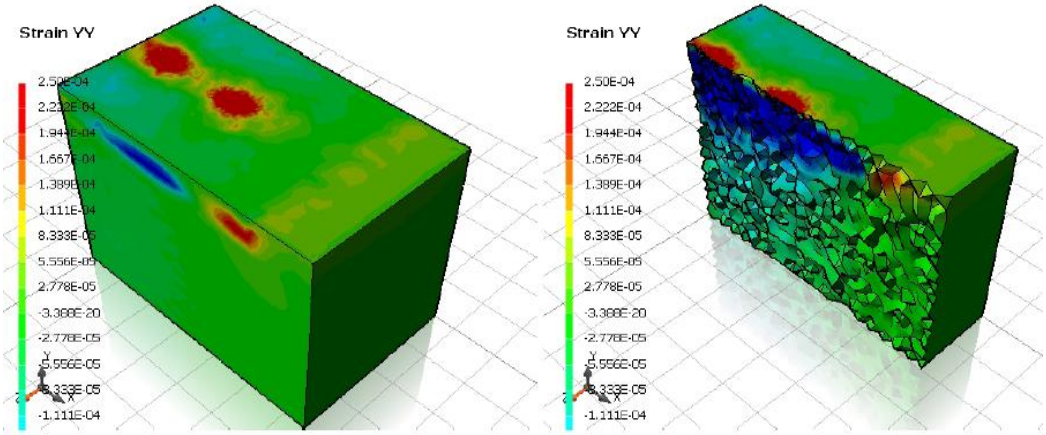

Figure 5.36 Vertical Strain Profile for 100% Shredded Tire (Double Base) - Treated Subgrade

5.7.4 Shear Strain Analysis

Road model predicted shear strain results are shown below in Table 5.5 and Figure 5.37. The 100% shredded tire section constructed at Adolph Way is prone to undergoing failure due to shear in Saskatchewan field state conditions under primary load limits.

Table 5.5 Model Predicted Maximum Shear Strains on All Layers at Primary Weight Limits

Road Name	Maximum Shear Strain by Layer (με)			
	HMAC	Base	Subbase	Subgrade
100% Shredded Tire	703	1171	1848	4172
Crushed Rock	479	754	499	1466
100% Shredded Tire	660	1119	1623	1656
Crushed Rock	473	731	481	911
1Tire:1Sand	606	1006	1330	1654
1Tire:2Sand	538	888	908	1322
1Tire:3Sand	521	846	770	1204
100% Shredded Tire (D.B)	511	766	790	860

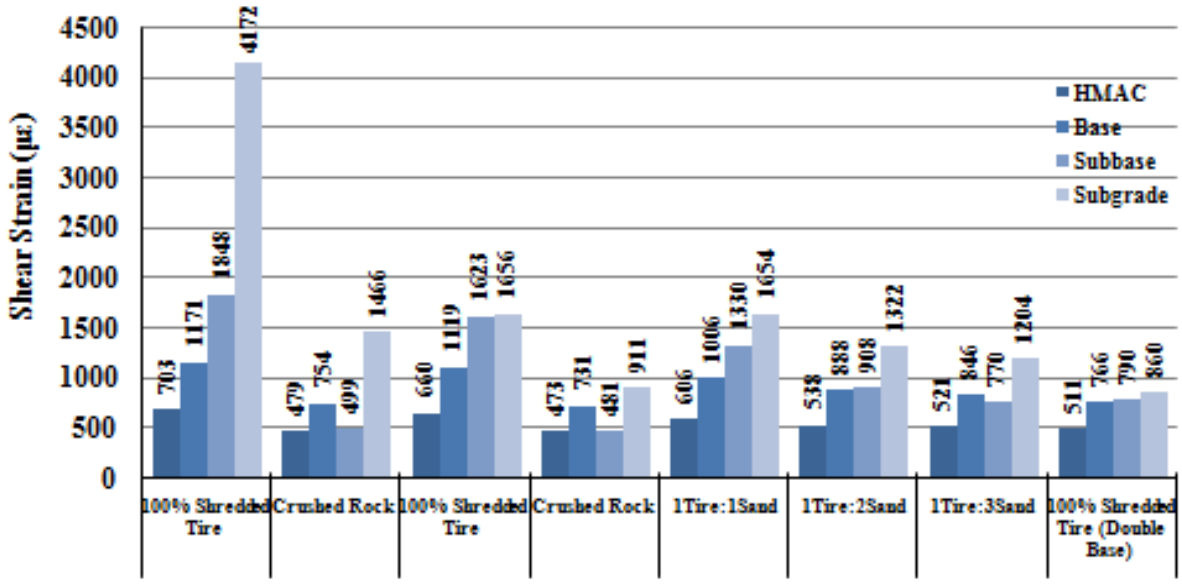

Figure 5.37 Model Predicted Shear Strains on Layers at Primary Weight Limits

The reason for the predicted failure was drawn from the fact that the 100% shredded tire road constructed on the untreated subgrade recorded the highest shear strain values for each respective layer. The lowest magnitude of shear strains were measured in the crushed rock road constructed on treated subgrade. 100% shredded tire (double base) structure recorded lower shear strain values than the shredded tire/sand mix roads. It is therefore important to note the 100% shredded tire (double base) road would be able to better withstand shear failure than the roads constructed with shredded tire/sand mix as subbase. The double base layer thickness for the 100% shredded tire (double base) road would account for the improved structural performance.

5.8 Chapter Summary

Field experimentation of shredded tire was conducted on a Saskatoon residential road section (Adolph Way) to compare the structural performance of a shredded tire section with City of Saskatoon crushed rock section.

Preconstruction visual site inspection revealed numerous fatigue cracks along wheel paths and several other severe road distress features. Most of the distresses were associated with freeze-thaw cycle effects that were facilitated by high groundwater table around site.

Two sections, each of 50m length, were constructed: shredded tire test section constructed with shredded tire as subbase material and a crushed rock section using crushed rock as subbase. Similar design geometry and materials were proposed for both sections. The base layer and overlay were to be constructed with 120mm RAP (existing pavement mixed with base) and 50mm HMAC, respectively.

Structural assessment of substructure was performed using a water truck to determine if the substructure was structurally sound for paving. Deflections higher than acceptable City of Saskatoon structural asset management standards (i.e. 1.0mm) were found to occur on both control and test section. The entire section was excavated and the subgrade was found to be wet.

The subgrade was later treated by mixing the top 100mm with clean sand. The entire section was reconstructed using design for the crushed rock section on the entire road.

Subsequent substructure structural assessment using proof rolling showed no deflection on the entire road section.

PSIPave3D^{TM} was further used to evaluate the behaviour of the shredded tire section and the control crushed rock section. Both untreated and treated subgrade conditions experienced at Adolph Way were modeled. Subgrade condition was found to have a significant effect on the measured peak surface deflections and strain responses. 100% shredded tire and crushed rocks modeled on the treated subgrade deflected less than when modeled on the untreated subgrade. Considering the treated subgrade, the deflection of the 100% shredded tire road was higher than acceptable. Increasing the base layer thickness (twice as thick) of the 100% shredded tire significantly reduced the peak surface deflection and strains measured. The thickness of the base layer of shredded tire road could be deemed to have a significant effect on the structural performance. The peak surface deflection and measured strains were also seen to decrease with increase in the quantity of sand in the subbase of shredded tire/sand roads.

CHAPTER 6 CAPITAL COST ANALYSIS

City of Saskatoon Green Street Infrastructure program has over the years experimented with the use of recycled materials such as asphalt rubble and crushed Portland cement concrete (PCC) in numerous projects within the city. The outcome of these projects has been a tremendous achievement in all aspects of sustainable development namely social, environmental and economic areas (Foth et al 2011). The cost of road projects is of great importance to stockholders in our society. Design and construction of efficient road infrastructure that meets a budget has been the main priority of highway engineers.

Economic analysis in this research was limited to estimated capital cost involved in the construction of the shredded tire/sand mixes and City of Saskatoon local road subbase layers. Life cycle cost analysis is not considered in this research since this is only a preliminary study and the life cycle performance of shredded tire systems has not yet been fully studied in Saskatchewan field state conditions.

Capital cost analysis involves the evaluation of design cross sections modeled in Chapter 4. For the purpose of this research, similar road overlay material as well as base and subgrade materials were assumed for all roads and were therefore factored out of the capital cost analysis to enable direct comparison of cost based on only subbase layer material type.

Unit prices of subbase construction materials are based on prices used by most contractors within Saskatoon as of October 2013. Table 6.1 shows the unit cost of materials used. Based on the unit prices obtained the capital cost of the subbase layer of each road section was estimated. Figure 6.1 shows a detailed design cross section for a typical City of Saskatoon structure assumed as a fixed structure for all roads. Each subbase layer was of 225mm thickness with varying material type. Detailed cross sectional designs of each of the roads considered are identified in Appendix H.

Table 6.1 Unit Price Estimates for Subbase/Drainage Materials

No.	Item	Unit	Unit Price
1	Shredded Tire	m^3	$13.00
2	Sand	m^3	$26.00
3	Type 6 Subbase	m^3	$26.00
4	Crushed Rock	m^3	$62.00
5	Granular Base	m^3	$40.00

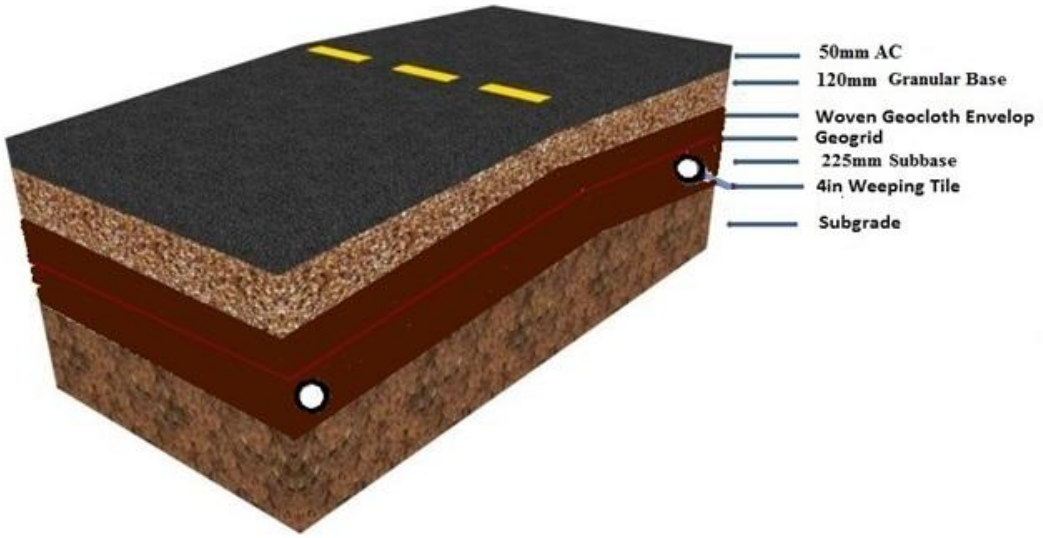

Figure 6.1 Typical City of Saskatoon Local Road Design

Table 6.2 and Figure 6.2 show the initial capital cost of the subbase material for each of the roads modeled. Deductions made from the information provided include the fact that the 100% shredded tire layer was priced as the least expensive at $\$2.93/m^2$ but is not considered a good option since it will fail structurally in the field upon loading. The costs of shredded tire/sand mixes were found to increase with increase in the quantity of sand. For instance, the capital cost for the 1Tire:1Sand layer was $\$4.39/m^2$ and this was seen to increase to $\$4.88/m^2$ and $\$5.12/m^2$ in the 1Tire:2Sand and 1Tire:3Sand, representing 11% and 16% increments in cost, respectively. The increase in the cost could be associated to the increase in quantity of sand, which is more expensive than shredded tire.

Table 6.2 Estimated Capital Cost ($/m^2) of Subbase/Drainage Layers

Road Name	Total Subbase Cost ($/m^2)
100% Shredded Tire	2.93
1Tire: 1Sand	4.39
1Tire: 2Sand	4.88
1Tire: 3Sand	5.12
Sand	5.85
SMHI Type 6 Subbase	5.85
Granular Base	9.00
Crushed Rock	13.95

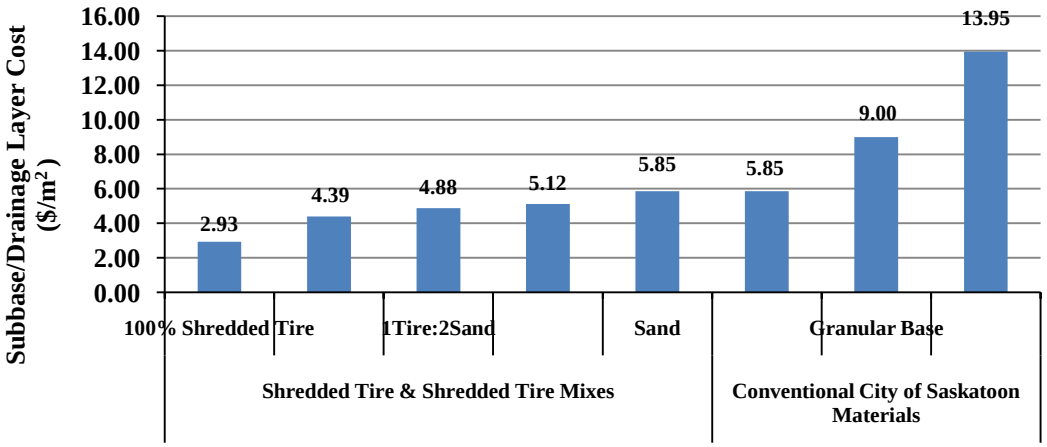

Figure 6.2 Total Capital Cost of Subbase/Drainage Layers

The sand road had an estimated subbase layer cost higher than those of the 100% shredded tire and shredded tire/sand mixes. To illustrate, sand subbase layer was estimated at $5.85/m^2 which is approximately 14.3% higher than the cost of 1Tire:3Sand and 20% higher than that of 1Tire:2Sand subbase layers. Considering the cost and structural support behaviours, 1Tire:2Sand and 1Tire:3Sand will make better cost effective options than the sand road.

All the conventional City of Saskatoon subbase layers considered in this research were found to be more expensive than the shredded tire and shredded tire/sand roads. SMHI Type 6 subbase layer was estimated at a cost of $5.85/m^2, which is 14.3% higher than the cost of 1Tire:3Sand. Granular base layer was also estimated at a cost of $9.00/m^2, representing an approximately 75.8% increase in cost as compared to the 1Tire:3Sand.

The fact the granular base layer is more expensive than the shredded tire/sand mixes and also less permeable than the mixes makes it a less cost efficient option for mitigating frost action. The granular base layer due to its poor drainage (less permeable than sand and comparable to silts) will tend to retain moisture during spring, thereby causing reduced bearing capacity leading to failure.

The crushed rock layer was found to have the highest cost of $\$13.95/m^2$. The high cost of this material is due to cost involved in crushing and also due to the fact that it is a depleting natural resource. The cost of the crushed rock layer is approximately 172.4% higher than the cost of the 1Tire:3Sand layer.

In the case where recycled asphalt pavement is available for use as a base material in low volume residential roads, the 100% shredded tire (double base) road design (50mm HMAC, 225mm RAP base and 225mm 100% shredded tire subbase) determined in Chapter Five could be incorporated. The recycled asphalt layer (at $\$24/m^3$ unit price) will be priced at $\$5.4/m^2$ while the base layer used for each of the roads in this research is at an estimated cost of $\$4.8/m^2$. However, the fact that its subbase layer of 100% shredded tire was estimated at $\$2.93/m^2$ makes the 100% shredded tire (double base) less costly as compared to 1Tire:2Sand, 1Tire:3Sand and all City of Saskatoon roads considered in this research. The cost of excavation for an extra 100mm will not make much of a difference in total cost. The 100% shredded tire (double base) design is therefore a good alternative to consider aside from the 1Tire:2Sand and 1Tire:3Sand roads.

Although this research is limited to only capital cost analysis, it is important to note that other costs such as haulage cost and cost of compaction of the subbase layer materials will affect the total cost of the roadway. The 100% shredded tire road will save money in terms of haulage cost due to its lightweight as compared to the roads constructed with conventional aggregates. Minimal static compaction will also be required for building the shredded tire road as compared to conventional mineral aggregates. Vibratory compaction of shredded tires is highly inefficient in maximizing density of compaction. Extra cost will be incurred in order to compact the crushed rock, SMHI Type 6, sand and granular base layers since vibratory compaction will be required. Considering the haulage cost and cost of compaction, the total cost will be seen to increase with increase in the quantity of sand in the mixes as well.

6.1 Estimated Number of Waste Tires for Road Construction

Table 6.3 below shows the estimated number of waste tires that could be recycled as shredded tire for building the subbase of a 100m two-lane roadway for each of the roads modeled.

Table 6.3 Estimated Number of Waste Tires of Road Sections

Road Name	Number of Tires (Passenger Car Tire Equivalent)
100% Shredded Tire	27,750
1Tire: 1Sand	13,875
1Tire: 2Sand	9,263
1Tire: 3Sand	694
100% Shredded Tire (double base)	27,750

The number of scrap tires required to construct each roadway directly represents the number of waste tires and their accompanying environmental sanitation problems that could be solved by recycling these tires into aggregates. The number of tires required is observed to decrease for roads with a higher amount of sand. 1Tire:2Sand and 1Tire:3Sand roads could claim 9,263 and 694 waste tires for each 100m two lane roadway, respectively – that frees up a lot of landfill space and drastically cuts down associated environmental problems.

6.2 Chapter Summary

Capital cost analysis for the roads proved the shredded tire/sand mix subbase layers to be less costly than all City of Saskatoon subbase layers. Although the 100% shredded tire subbase layer was estimated at the least cost, it was not considered a good option because of its poor structural performance behavior.

Both 1Tire:2Sand and 1Tire:3Sand proved to be the most cost efficient roads considering the fact that they were lesser in cost than the City of Saskatoon subbase layers and also performed efficiently in terms of providing structural support and drainage.

Crushed rock and granular base were more expensive and accounted for minimum extra costs of approximately 172% and 75% relative to the cost of 1Tire:3Sand.

CHAPTER 7 SUMMARY, CONCLUSIONS AND RECOMMENDATIONS

Frost action and substructure moisture are major contributing factors to road structure failure in Saskatchewan. Few research projects have incorporated the use of shredded tires as a road drainage layer material to mitigate frost action. Based on the results of the investigation performed herein, shredded tires have been generally classified as a good thermal insulation and drainage layer material for frost mitigation, but poor in terms of structural performance. With regard to the increase in the number of waste tires on our landfills and growth of the tire recycling industry in Saskatchewan and Canada as a whole, this research aimed at evaluating and improving the structural strength of shredded tire materials used in roads to mitigate frost action.

7.1 Summary and Conclusions

It was hypothesized that the mechanical behavior of shredded tires can be improved by blending with free draining sand. The specific objectives of this research include:

- ***Objective 1: Quantify the mechanical properties of shredded tires and investigate the mechanical behavior of mixes of shredded tires with and without sand blended into the tire matrix as compared to conventional subbase and base coarse materials;***

Based on CBR and confined compressive test results obtained, 100% shredded tire exhibited low mechanical stiffness. Blending shredded tire with sand significantly improved the structural stiffness. Unsoaked CBR test conducted on samples showed 100% shredded tire materials yielded a CBR value as low as 1.33%. The CBR was observed to increase with increase in quantity of sand to 9.6% with 1Tire:3Sand. Confined frequency sweep characterization measured the stiffness of 100% shredded tire at 5MPa. Shredded tire/sand mix of 1Tire:1Sand yielded a stiffness of 30MPa and was observed to increase to 158MPa in 1Tire:3Sand. The stiffness of 1Tire:2Sand and 1Tire:3Sand were higher than conventional SMHI Type 6 subbase which was quantified at a stiffness of 94MPa.

Therefore, it can be concluded that shredded tires when blended with sand can significantly improve the mechanical stiffness behavior to that equal to or greater than conventional high quality subbase.

- ***Objective 2: Determine the permeability of shredded tires and investigate the effect of sand on the permeability of shredded tire/sand mixes as compared to conventional granular base and subbase materials;***

Permeability characterization showed shredded tire as free draining with a high permeability of 1.42cm/s. Increasing the quantity of sand in the mix yielded a significant decrease in the permeability with the mixes as compared to the permeability of 100% shredded tire. For instance 1Tire:1Sand yielded a permeability of 0.0115cm/s while 1Tire:3Sand yielded 0.0026cm/s. All shredded tire/sand mixes had higher permeability than sand. SMHI Type 6 subbase and granular base materials used in the City of Saskatoon yielded permeabilities less than sand and the shredded tire mixes considered in this research. Granular base was considered to provide inefficient drainage at a low permeability of 0.000025cm/s. SMHI Type 6 subbase was considered to have a permeability of 0.0018cm/s. Crushed rock was considered to have permeability comparable to the shredded tires and sand mixes.

Therefore, it can be concluded that shredded tires can provide adequate drainage properties with the addition of up to three parts of sand.

- ***Objective 3: Compare the structural primary response behavior and capital cost of alternate road structures constructed with shredded tires and mixes of shredded tire and sand as a free draining subbase material compared to conventional drainage layers and road structures.***

Structural performance analysis of shredded tire and shredded tire/sand road models were evaluated and compared to those of conventional City of Saskatoon road models. Model predicted results indicated the 100% shredded tire road to be a poor structure with a measured deflection of 2.19mm, which falls within the poor deflection threshold. As the quantity of sand in the subbase mix was increased the resultant peak surface deflection was found to decrease significantly. The peak surface deflection of 1Tire:2Sand and 1Tire:3Sand were both within the acceptable good deflection threshold ($\leq$ 1.0mm). Both 1Tire:2Sand and 1Tire:3Sand road models performed more efficiently than SMHI Type 6 subbase road model which performed fairly at 1.14mm. Crushed rock and granular base roads recorded good peak surface deflection at 0.73mm and 0.89mm, respectively.

Capital cost analysis showed the 100% shredded tire and shredded tire/sand roads to be generally less expensive than all City of Saskatoon road structures considered in this research. Material cost estimation for the subbase layers quantified 100% shredded tire layer as the least expensive of all the subbase at $\$2.93/m^2$ while crushed rock layer was priced at the highest value of $\$13.95/m^2$ considering similar layer thickness of 225mm for all roads. The cost of the roads was seen to increase with increase in the amount of sand. The cost of 1Tire:3Sand was estimated at $5.12/m^2$ which is 172% cheaper than the crushed rock considering the fact that 1Tire:3Sand road will also perform to acceptable City of Saskatoon standards.

Field test sections constructed at Adolph Way validated shredded tire constructability in Saskatchewan. Aside from the 1Tire:2Sand and 1Tire:3Sand roads, modeled results and analysis of simulations also proved the improved 100% shredded tire (double base) structure to be another cost efficient option in terms of structural performance and drainage. Provided the RAP base layer of a 100% shredded tire road is made thicker than the shredded tire subbase layer (twice as thick for a granular base), the structure will be able to perform to acceptable standards as seen in the 100% shredded tire road (double base).

7.2 Future Research and Recommendations

This research focused on characterizing the structural stiffness of shredded tire and shredded tire/sand mixes up to one part tire shreds and three parts sand. Results and findings from this research provided relevant information regarding the structural performance behavior of shredded tire and the effect of mixing with sand.

This research applied the use of modified test procedures and sample size variations to characterize the properties of shredded tire. There is the need to adopt full scale testing of shredded tire materials to fully characterize their physical and mechanistic material properties. Laboratory apparatus and test procedures need to be designed for testing shredded tire materials as well.

There is the need for further field test sections to be constructed and structurally evaluated in order to validate the modeled results and also to ascertain the life cycle performance of shredded tire systems in Saskatchewan field state conditions.

LIST OF REFERENCES

American Automobile Association (AAA). 2009 http://aaa.com. Accessed: [August 4, 2011]

Alberta Recycling Management Authority. 2009. Tire Recycling Program. http://www.albertarecycling.ca/RecyclingMain.aspx?id=84&ekmensel=a681a8bf_8_24_btnlink Accessed: [September 12, 2011]

Andersland, O.B. and Ladanyi, B. 1994. Frozen Ground Engineering. Chapman & Hall Inc. New York.

Anne and Russ Evans. 2006 The Composition of a Tyre: Typical Components Project Code, The Waste & Resources Action Programme, 2006

American Association of State Highway and Transportation Officials (AASHTO). 2002. Guide for Mechanistic-Empirical Design of New and Rehabilitated Structures. Washington, D.C.

ASTM D422, 2. 2006, Standard Test Method for Particle-Size Analysis of Soils, Annual Book of ASTM Standards, American Society for Testing and Materials. West Conshohocken, PA: ASTM International.

ASTM D698, 2. 2006, Laboratory Compaction Characteristics of Soil using Standard Effort, Annual Book of ASTM Standards, American Society for Testing and Materials. West Conshohocken, PA: ASTM International.

ASTM D1883, 2. 2007, Standard Test Method for CBR (California Bearing Ratio) of Laboratory Compacted Soils, Annual Book of ASTM Standards, American Society for Testing. West Conshohocken, PA: ASTM International.

Atterberg, A. 1911. On the Investigation of the Physical Properties of Soils and on the Plasticity of Clays. Int. Mitt. Fur Bodenkunde, I, pp. 10-43.

Baker, T.E., Alen, T.M. and Pierce, L.M. 2003. Evaluation of the Use of Scrap Tires in Transportation Related Applications in the State of Washington. Washington State Department.

Berthelot, C. 1999. Mechanistic Modeling of Saskatchewan Specific Pavement Studies-9A Asphalt Concrete Pavements. Ph.D. Thesis, Department of Civil Engineering, Texas A&M University, College Station, Texas.

Berthelot, C., and Widger, A. 2004. Mechanistic Investigation of Granular Base and Subbase Materials: A Saskatchewan Case Study. In Proceedings of the Annual Meeting of the Transportation Association of Canada, Quebec City, Quebec, 19–22 September 2004. Transportation Association of Canada, Ottawa, Canada.

Berthelot, C., Crockford, B., White, S., and Sparks, G. 1997. Mechanistic Quality Control/Quality Assurance Evaluation of Saskatchewan Specific Pavement Studies-9A Asphalt Mixes. In Proceedings of 42nd Annual Conference of Canadian Technical Asphalt Association, Ottawa, Ontario, 16–19 November 1997. Canadian Technical Asphalt Association, Victoria, B.C.

Berthelot, C., Gerbrandt, R., and Baker, D. 2000. Full Depth Cold In-place Recycling Stabilization for Low Volume Road Strengthening: A Case Study On HWY 19-06, 2000 Annual Conference of the Transportation Association of Canada, Edmonton, Alberta.

Berthelot, C., Podborochynski, D., Marjerison, B., and Gerbrandt, R. 2009. Saskatchewan Field Case Study of Triaxial Frequency Sweep Characterization to Predict Failure of a Granular Base across Increasing Fines Content and Traffic Speed Applications. American Society of Civil Engineering, Journal of Transportation Engineering. Reston, USA. Vol. 135, No.11. p.p. 907-914.

Berthelot, C., Soares, R., Haichert, R., Podborochynski, D. 2012. Quantifying the Impact of Truck Axle Groups on Rural and Urban Pavement Structure Performance. Pavement Performance Case Studies Session of the 2012 Annual Conference of the Transportation Association of Canada New Brunswick.

Berthelot, C., Soares, R., Haichert, R., Podborochynski, D., Prang, C., Guenther, D. 2011. City of Saskatoon Mechanistic Pavement Structure Modeling. Annual Conference of the Transportation Association of Canada Poster 2011.

Berthelot, C., Soares, R., Haichert, R., Podborochynski, D., Guenther, D., Kelln, R. 2012. Modeling the Structural Response of Urban Sub-Surface Drainage Systems. Presented at the Transportation Research Board 91st Annual Meeting. Washington, D.C.

Beskow, G. 1935. Soil Freezing and Frost Heaving with Special Application To Roads and Railroads. The Swedish Geological Society, C, no. 375, Year Book no.3 (Translated by J.O. Osterberg). Technological Instittute, Northwestern University.

Boyd, D. W. 1973. Normal freezing and thawing degree-days for Canada. Environment Canada, Atmos. Environ., Rep. CL 14-73.

Canadian Automobile Association (CAA) Registration Statistics. 2009. http://caa.ca/automotive Accessed: [August 13, 2011].

Chamberlain, E.J. 1981. Frost Susceptibility. Review of Index Tests.US Cold Regions Research and Engineering Laboratory Monograph 81-2, CRREL, Hanover, N.H.

Doré, G., and Zubeck, H. 2008. Cold Regions Pavement Engineering, McGraw-HilMcGraw-Hill.

Doré, Guy; Zubeck, H.K. 2009. **Cold** Regions Pavement Engineering. McGraw-Hill.

Dresher, A., Newcomb, D., and Bouhaja, M. 1992. Development of Design Guideline For Use of Shredded Tires as a Lightweight Fill in Road Subgrade and Retaining Walls. Department of Civil and Mineral Engineering, University of Minnesota., August 1992.

Penner, E. 1959. The Mechanism of Frost Heaving in Soils. Highway Research. Board . Bulletin Number. 225.

Everett, D.H. 1961. The Thermodynamics of Frost Action - Porous Solids. Trans. Faraday Soc., Vol. 58, p. 1541-1551.

Everett, D.H. and Haynes, J.M. 1965. Capillary Properties of some Model Pore Systems with Reference to Frost Damage. RILEM Bull. N.S. 27,p. 31-38.

G. Beskow. 1991. The Swedish Geological Society, C, No. 375, Year Book no. 3. Technological Institute, Northwestern University, 1935. Reprinted in Historical Perspectives in Frost Heave Research (P. B. Black and M. J. Hardenberg, eds.) CRREL Special Report No.91-23, pp 37–157, 1991.

Guthrie WS, Hermansson A. 2003. Frost Heave and Water Uptake Relations in Variably Saturated Aggregate Base Materials. Transportation Research Record: Journal of the Transportation Research Board 1821: 13–19.

Hallet, B. & Waddington, E.C. 1992. Buoyancy Forces Induced by Freeze-Thaw in the Active Layer: Implications for Diapirism and Soil Circulation. Periglacial Geomorphology, Wiley, Chichester, 251–279.

Head, K.H. 1982. Manual of Soil Laboratory Testing. Vol.2, Pentech Press Ltd., London.

Michael, H. 1992. Design and Construction of Asphalt Paving Materials with Crumb Rubber. Transportation Research Record No. 1339, Transportation Research Board, Washington, DC, 1992.

Hilf, J.W. 1975. Compacted Fill. In Foundation Engineering Handbook, Winterkorn, H.F.and Fang, H.Y. Eds, Van Nostrand Reinhold Company, New York, NY. 1975.

Hoppe, E. J. 1996. The Influence of Fines on Strength and Drainage Characteristics of Aggregate Bases. Virginia Transportation Research Council, Charlottesville, VA, 33 pp.

Horiguchi, K. 1987. Effect of Cooling Rate on Freezing of Saturated Soil. Cold Reg.Sci. Technol., Vol. 14, pp. 147-153.

Hu, X., Hu, S., and Walubita, L.F. 2008. Investigation of Fatigue Cracking :Bottoms – Up or Top-Down. Texas Transportation Institute, Texas A&M University, College Station, Texas, USA.

Humphrey, D.N. 2006. Civil Engineering Applications of Tire Derived Aggregate. Course Notes, Prepared for California Integrated Waste Management Board.

Humphrey, D.N., and Katz, L.E. 2000. Five-year Field Study of the Effect of Tire Shreds Placed above the Water Table on Groundwater Quality. Preprint No. 00-0892. Transportation Research Board, Washington, D.C.

Humhprey, D.N., Katz, L.E. and Blumenthal, M. 1997. Water Quality Effects of Tire Chip Fill Above the Groundwater Table. Testing Soil Mixed with Waste or Recycled Materials. ASTM STP 1275, ASTM Philadelphia, Pa.,1997, pp. 299-313.

Humphrey, Dana N. and Robert A. E. 1993. Tire Chips as Subgrade Insulation - Field Trial. Proceedings of the Symposium on Recovery and Effective Reuse of Discarded Materials and By-Products for Construction of Highway Facilities, Federal Highway Administration, Denver, Colorado, October, 1993.

Kessler, M.A., Murray, A.B., Werner, B.T. & Hallet, B. 2001. A Model for Sorted Circles as Self-Organized Patterns. Journal of Geophysical Research, 106, 13287–13306.

Keystone Retaining Wall Systems, 2003, Silt/Clay Soils - Atterberg Limits 2003.

Knutson, A. 1993. Frost Action in Soils. Norwegian Road Research Laboratory, Oslo, 40 pp.

J. G. Dash. 1989. Thermomolecular Pressure in Surface Melting: A Motivation for Frost Heave.Science, 246:1591, 1989.

Jahren, C. T. 2001. Best Practices for Maintaining and Upgrading Aggregate Roads in Australia and New Zealand. Minnesota Department of Transportation, St. Paul, MN, 75 pp.

Janoo, V. C., Eaton, R., and Barna, L. 1997. Evaluation of Airport Subsurface Materials. U.S. Army Cold Regions Research and Engineering Laboratory, Hanover, NH, 32 pp.

Johnson, T.C. 1974. Is Graded Aggregate Bases the Solution in Frost Areas? USA Cold Regions Research and Engineering Laboratory.

Konrad, J.M. 1994. Frost Heave in Soils. Concept and Engineering. Sixteenth Canadian Geotechnical Colloquium. Canadian Geotechnical Journal, **31**: 233–245.

Konrad, J.-M., Dore, G., and Roy, M. 1996. Field Observations of Instrumented Highway Sections with Different Frost Protections. Proceedings of the Eighth International Conference on Cold Regions Engineering, Fairbanks, Alaska, p. 652-663.

Krantz, W.B. 1990. Self-Organization Manifest as Patterned Ground in Recurrently Frozen Soils. Earth-Science Reviews 29, 117–130.

Lawrence, B., Humphrey, D., and Chen, L.H. 1999. Field Trial of Tire Shreds as Insulation for Paved Roads. Proceedings of Tenth International Conference on Cold Regions Engineering: Putting Research into Practice, J.E. Zufelt, ed., ASCE, pp. 428-439

Loch, J., and Kay, B. D. 1978. Water Redistribution in Partially Frozen, Saturated Silt Under Several Temperature Gradients and Overburden Loads. Soil Sci. Soc. Amer. Proc,Vol. 42, pp. 400-406.

Marachi, N.D., Chang C.K., and Saed, H.B. 1972. Evaluation of properties of rock fill materials. Journal of the Soil Mechanics and Foundation Division, ASCE, 98:95-114.

Martin, R.T. 1959. Rhythmic Ice Banding in Soil. Highway Res. Board Bull. 218, NASINRC, Washington, p. 11-23.

Miller, R. D. 1977. Lens Initiation in Secondary Heaving, Int. Symp. on Frost Action in Soils, Lulea University of Technology, Sweden, Vol. 2. pp. 68-74.

Muench, S. 2004. Washington DOT Pavement Online Guide. Accessed on July 20011.

Nix, F.P., Boucher, M. and Hutchinson, B. 1992: Road Costs; in Directions: The Final Report of the Royal Commission on National Passenger Transportation, v. 4, p. 1014.

Nordal, R.S. 1973. Frost Heave and Bearing Capacity during Spring Thaw at the Vormsund Test Road. Proc. Symp. Frost Action Roads, Oslo,p. 159-163.

Ontario Tire Stewardship. 2009. Tire Recycling in Ontario. https://www.ontariots.ca/?q=TireRecOntario Accessed: [April 12, 2011]

Pehlken , A., Essadiqi, E. 2005. Scrap Tire Recycling in Canada, .CANMET Materials Technology Laboratory. MTL 2005-08(CF), August 2005.

Penner, E. 1957. Soil Moisture Tension and Ice Segregation. Highway Res. Board Bull. 168, NASINRC, Washington, p. 50-64.

Penner, E. 1959. The Mechanism of Frost Heaving in Soils. Highway Research Board., Bulletin No. 225., P 1-22.

Penner, E. 1959. Pressures Developed in a Porous Granular System as a Result of Ice Segregation. Highway Res. Board, SR40,p. 191-199.

Penner, E. 1968. Pressures Developed During the Unidirectional Freezing of Water-Saturated Porous Materials. International Conf. on Low Temperature Science, Sapporo, Japan. Vol. 1, Part 2, p. 1401-1412.

Penner, E. 1976. Grain Size as a Basis for Frost –Susceptibility Criteria. Proc. Second Conf. Soil-Water Problems in Cold Regions, Edmonton, Alta., p. 103-109.

Penner E. Ueda T. 1977. The Dependence of Frost Heaving on Load Applications. In Proceedings of the Symposium on Frost Action in Soils. Balkema: University of Lulea, Lulea, Sweden; 92–101.

Prang, C., and Berthelot, C. 2009. Performance Valuation Model for Urban Pavements. Transportation Research Board of the National Academies Annual Meeting, Jan 10-15, 2009.

Rempel, A.W., Wettlaufer, J. S., and Worster, M. G. 2004. Premelting dynamics in a continuum model of frost heave. J. Fluid Mech., 498:227–244.

Reschner, k. 2008. Scrap Tire Recycling. A Summary of Prevalent Disposal and Recycling Methods. Langobardenallee 6. Berlin, Germany. July, 2008.

Rubber Manufacturers Association 2011. U.S. Scrap Tire Management Summary 2005-2009. Washington, DC., October 2011.

Saskatchewan Ministry of Highways and Infrastructure (SMHI). 2009. Surfacing Manual. SMHI Internal Document, Saskatchewan.

Schnormeier, Russell. 1995. Recycled Tire Rubber in Asphalt. Presented at the 71st Annual Meeting of the Transportation Research Board, Washington, DC, 1992.

Scrap Tire Management Council. 1995. Scrap Tire Use/Disposal Study 199 Update, Washington, DC, February, 1995.

Sheng D, Axelsson K, and Knuttson S. 1995. Frost Heave due to Ice Lens Formation in Freezing Soils. 1. Theory and Verification. Nordic Hydrology 26: 125–146.

Soares, R., Haichert, R., Podborochynski, D., and Berthelot, C., 2012. Modeling the In Situ Performance of Cement Stabilized Granular Base Layers of Urban Roads. Transportation Research Board 2012.

Soares, R., Haichert, R., Podborochynski, Guenther, D., Berthelot, C. 2012. Modeling the In situ Performance of Granular Materials Stabilized with Cement. Characterization of Granular and Stabilized Materials of the 2012 Annual Conference of the Transportation Association of Canada New Brunswick.

Solid & Hazardous Waste Education Centre, (SHWEC) 2012. Material Manufacturing and Recycling: Tires. Waste Education Series – University of Wesconsin.

SSTC. 2009. Saskatchewan's Used Tire Recycling Program ww.scraptire.sk.ca/index.php?option=com_content&task=view&id=14&Itemid=31. [April 12, 2011]

Spencer, R. 1991. New Approaches to Recycling Tires. Biocycle**,** March 1991.

Sridharan, A., and Gurtug, Y. 2005. Compressibility Characteristics of Soils. Geotechnical and Geological Engineering..Springer (2005). 23**:** 615-634.

Terier Shredders – Leader in Machinery for the Waste Recycling – 2011. https://www.terier.cz/en/ Accessed: [April 12, 2011].

Theyse, H.L., 2002. Stiffness, Strength, and Performance of Unbound Aggregate Material: Application of South African HVS and Laboratory Results to California Flexible Pavements. University of California Pavement Research Center.

Van Deusen, D. 1998. Improved Spring Load Restriction Using Mechanical Analysis, Cold Regions Impact of Civil Works, Ninth International Conference on Cold Regions Engineering, pp 188 – 199.

Waalkes, S.M. 2003. Cold Weather & Concrete Pavements: Troubleshooting & Tips to Assure a Long-Life Pavement. Long-Life Pavements – Contributing to Canada's Infrastructure (A). Session of the 2003 Annual Conference of the Transportation Association of Canada St. John's, Newfoundland and Labrador.

White, T.D. and Coree, B.J. 1990. Threshold Pavement Thickness to Survive Spring Thaw. Proceedings of the Third International Conference on Bearing Capacity of Roads and Airfields, Throndeim, Norway, pp.41-51.

Xu, J. 2008. Mechanistiv Evaluation of Granular Base Stabilization Systems in Saskatchewan. MSc. Thesis, Department of Civil Engineering, University of Saskatchewan, Saskatoon, Saskatchewan.

Yang, S., Lohnes, R.A., Kjartanson, B.H. 2002. Mechanical Properties of Shredded Tires, Geotechnical Testing Journal, Vol. 25, No. 1, March 2002, pp. 44-52

APPENDIX A

RESEARCH WORK PLAN

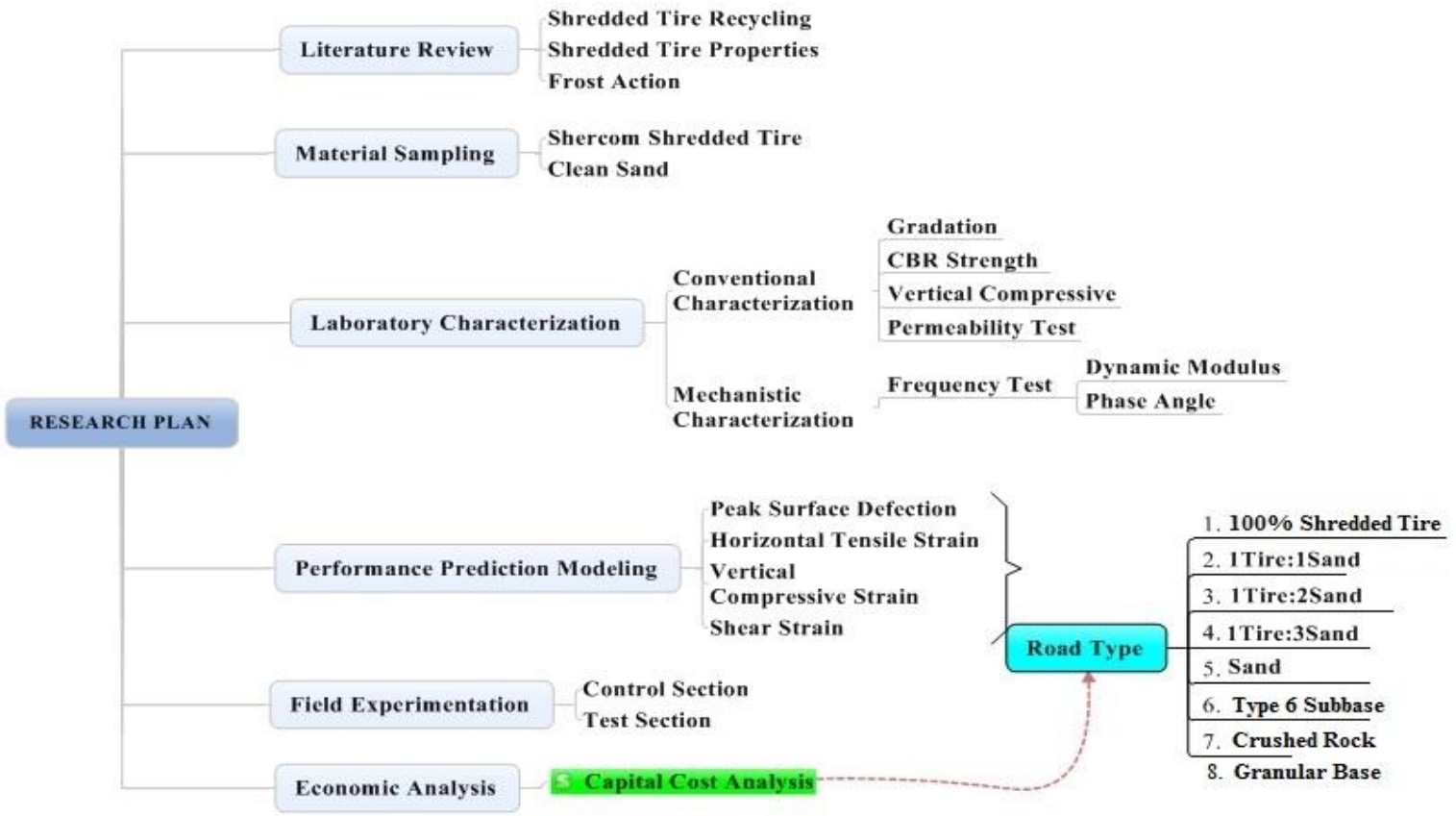

Figure A1 Research Work Plan

APPENDIX B

GRADATION TEST RESULTS

Table B1. Gradation for 100% Shredded Tire

Sieve Opening (mm)	Soil Retained (g)	% retained	Cumulative % retained	Cumulative % passing
31.5	0	0	0	100
25	19	1	1	99
20	57	3	4	96
18	779	41	45	55
16	703	37	82	18
12.5	228	12	94	6
9	76	4	98	2
5	38	2	100	0
2	0	0	100	0
0.9	0	0	100	0
0.4	0	0	100	0
0.16	0	0	100	0
0.071	0	0	100	0
Pan	0	0	100	0

Table B2. Gradation for 1Tire:1Sand Mix

Sieve Opening (mm)	Soil Retained (g)	% retained	Cumulative % retained	Cumulative % passing
31.5	0	0	0	100
25	19	1	1	99
20	57	3	4	96
18	323	17	21	79
16	209	11	32	68
12.5	171	9	41	59
9	38	2	43	57
5	19	1	44	56
2	152	8	52	48
0.9	304	16	68	32
0.4	551	29	97	3
0.16	38	2	99	1
0.071	19	1	100	0
Pan	0	0	100	0

Table B3. Gradation for 1Tire:2Sand Mix

Sieve Opening (mm)	Soil Retained (g)	% retained	Cumulative % retained	Cumulative % passing
31.5	0	0	0	100
25	19	1	1	99
20	57	3	4	96
18	114	6	10	90
16	133	7	17	83
12.5	95	5	22	78
9	38	2	24	76
5	0	0	24	75
2	19	1	25	65
0.9	190	10	35	40
0.4	475	25	60	4
0.16	684	36	96	1
0.071	57	3	99	0
Pan	19	1	100	0

Table B4. Gradation for 1Tire:3Sand Mix

Sieve Opening (mm)	Soil Retained (g)	% retained	Cumulative % retained	Cumulative % passing
31.5	0	0	0	100
25	19	1	1	99
20	19	1	2	98
18	171	9	11	89
16	76	4	15	85
12.5	76	4	19	81
9	19	1	20	80
5	19	1	21	79
2	171	9	30	70
0.9	551	29	59	41
0.4	684	36	95	5
0.16	57	3	98	2
0.071	38	2	100	0
Pan	0	0	100	0

Table B6. Gradation for Sand

Sieve Opening (mm)	Soil Retained (g)	% retained	Cumulative % retained	Cumulative % passing
31.5	0	0	0	100
25	0	0	0	100
20	0	0	0	100
18	0	0	0	100
16	0	0	0	100
12.5	0	0	0	100
9	0	0	0	100
5	19	1	1	99
2	228	12	13	87
0.9	627	33	46	54
0.4	893	47	93	7
0.16	114	6	99	1
0.071	19	1	100	0
Pan	0	0	100	0

APPENDIX C

CALIFORNIA BEARING RATIO TEST RESULTS

Table C1. California Bearing Ratio Results for 100% Shredded Tires

Dspl. (mm)	Force (lbf) Specimen						CBR (%) Specimen						Mean CBR (%)	STD	CV%
	1	2	3	4	5	6	1	2	3	4	5	6			
0.64	30	30	20	30	30	20									
1.27	30	30	30	30	30	30									
1.91	30	30	30	40	40	30									
2.54	40	40	40	40	50	30	1.3	1.3	1.3	1.3	1.7	1.0	1.3	0.2	15.8
3.18	40	40	40	40	50	30									
3.81	40	50	40	40	50	40									
4.45	40	50	40	50	50	40									
5.08	50	60	50	50	50	50	1.1	1.3	1.1	1.1	1.1	1.1			
7.62	50	60	50	70	60	50									
10.16	70	70	80	90	70	70									
12.7	90	90	100	90	90	80									

Table C2. California Bearing Ratio Results for 1Tire:1Sand Mix

Dspl. (mm)	Force (lbf) Specimen						CBR (%) Specimen						Mean CBR (%)	STD	CV%
	1	2	3	4	5	6	1	2	3	4	5	6			
0.64	50	60	40	60	50	40									
1.27	60	60	50	70	50	50									
1.91	60	60	70	70	70	80									
2.54	70	60	80	80	70	90	2.3	2.0	2.7	2.7	2.3	3.0			
3.18	80	80	90	110	80	90									
3.81	100	80	110	120	90	100									
4.45	110	110	150	130	100	110									
5.08	140	120	160	150	110	110	3.1	2.7	3.6	3.3	2.5	2.5	2.9	0.5	16.2
7.62	170	150	190	180	220	190									
10.16	190	190	240	250	250	280									
12.7	220	210	300	290	280	350									

Table C4. California Bearing Ratio Results for 1Tire:2 Sand Mix

Dspl. (mm)	Force (lbf) Specimen						CBR (%) Specimen						Mean CBR (%)	STD	CV%
	1	2	3	4	5	6	1	2	3	4	5	6			
0.64	60	50	70	70	60	80									
1.27	80	100	90	80	90	90									
1.91	120	150	170	140	120	180									
2.54	180	190	210	220	200	210	6.0	6.3	7.0	7.3	6.7	7.0	6.7	0.5	7.3
3.18	210	210	230	240	210	240									
3.81	240	230	260	270	240	270									
4.45	270	260	270	280	270	300									
5.08	300	290	290	290	280	310	6.7	6.5	6.5	6.5	6.3	6.9			
7.62	420	400	370	360	390	450									
10.16	530	470	560	430	470	640									
12.7	600	560	640	590	630	790									

Table C5. California Bearing Ratio Results for 1Tire:3Sand Mix

Dspl. (mm)	Force (lbf) Specimen						CBR (%) Specimen						Mean CBR (%)	STD	CV%
	1	2	3	4	5	6	1	2	3	4	5	6			
0.64	50	70	50	80	70	60									
1.27	90	100	80	90	100	100									
1.91	140	130	150	140	130	140									
2.54	190	200	180	200	190	180	6.3	6.7	6.0	6.7	6.3	6.0			
3.18	250	260	220	260	250	220									
3.81	310	330	360	350	300	280									
4.45	370	370	400	470	390	350									
5.08	440	410	410	430	430	460	9.8	9.2	9.2	9.6	9.6	10.3	9.6	0.4	4.4
7.62	700	810	780	820	580	650									
10.16	940	970	890	910	880	870									
12.7	1100	1300	100	1200	1000	900									

Table C5. California Bearing Ratio Results for Sand

Dspl. (mm)	Force (lbf) Specimen						CBR (%) Specimen						Mean CBR (%)	STD	CV%
	1	2	3	4	5	6	1	2	3	4	5	6			
0.64	70	60	40	60	70	80									
1.27	110	80	70	100	90	110									
1.91	150	100	130	140	120	160									
2.54	190	190	180	180	140	200	6.3	6.3	6.0	6.0	4.7	6.7			
3.18	230	180	220	230	190	230									
3.81	270	220	260	260	220	290									
4.45	300	290	300	340	260	320									
5.08	370	340	330	400	310	360	8.3	7.6	7.4	8.9	6.9	8.0	7.8	0.7	9.07
7.62	490	420	460	560	430	460									
10.16	670	580	610	630	510	610									
12.7	870	700	790	840	590	749									

APPENDIX D

CONFINED COMPRESSIVE STRESS TEST RESULTS

Table D1. Confined Compression Test Results for 100% Shredded Tires

Sample	Peak Load (KN)	Compressive Strength (KPa)
1	0.11	0.602943422
2	0.1	0.548130384
3	0.12	0.657756461
4	0.09	0.493317346
5	0.1	0.548130384
6	0.12	0.657756461
Mean	0.10666667	0.58467241
STD	0.0121106	0.066381886
CV (%)	11.3536888	11.35368883

Table D2. Confined Compression Test Results for 1Tire:1Sand

Sample	Peak Load (KN)	Compressive Strength (KPa)
1	1.46	8.00270
2	1.31	7.18051
3	1.67	9.15378
4	1.52	8.33158
5	1.7	9.31822
6	1.57	8.60565
Mean	1.53833333	8.43207
STD	0.14358505	0.78703
CV (%)	9.33380609	9.33381

Table D3. Confined Compression Test Results for 1Tire:2Sand Mix

Sample	Peak Load (KN)	Compressive Strength (KPa)
1	8.4	46.04295226
2	7.9	43.30230034
3	7.7	42.20603957
4	7.6	41.65790919
5	8.1	44.39856111
6	7.3	40.01351804
Mean	7.83333333	42.93688008
STD	0.38815804	2.127612174
CV (%)	4.95520906	4.955209065

Table D4. Confined Compression Test Results for 1Tire:3Sand Mix

Sample	Peak Load (KN)	Compressive Strength (KPa)
1	12.2	66.8719
2	11.9	65.2275
3	10.9	59.7462
4	11.8	64.6794
5	12.5	68.5163
6	12.8	70.1607
Mean	12.0166667	65.867
STD	0.6615638	3.62623
CV (%)	5.50538533	5.50539

Table D5. Confined Compression Test Results for Sand

Sample	Peak Load (KN)	Compressive Strength (KPa)
1	10.7	58.65
2	9.1	49.88
3	9.5	52.07
4	10.9	59.75
5	11.1	60.84
6	9.8	53.72
Mean	10.183333	55.82
STD	0.8256311	4.52553
CV (%)	8.1076701	8.10767

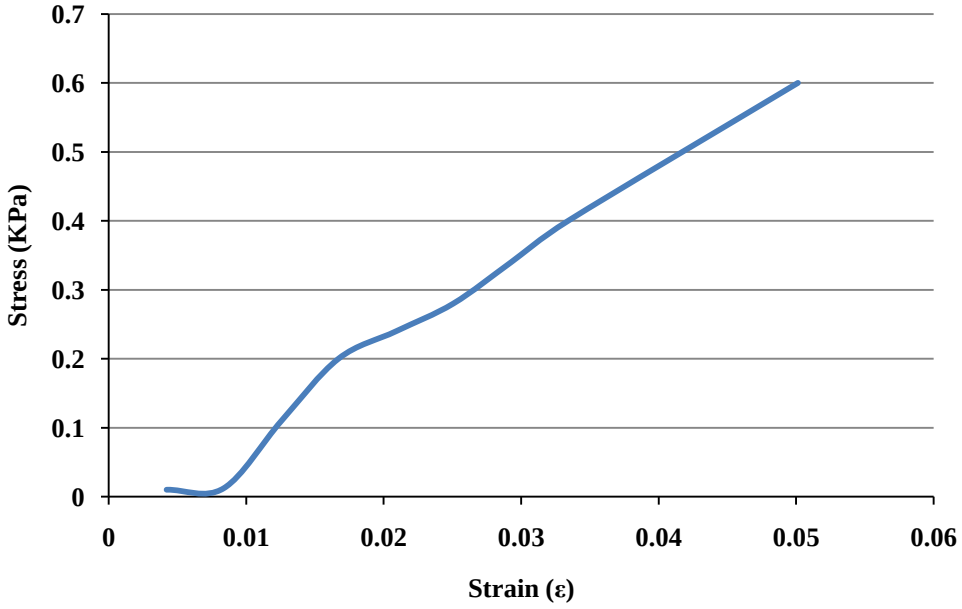

Figure D1. Stress Strain Curve for 100% Shredded Tire Sample

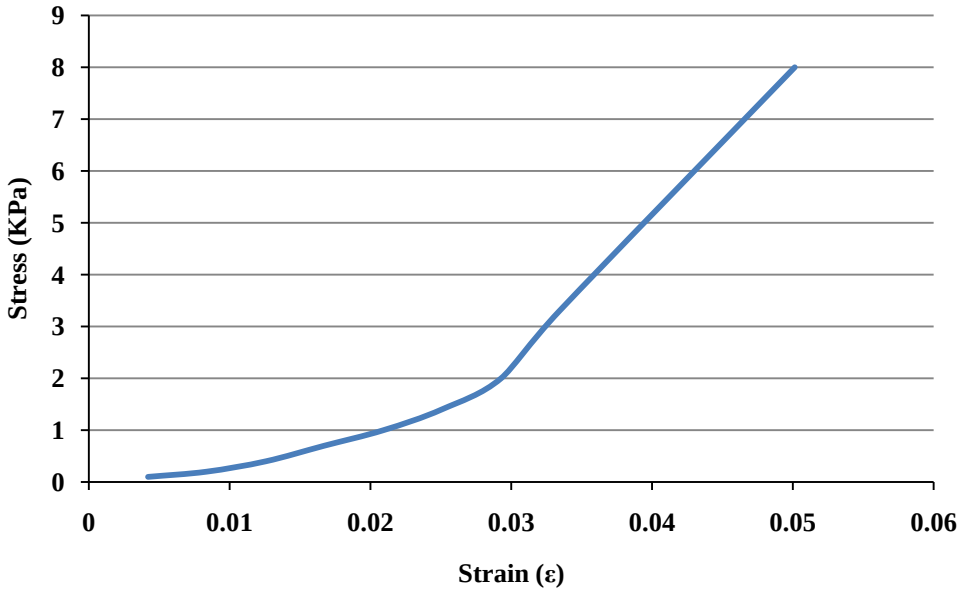

Figure D2. Stress Strain Curve for 1Tire:1Sand Sample

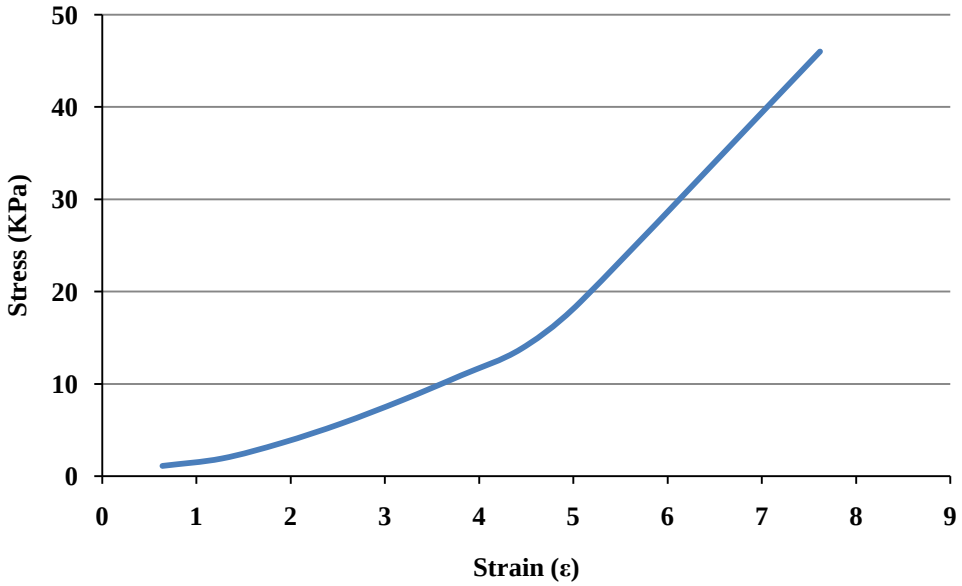

Figure D3. Stress Strain Curve for 1Tire:2Sand Sample

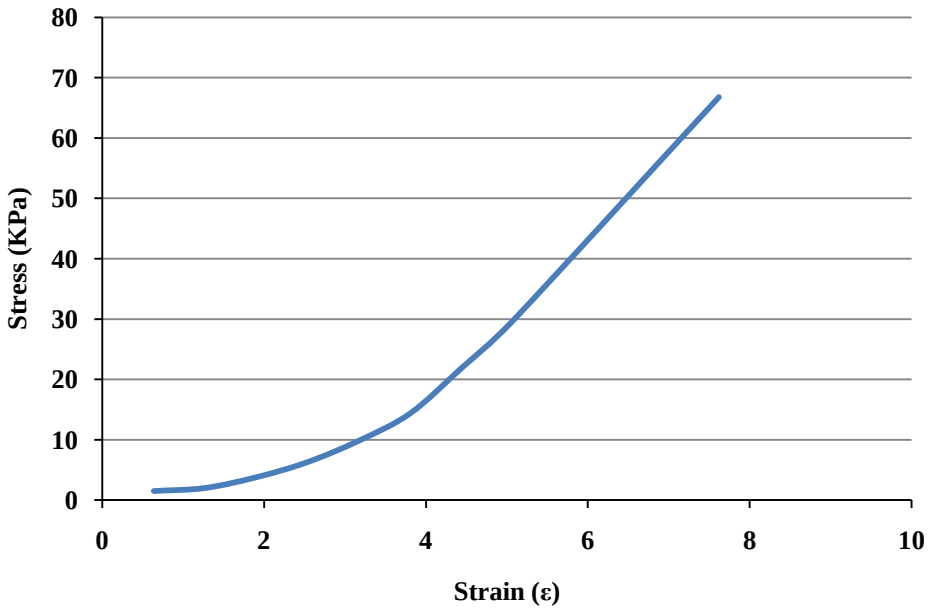

Figure D4. Stress Strain Curve for 1Tire:3Sand Sample

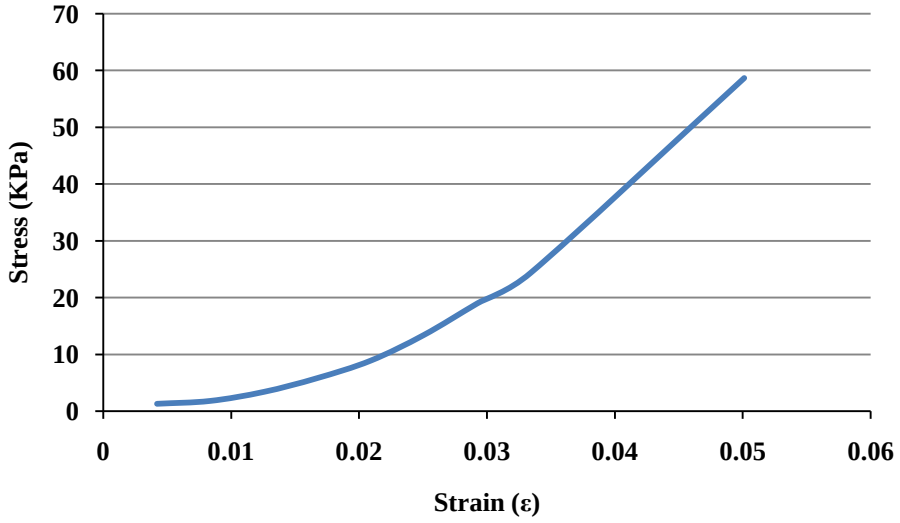

Figure D5. Stress Strain Curve for Sand Sample

APPENDIX E.

CONFINED FREQUENCY SWEEP TEST RESULTS

Table E1. Dynamic Modulus Results at 50 kPa Static and 25 kPa Dynamic Stress Loading States

Sample	Freq (Hz)	Dynamic Modulus E_d (MPa)		
100% Shredded Tire	5	7	4	4
Sand	5	128	132	118
1Tire:1Sand	5	26	36	28
1Tire:2Sand	5	102	121	107
1Tire:3Sand	5	171	164	139

Table E2. Phase Angle Results at 50 kPa Static and 25 kPa Dynamic Stress Loading States

Sample	Freq (Hz)	Phase Angle (^{o})		
100% Shredded Tire	5	29.7	36.7	28.4
Sand	5	13.6	15.1	14.2
1Tire:1Sand	5	18.7	15.9	14.3
1Tire:2Sand	5	16.4	13.9	17.1
1Tire:3Sand	5	14.2	13.6	15.1

APPENDIX F.

PERMEABILITY TEST RESULTS

Table F1. Permeability Test Results for 100% Shredded Tires

Sample	Time (s)	Permeability (cm/s)
1	4	1.370326
2	3	1.827101
3	5	1.096261
4	3	1.827101
5	4	1.370326
6	5	1.096261
Mean	5	1.42
STD	0.894427	0.330229
CV (%)	17.88854	23.25555

Table F2. Permeability Test Results for Sand

Sample	Time (s)	Permeability (cm/s)
1	4167	0.001315408
2	4421	0.001239833
3	4173	0.001313516
4	3984	0.001375829
5	4216	0.00130012
6	4414	0.0012418
Mean	4229.167	0.001297751
STD	166.2906	5.12779E-05
CV (%)	3.931995	3.951290338

Table F3. Permeability Test Results for 1Tire:1Sand Mix

Sample	Time (s)	Permeability (cm/s)
1	448	0.012235053
2	463	0.011838669
3	502	0.010918932
4	511	0.010726622
5	489	0.01120921
6	465	0.01178775
Mean	479.66667	0.011452706
STD	24.752104	0.00059071
CV (%)	5.1602719	5.157821336

Table F4. Permeability Test Results for 1Tire:2Sand Mix

Sample	Time (s)	Permeability (cm/s)
1	1678	0.003267
2	1732	0.003165
3	1812	0.003025
4	1624	0.003375
5	1649	0.003324
6	1783	0.003074
Mean	1713	0.003205
STD	75.23829	0.00014
CV (%)	4.392194	4.369326

Table F5. Permeability Test Results for 1Tire:3Sand Mix

Sample	Time (s)	Permeability (cm/s)
1	2085	0.002628923
2	2106	0.002602708
3	2125	0.002579437
4	2303	0.002380071
5	2117	0.002589185
6	1918	0.002857823
Mean	2109	0.002606358
STD	122.49245	0.000152304
CV (%)	5.808082	5.843552276

APPENDIX G.

DETAILED ROAD STRUCTURE DESIGN & MODEL PREDICTED STRAIN PROFILES

DETAILED CROSS SECTIONS

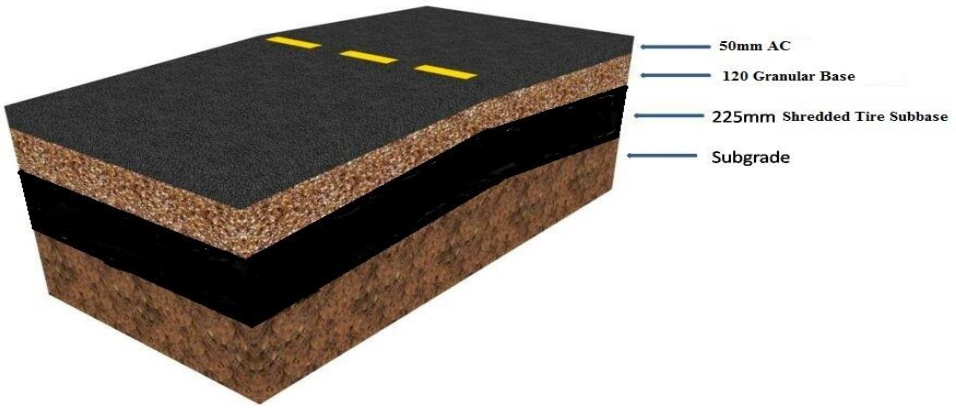

Figure G1. 100% Shredded Tire Test Section

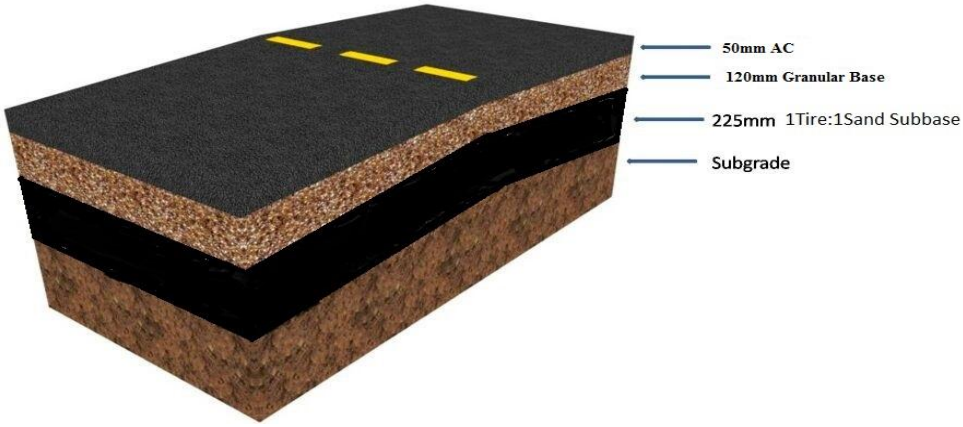

Figure G2. 1Tire:1Sand Road Cross Section

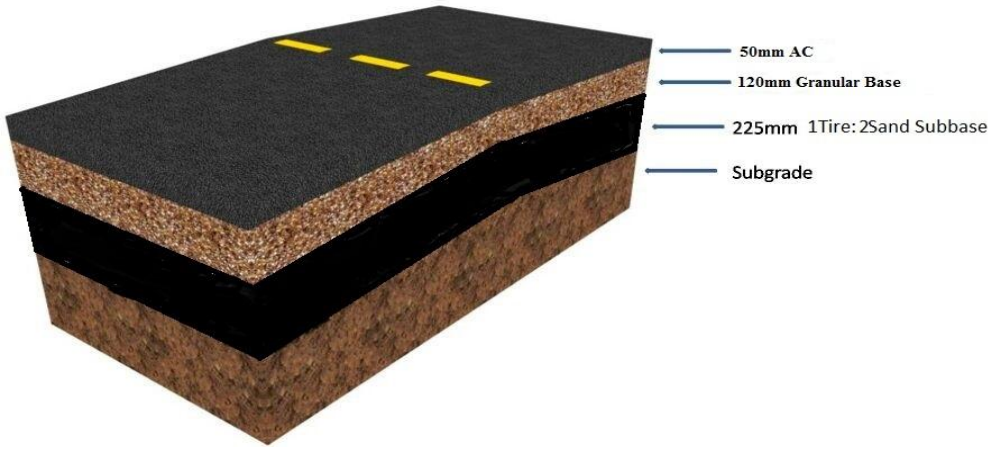

Figure G3. 1Tire:2Sand Road Cross Section

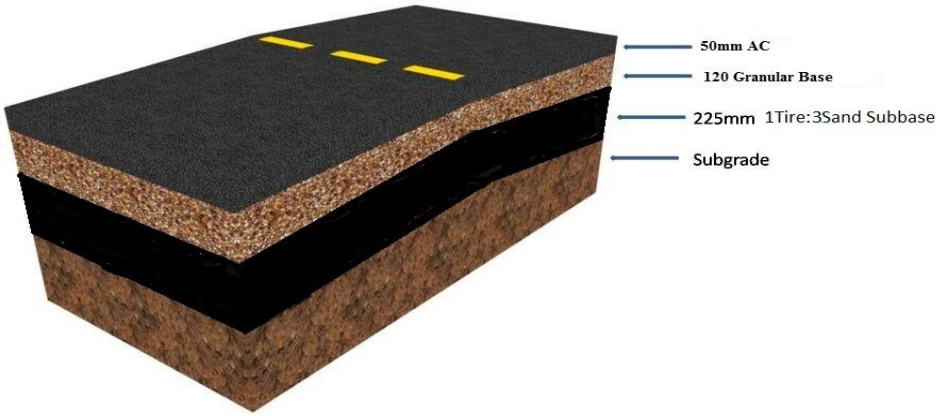

Figure G4. 1Tire:3Sand Road Cross Section

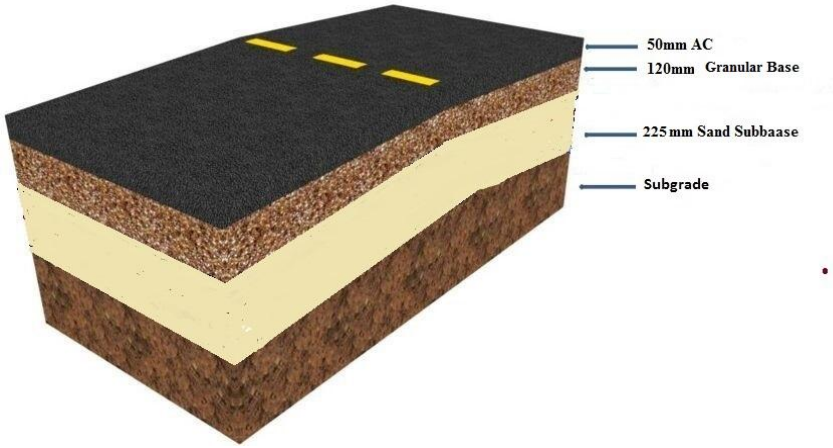

Figure G5. Sand Road Cross Section

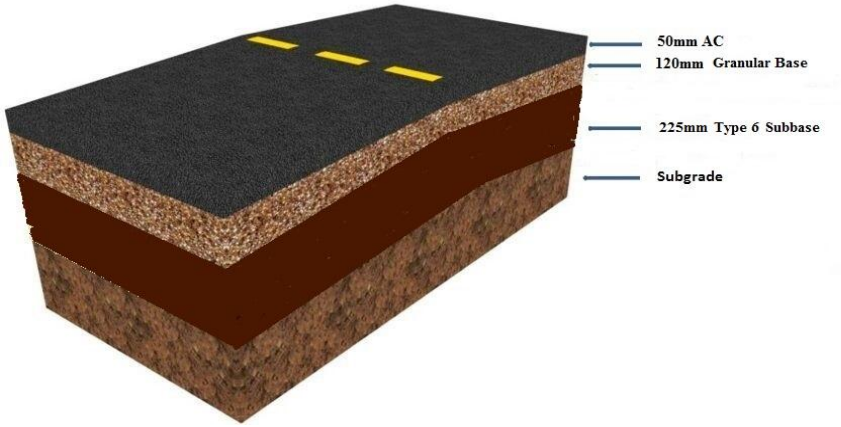

Figure G6. SMHI Type 6 Subbase Road Section

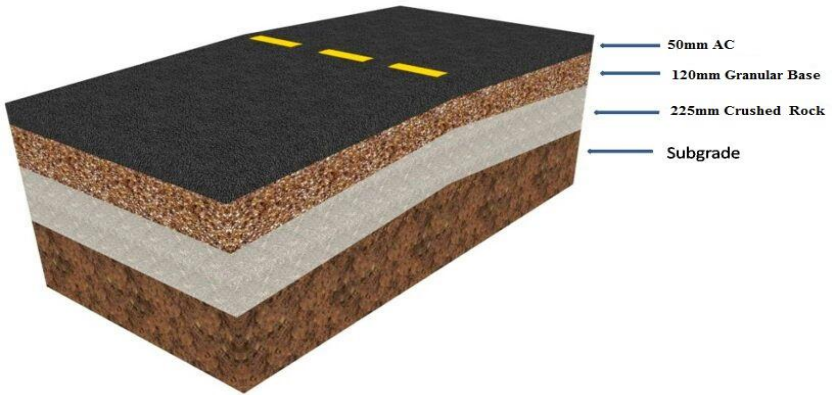

Figure G7. Crushed Rock Road Section

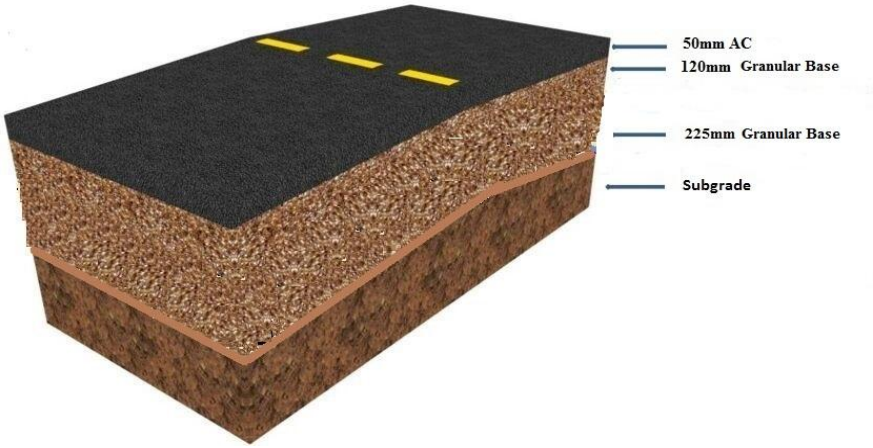

Figure G8. Granular Base Road Section

100% SHREDDED TIRE STRAIN PROFILES

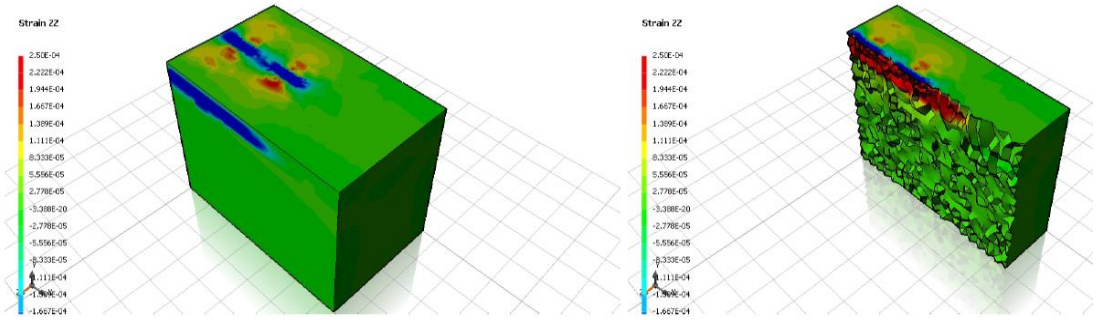

Figure G9. Horizontal Strain (Longitudinal) Profile for 100% Shredded Tire Section

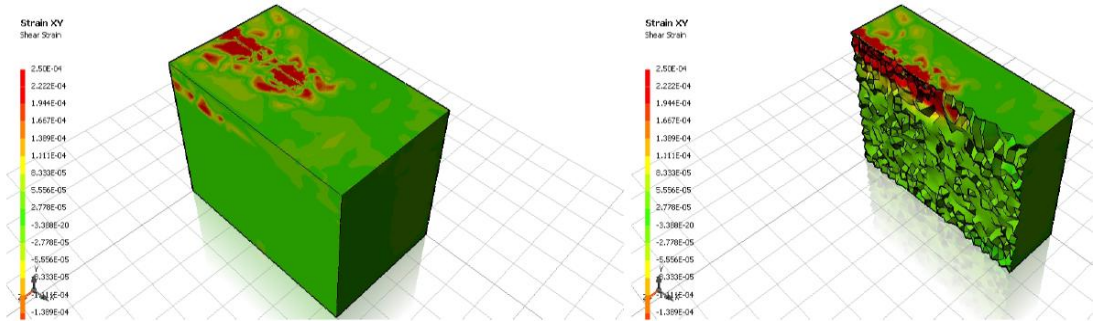

Figure G10. Shear Strain (XY) Profile for 100% Shredded Tire Section

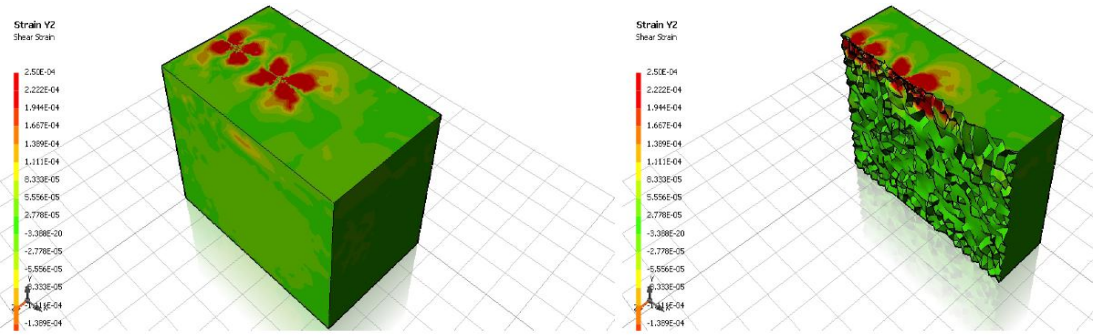

Figure G11. Shear Strain (YZ) Profile for 100% Shredded Tire Section

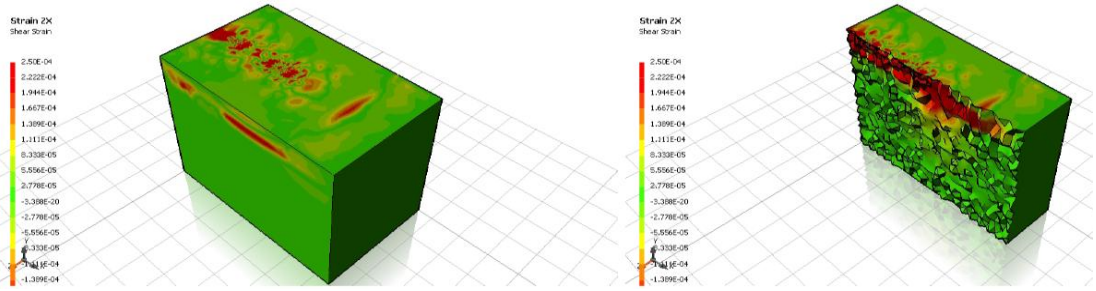

Figure G12. Shear Strain (ZX) Profile for 100% Shredded Tire Section

1TIRE:1SAND PROFILES

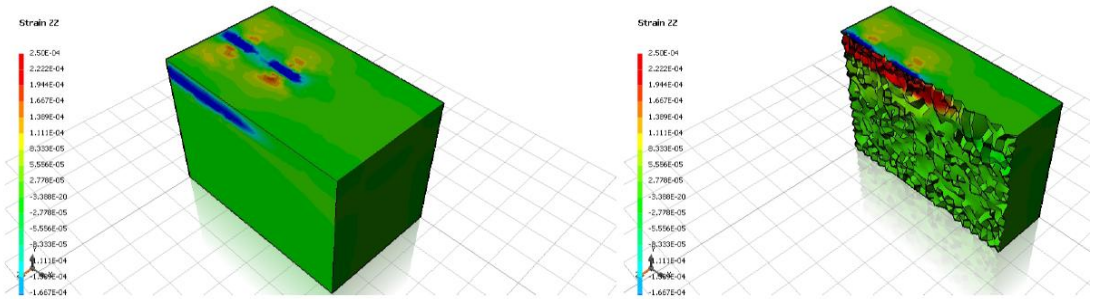

Figure G13. Horizontal Strain (Longitudinal) Profile for 1Tire:1Sand Road

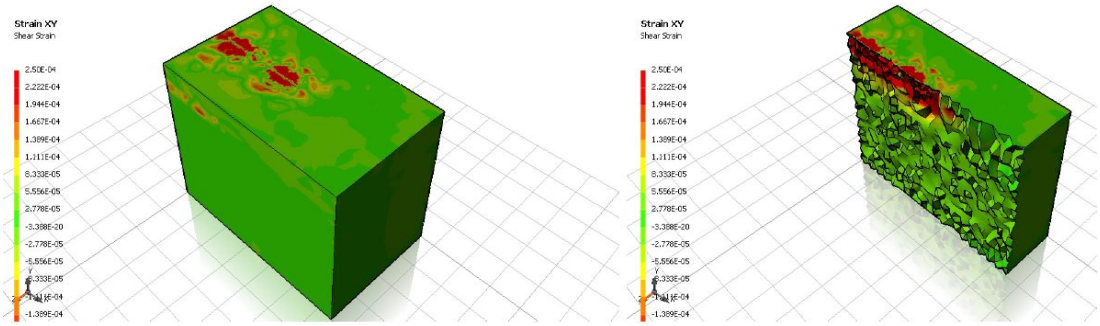

Figure G14. Shear Strain (XY) Profile for 1Tire:1Sand Road

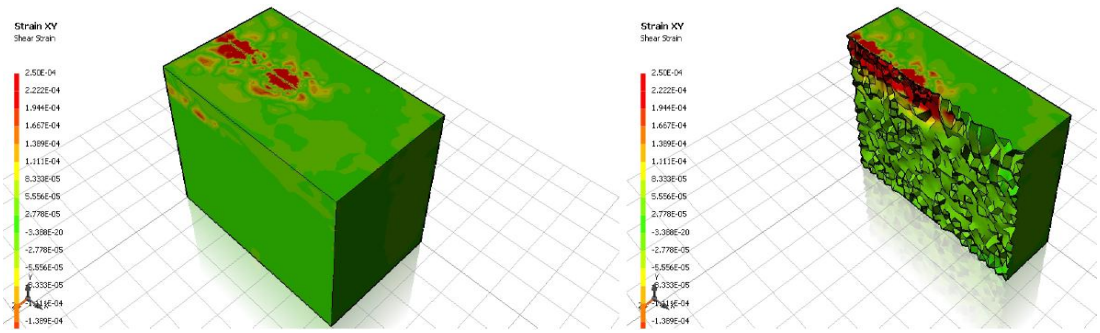

Figure G15. Shear Strain (YZ) Profile for 1Tire:1Sand Road

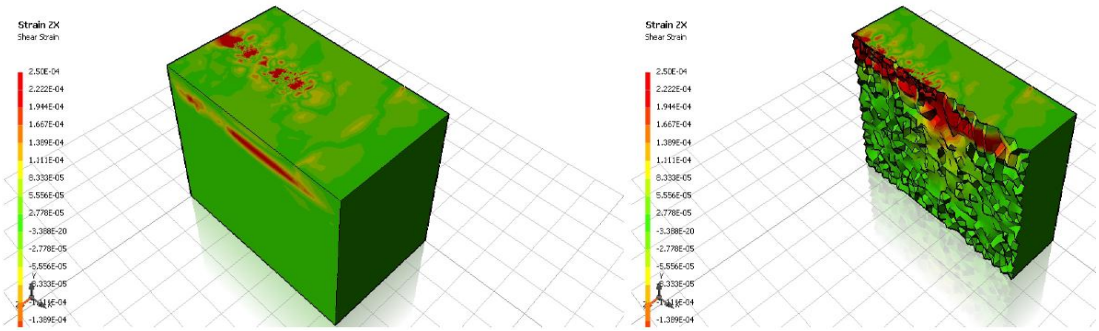

Figure G16. Shear Strain (YZ) Profile for 1Tire:1Sand Road

1TIRE:2SAND STRAIN PROFILE

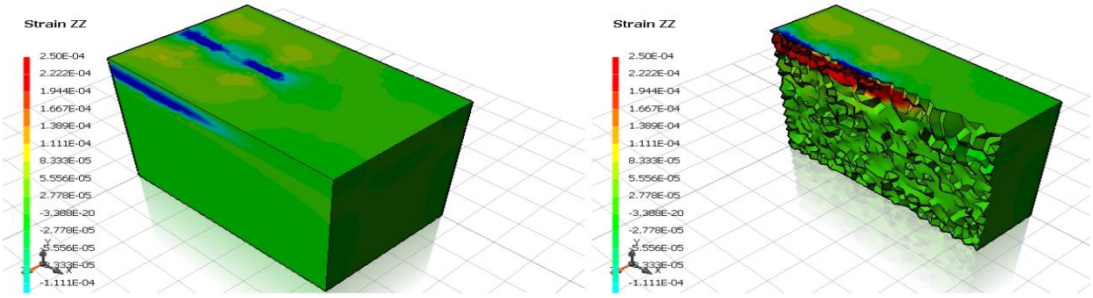

Figure G17. Horizontal Strain (Longitudinal) Profile for 1Tire:2Sand Road

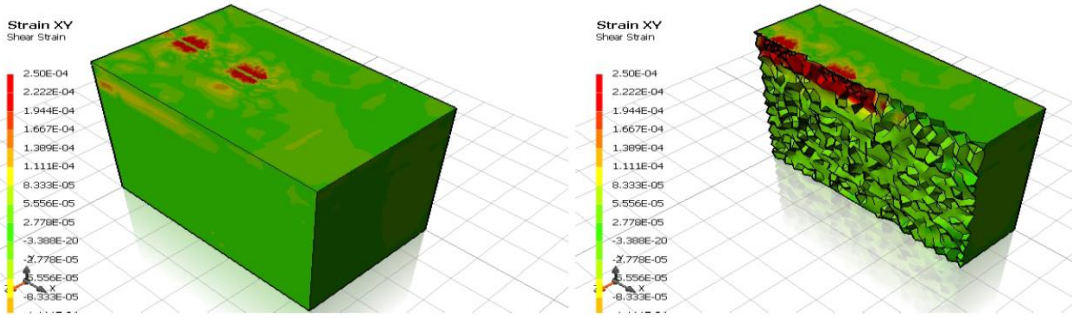

Figure G18. Shear Strain (XY) Profile for 1Tire:2Sand Road

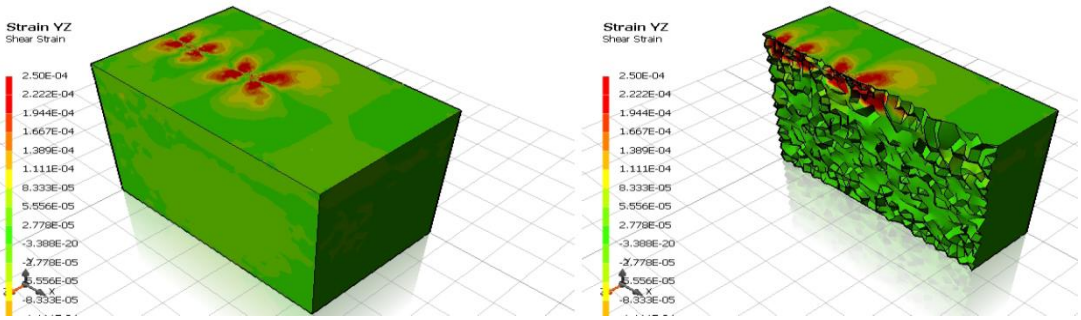

Figure G19. Shear Strain (YZ) Profile for 1Tire:2Sand Road

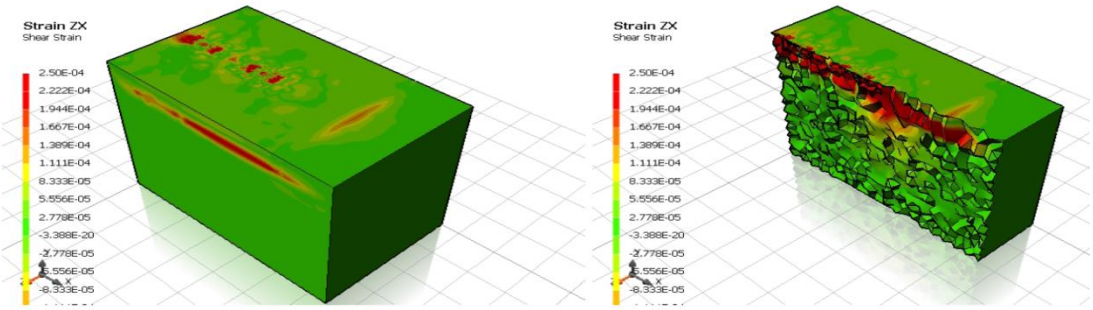

Figure G20. Shear Strain (ZX) Profile for 1Tire:2Sand Road

1TIRE:3SAND STRAIN PROFILES

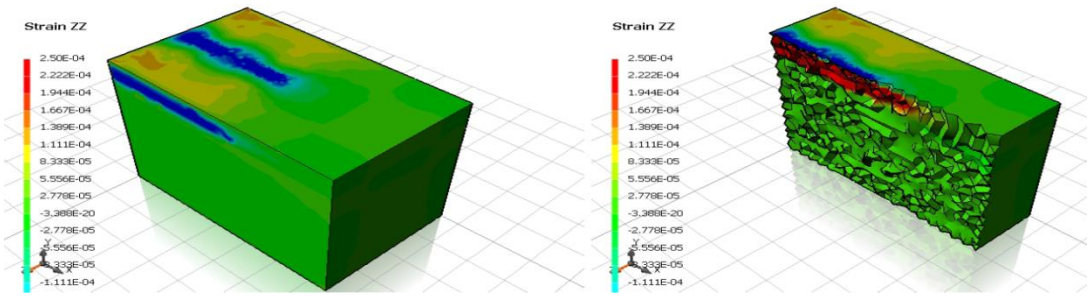

Figure G21. Horizontal Strain (Longitudinal) Profile for 1Tire:3Sand Road

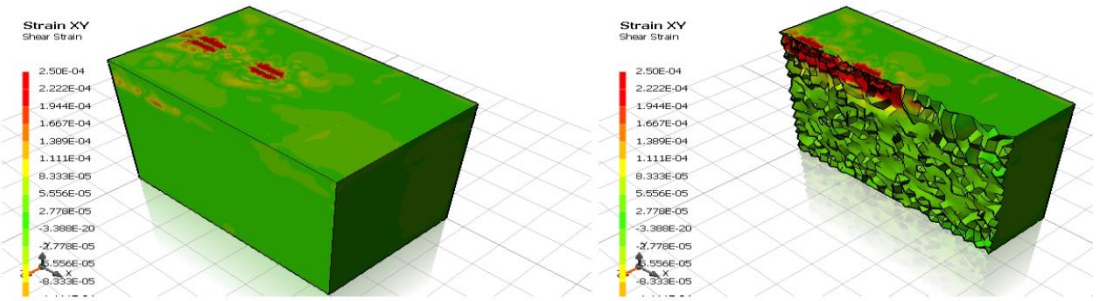

Figure G22. Shear Strain (XY) Profile for 1Tire:3Sand Road

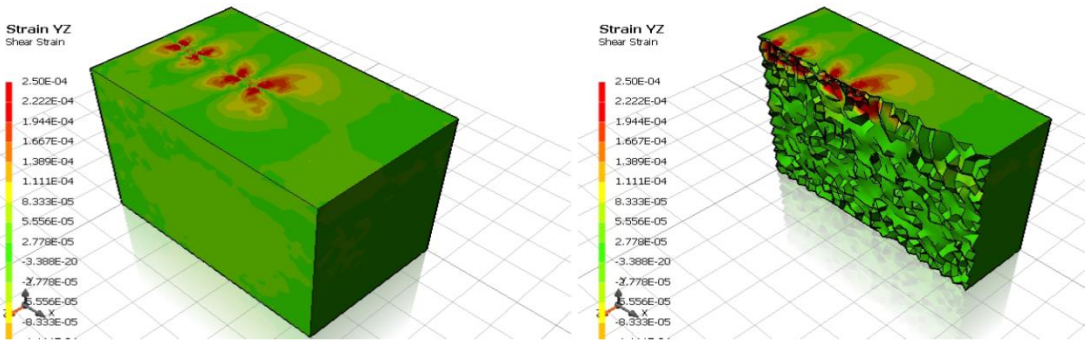

Figure G23. Shear Strain (YZ) Profile for 1Tire:3Sand Road

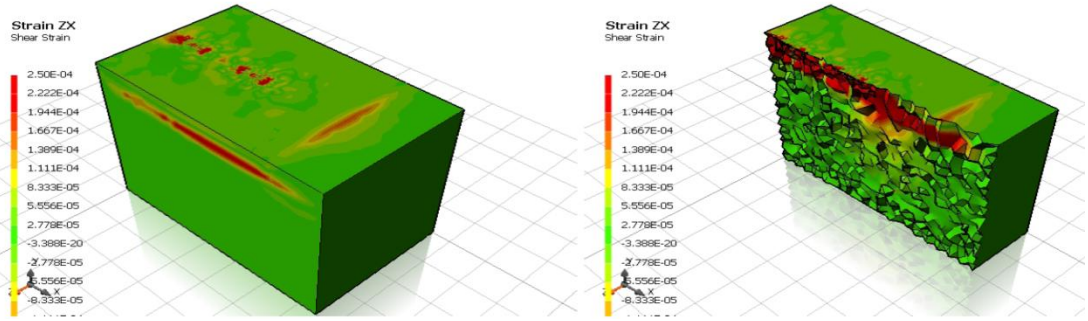

Figure G24. Shear Strain (ZX) Profile for 1Tire:3Sand Road

SAND ROAD PROFILES

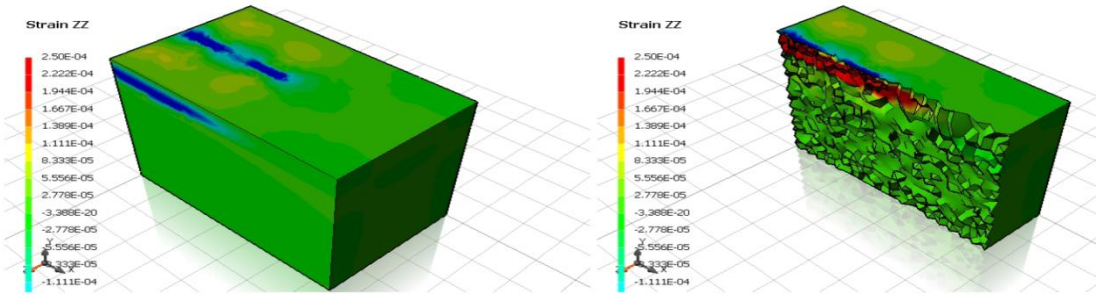

Figure G25. Horizontal Strain (Longitudinal) Profile for Sand Road

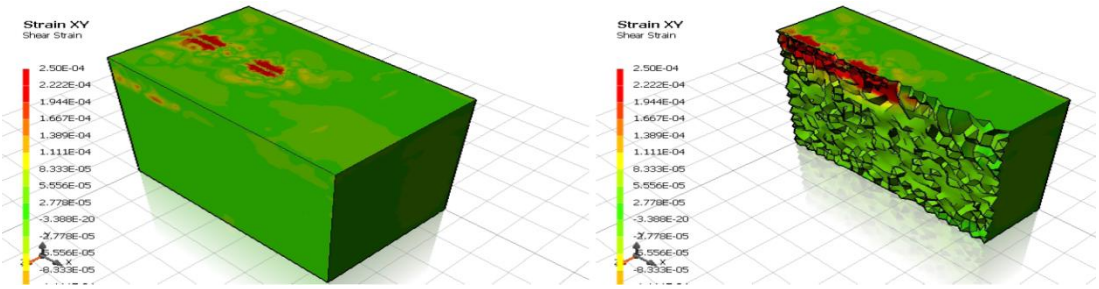

Figure G26. Shear Strain (XY) Profile for Sand Road

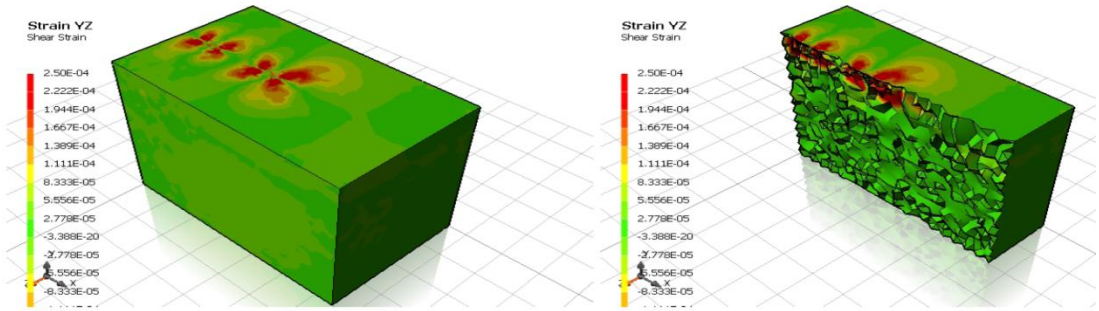

Figure G27. Shear Strain (YZ) Profile for Sand Road

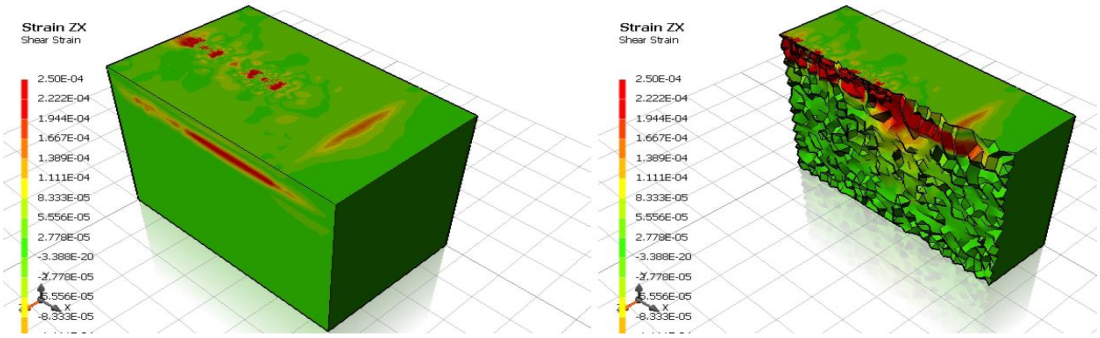

Figure G28. Shear Strain (ZX) Profile for Sand Road

SMHI TYPE 6 ROAD PROFILES

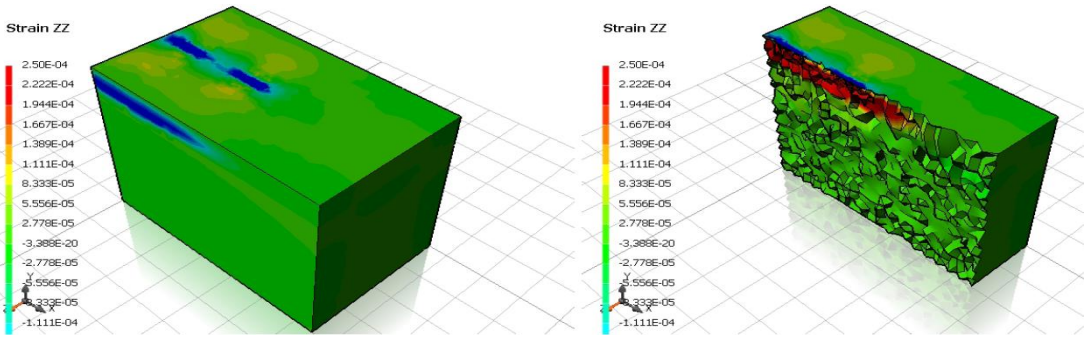

Figure G29. Horizontal Strain (Longitudinal) Profile for SMHI TYPE 6 Road

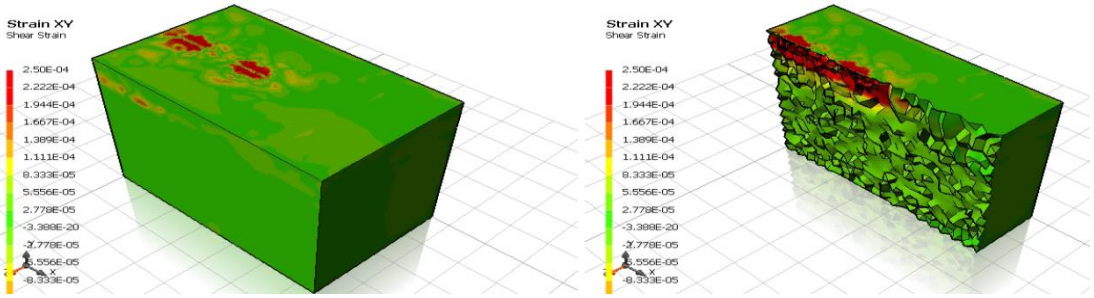

Figure G30. Shear Strain (XY) Profile for SMHI TYPE 6 Road

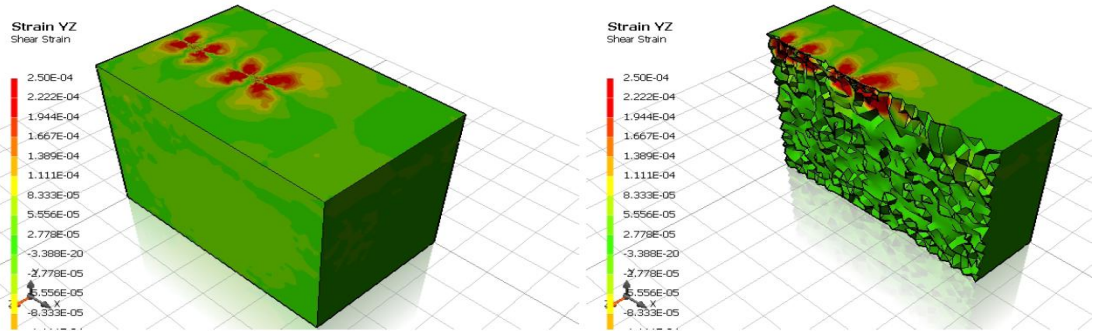

Figure G31. Shear Strain (YZ) Profile for SMHI TYPE 6 Road

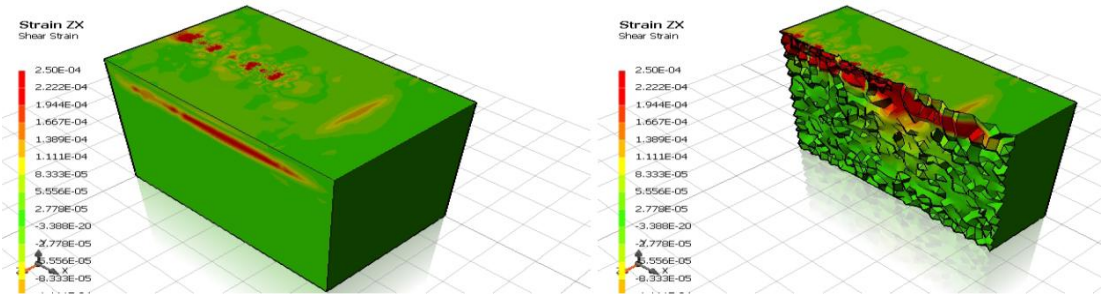

Figure G32. Shear Strain (ZX) Profile for SMHI TYPE 6 Road

GRANULAR BASE ROAD PROFILES

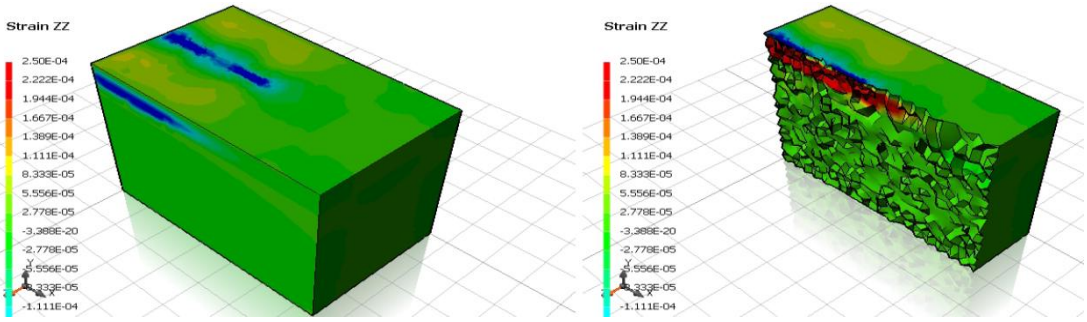

Figure G33. Horizontal Strain (Longitudinal) Profile for Granular Base Road

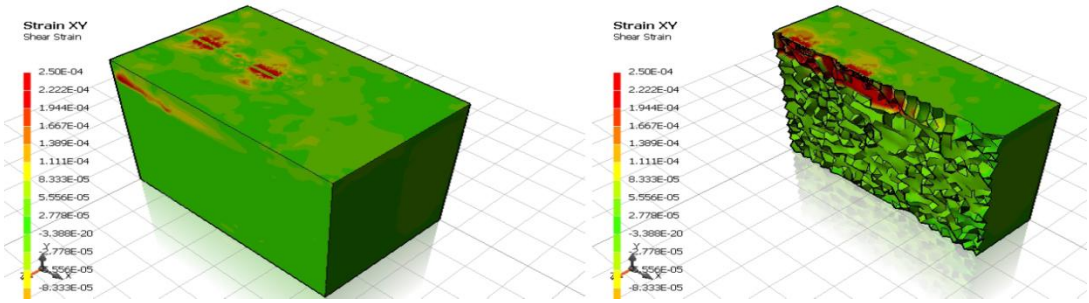

Figure G34. Shear Strain (XY) Profile for Granular Base Road

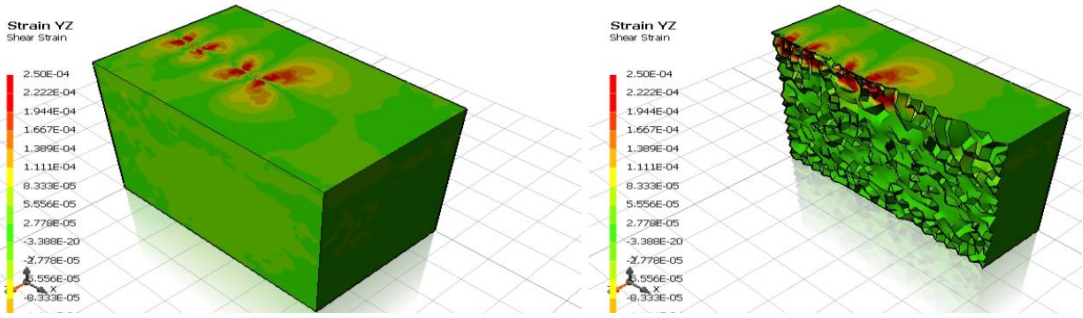

Figure G35. Shear Strain (YZ) Profile for Granular Base Road

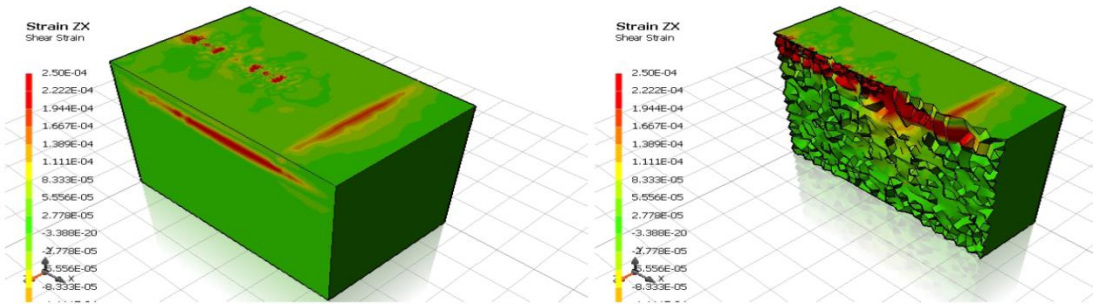

Figure G36. Shear Strain (ZX) Profile for Granular Base Road

CRUSHED ROCK SECTION

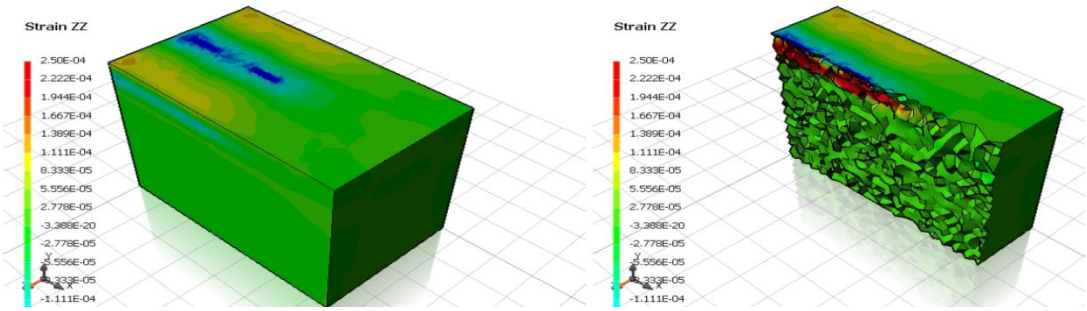

Figure G37. Horizontal Strain (Longitudinal) Profile for Crushed Rock Road

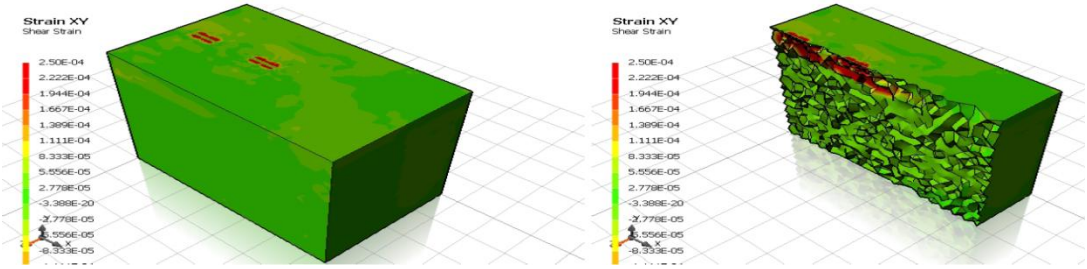

Figure G38. Shear Strain (XY) Profile for Crushed Rock Road

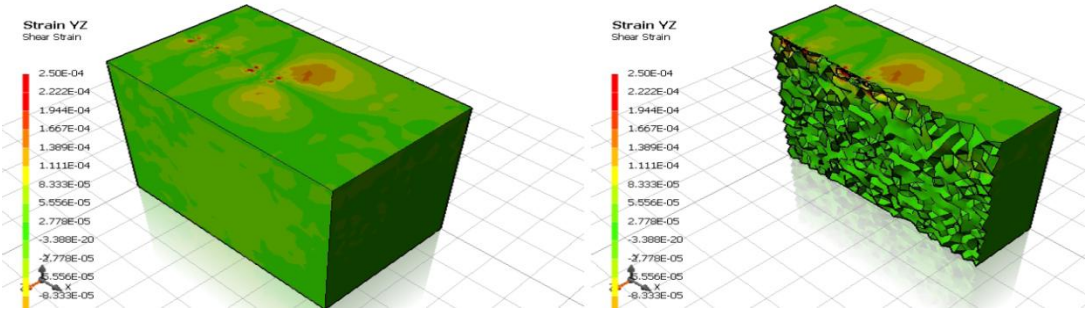

Figure G39. Shear Strain (YZ) Profile for Crushed Rock Road

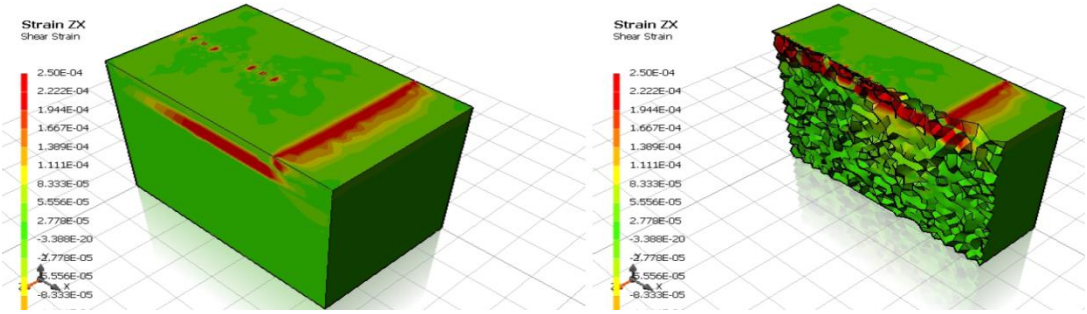

Figure G40. Shear Strain (ZX) Profile for Crushed Rock Road

100% SHREDDED TIRE (ADOLPH) SECTION - UNTREATED SUBGRADE

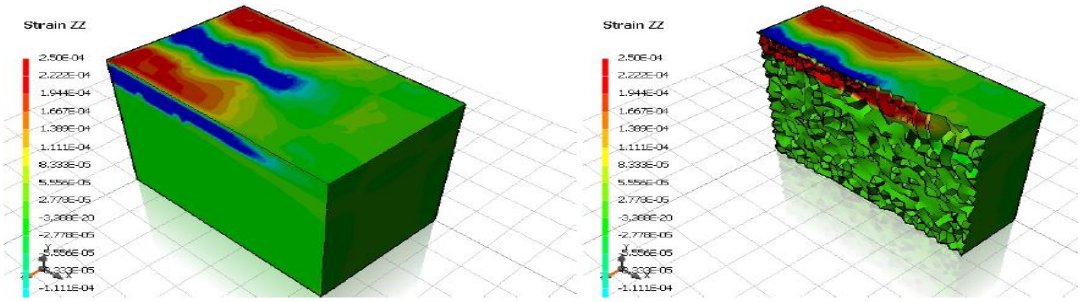

Figure G41. Horizontal Strain (Longitudinal) Profile for 100% Shredded Tire (Adolph) Section – Untreated Subgrade

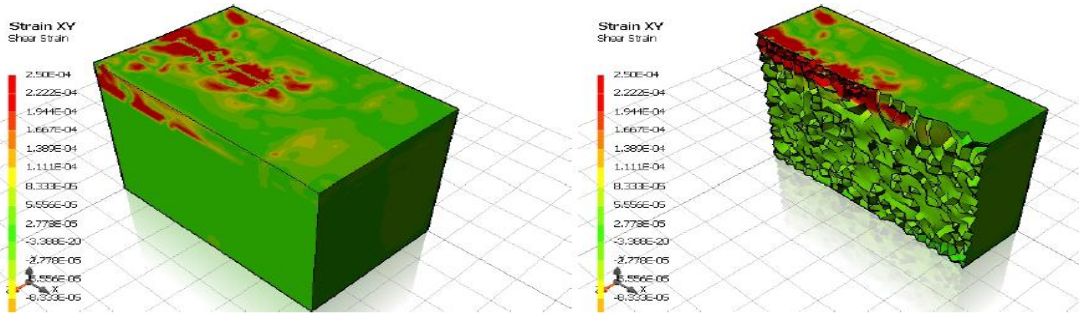

Figure G42. Shear Strain (XY) Profile for 100% Shredded Tire (Adolph) Section – Untreated Subgrade

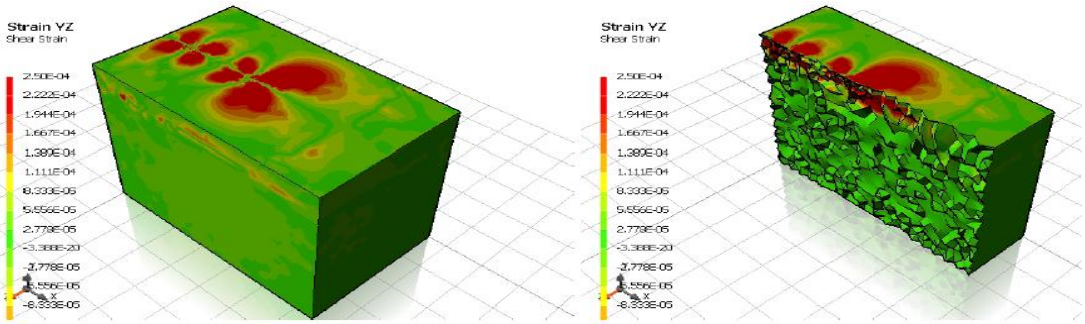

Figure G43. Shear Strain (YZ) Profile for 100% Shredded Tire (Adolph) Section – Untreated Subgrade

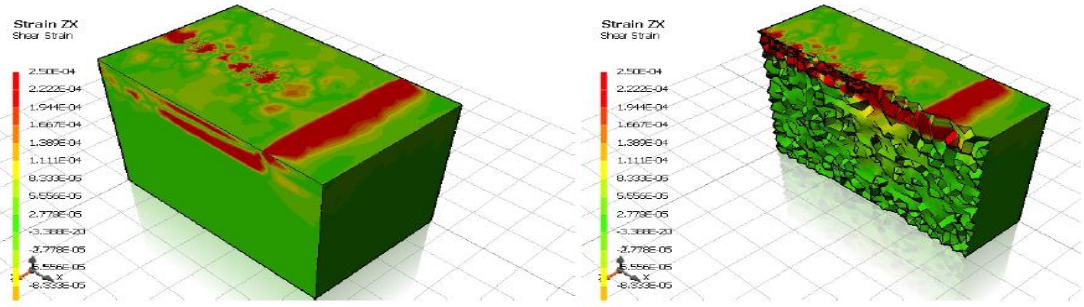

Figure G44. Shear Strain (ZX) Profile for 100% Shredded Tire (Adolph) Section – Untreated Subgrade

CRUSHED ROCK (ADOLPH) SECTION – UNTREATED SUBGRADE

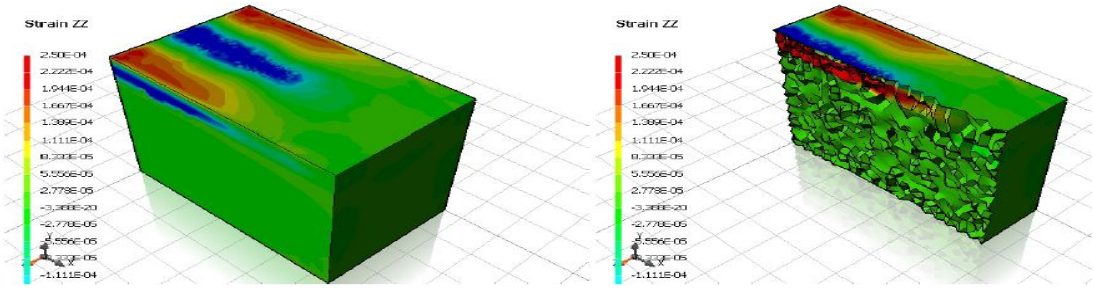

Figure G45. Horizontal Strain (Longitudinal) Profile for Crushed Rock (Adolph) Section – Untreated Subgrade

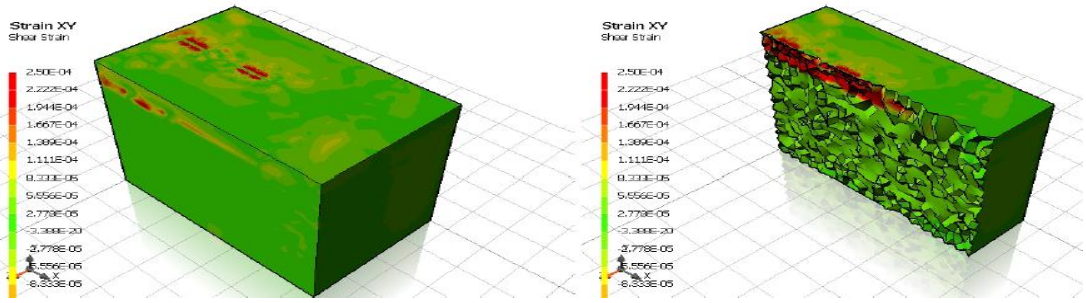

Figure G46. Shear Strain (XY) Profile for Crushed Rock (Adolph) Section – Untreated Subgrade

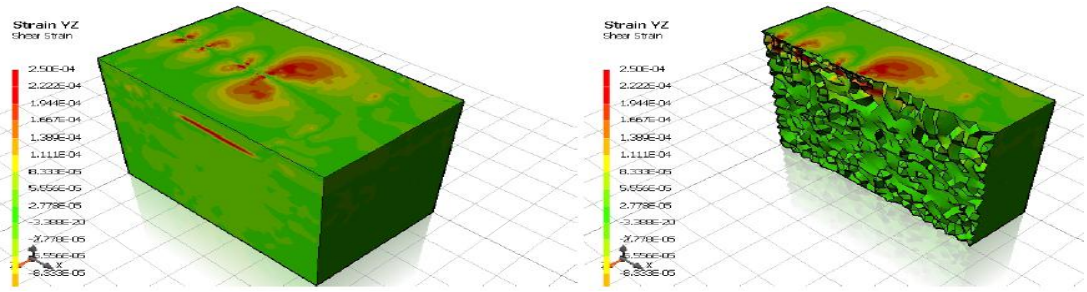

Figure G47. Shear Strain (YZ) Profile for Crushed Rock (Adolph) Section – Untreated Subgrade

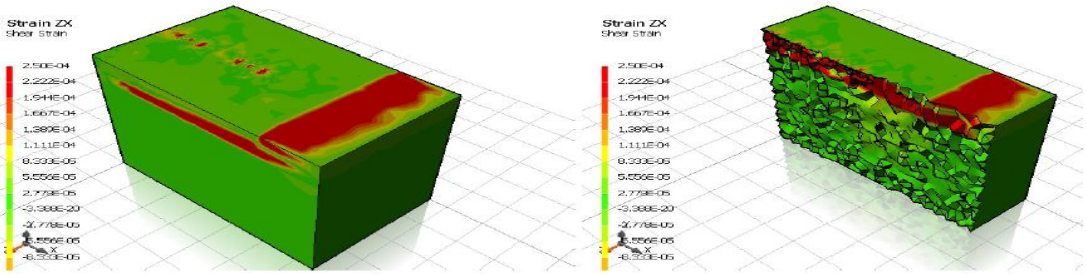

Figure G48. Shear Strain (ZX) Profile for Crushed Rock (Adolph) Section – Untreated Subgrade

100% SHREDDED TIRE SECTION - TREATED SUBGRADE

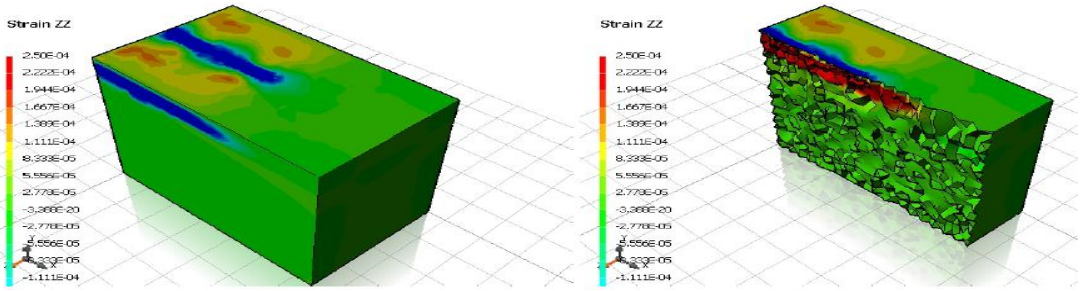

Figure G49. Horizontal Strain (Longitudinal) Profile for 100% Shredded Tire Section – Treated Subgrade

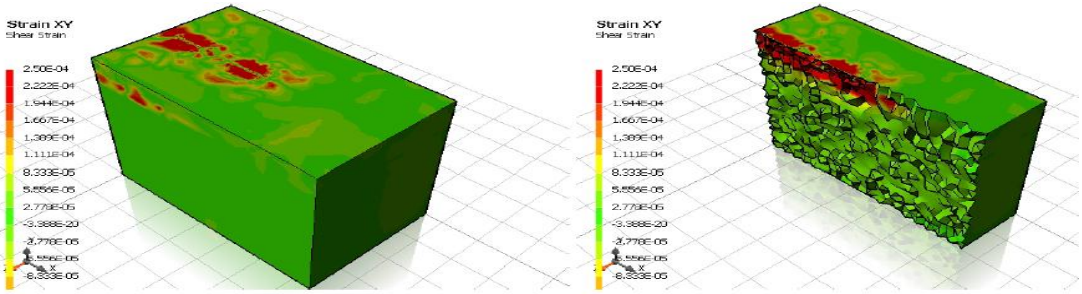

Figure G50. Shear Strain (XY) Profile for 100% Shredded Tire Section –Treated Subgrade

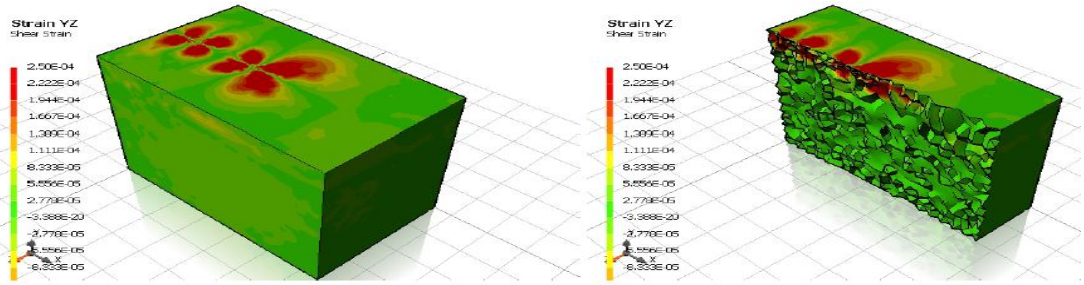

Figure G51. Shear Strain (YZ) Profile for 100% Shredded Tire Section – Treated Subgrade

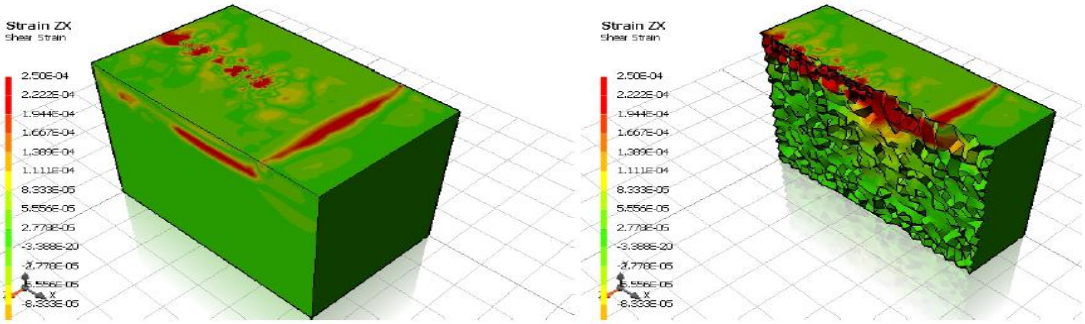

Figure G52. Shear Strain (ZX) Profile for 100% Shredded Tire Section – Treated Subgrade

CRUSHED ROCK SECTION – TREATED SUBGRADE

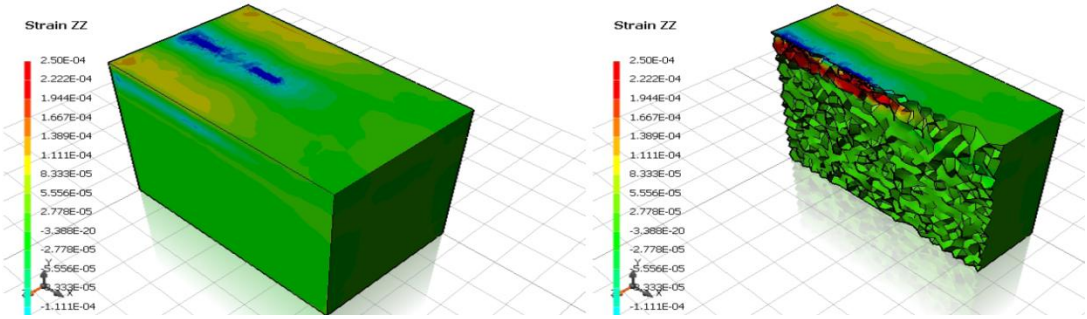

Figure G53. Horizontal Strain (Longitudinal) Profile for Crushed Rock Section – Treated Subgrade

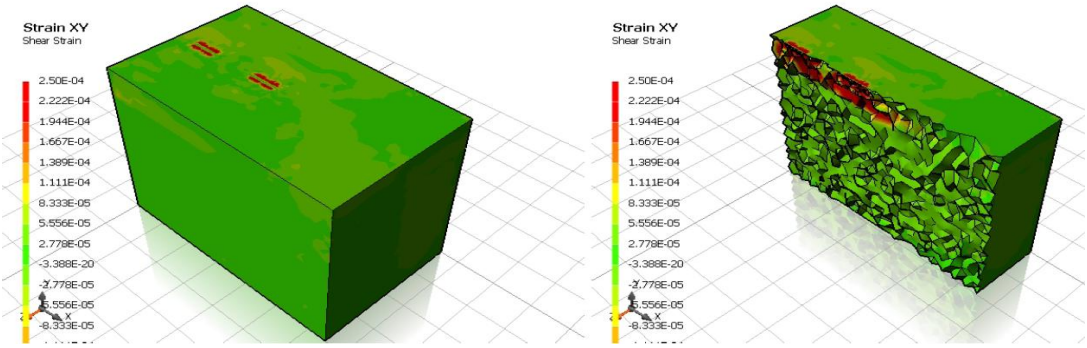

Figure G54. Shear Strain (XY) Profile for Crushed Rock Section – Treated Subgrade

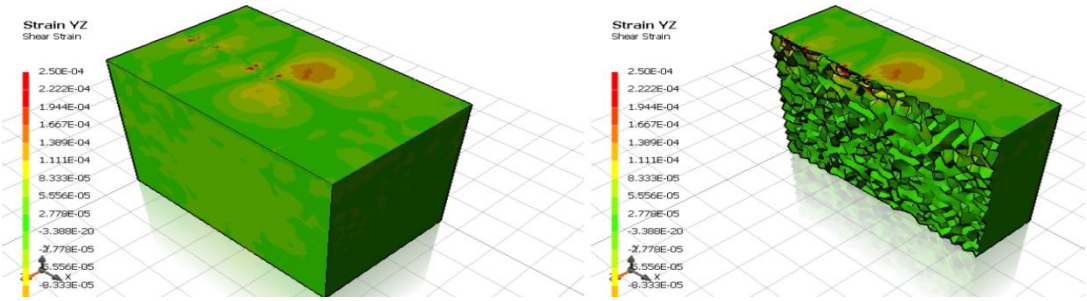

Figure G55. Section – Treated Subgrade

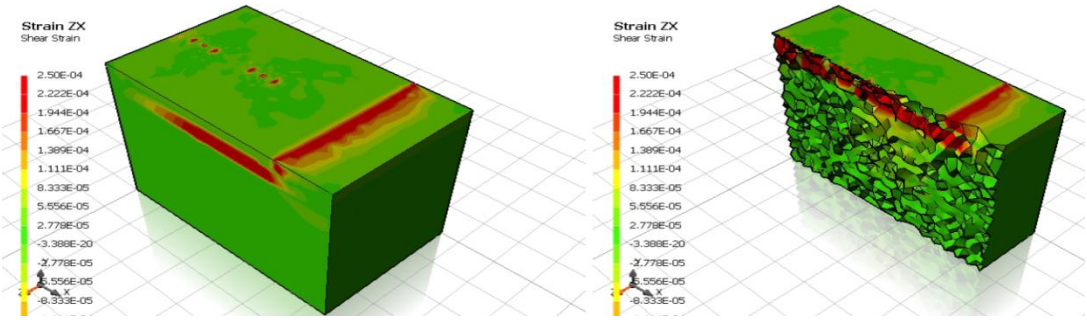

Figure G56. Shear Strain (ZX) Profile for Crushed Rock Section – Treated Subgrade

1TIRE:1SAND ROAD –TREATED SUBGRADE PROFILES

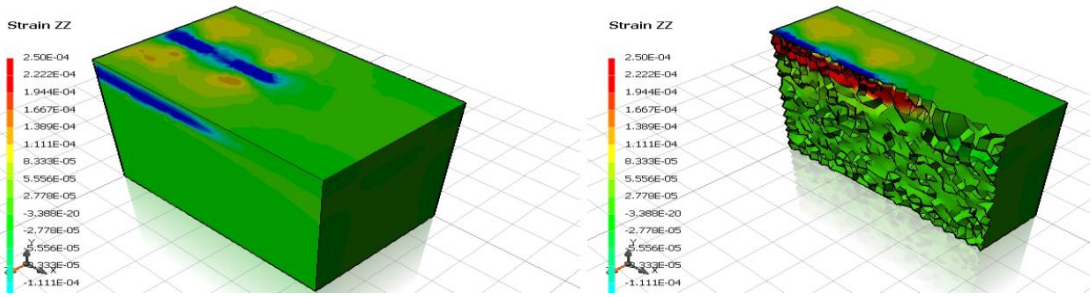

Figure G57. Horizontal Strain (Longitudinal) Profile for 1Tire:1Sand Road –Treated Subgrade

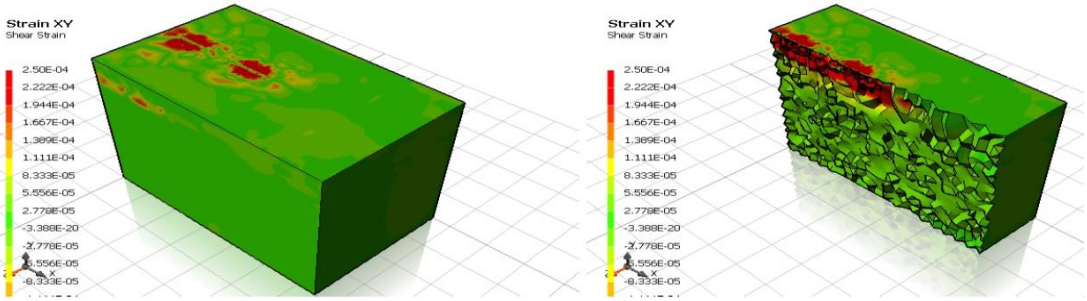

Figure F58. Shear Strain (XY) Profile for 1Tire:1Sand Road –Treated Subgrade

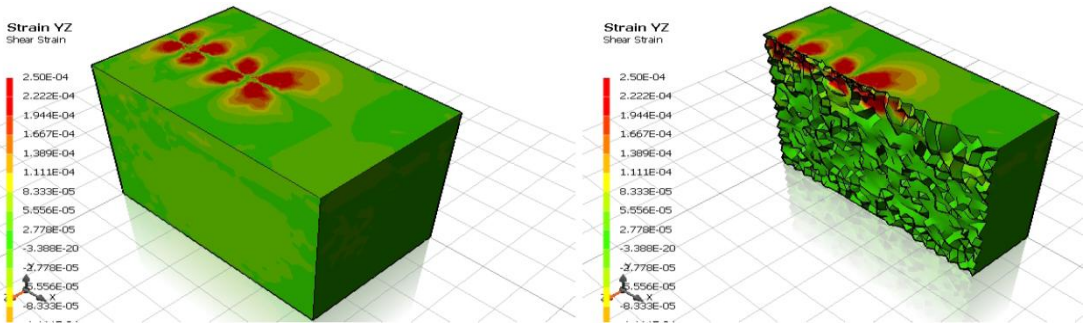

Figure F59. Shear Strain (YZ) Profile for 1Tire:1Sand Road –Treated Subgrade

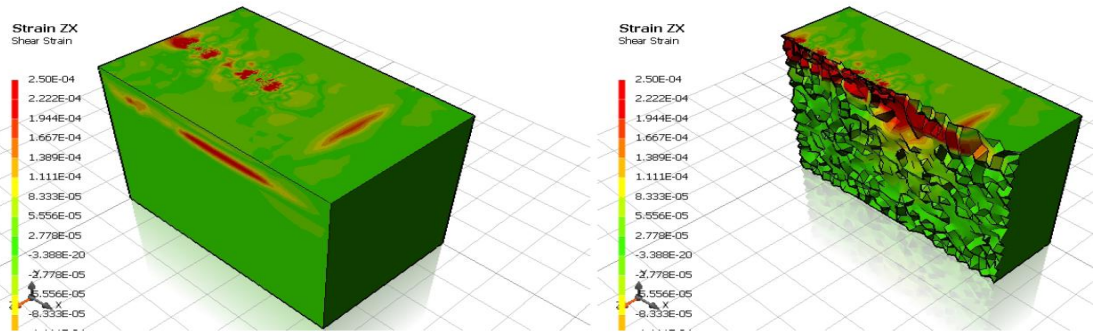

Figure F60. Shear Strain (YZ) Profile for 1Tire:1Sand Road –Treated Subgrade

1TIRE:2SAND ROAD –TREATED SUBGRADE PROFILE

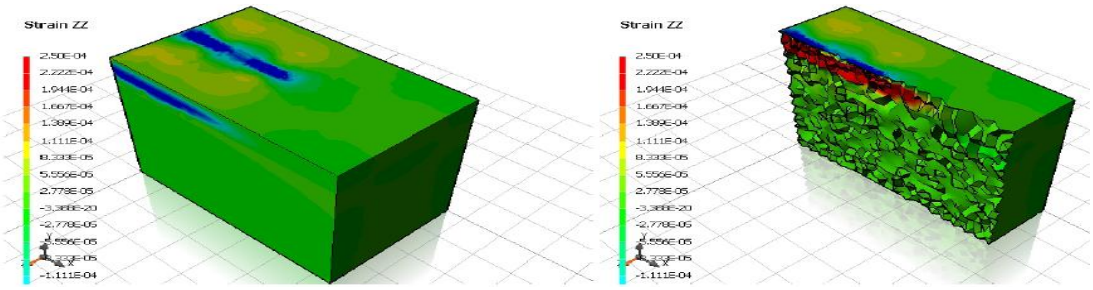

Figure G61. Horizontal Strain (Longitudinal) Profile for 1Tire:2Sand Road –Treated Subgrade

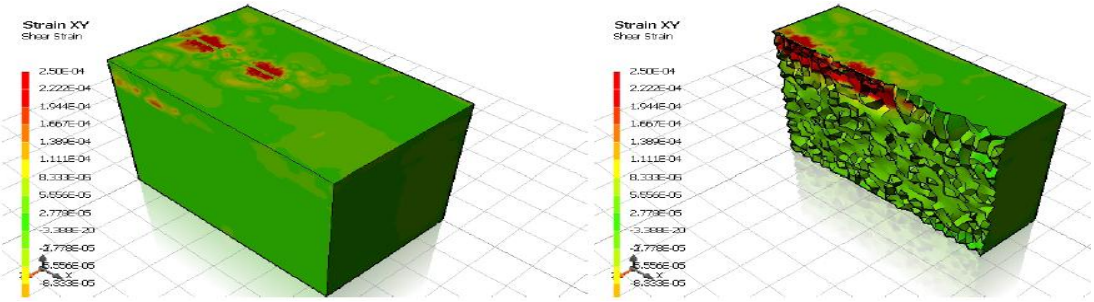

Figure G62. Shear Strain (XY) 1Tire:2Sand Road –Treated Subgrade

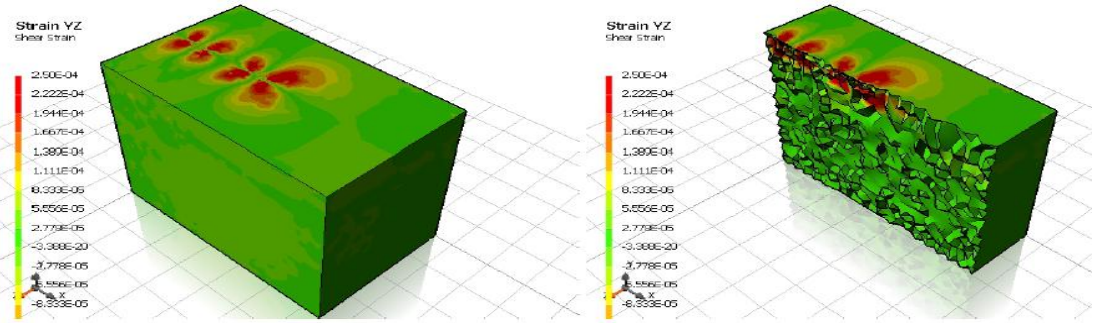

Figure G63. Shear Strain (YZ) Profile for 1Tire:2Sand Road –Treated Subgrade

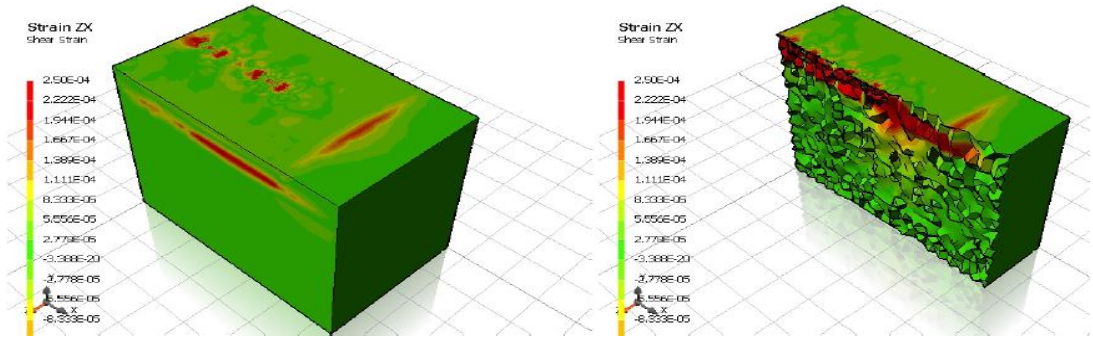

Figure G64. Shear Strain (ZX) Profile for 1Tire:2Sand Road –Treated Subgrade

1TIRE:3SAND ROAD –TREATED SUBGRADE PROFILES

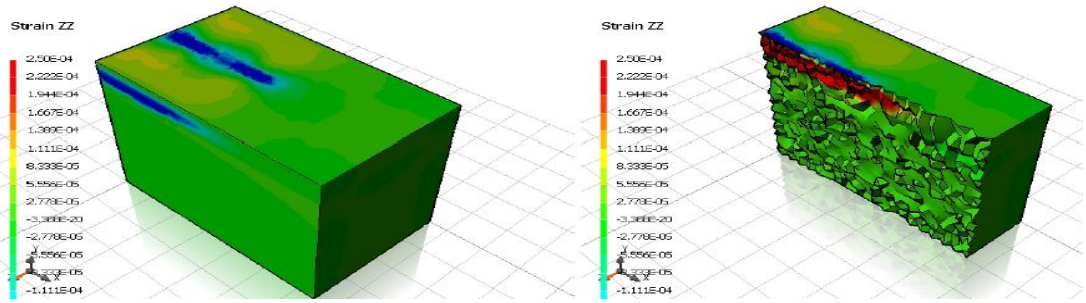

Figure G65. Horizontal Strain (Longitudinal) Profile for 1Tire:3Sand Road –Treated Subgrade

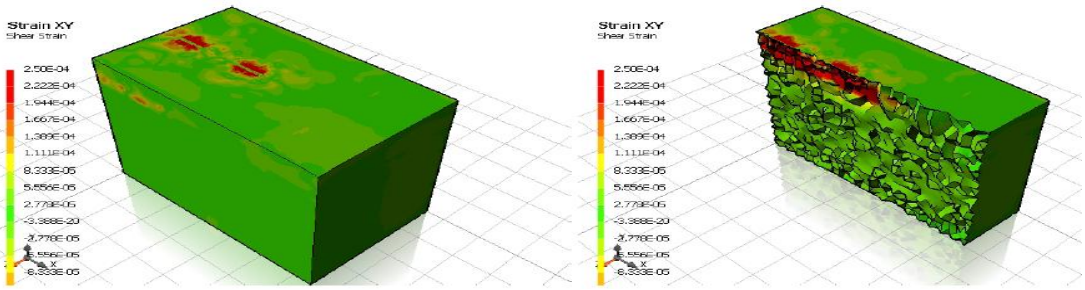

Figure G66. Shear Strain (XY) Profile for 1Tire:3Sand Road – Treated Subgrade

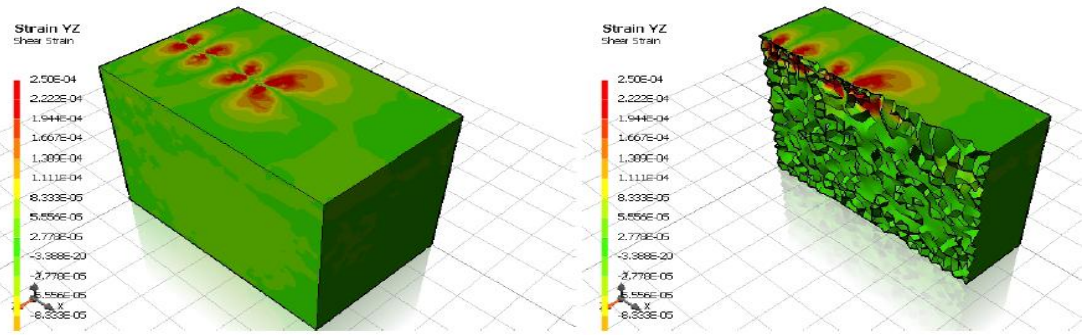

Figure G67. Shear Strain (YZ) Profile for 1Tire:3Sand Road –Treated Subgrade

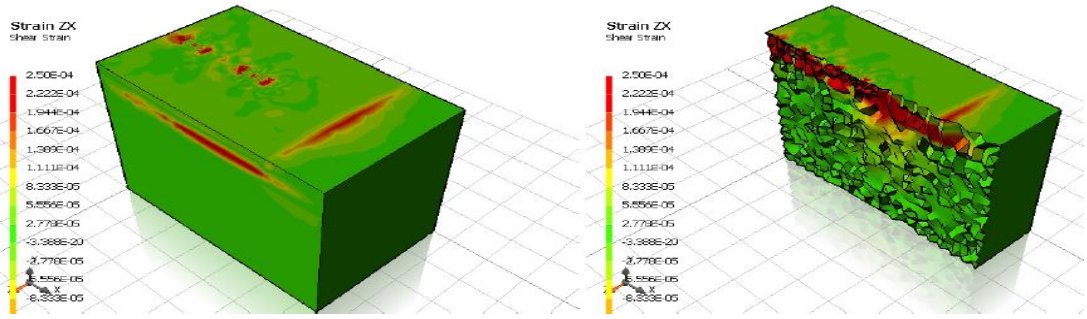

Figure G68. Shear Strain (ZX) Profile for 1Tire:3Sand Road – Treated Subgrade

100% SHREDDED TIRE (DOUBLE BASE) SECTION - TREATED SUBGRADE

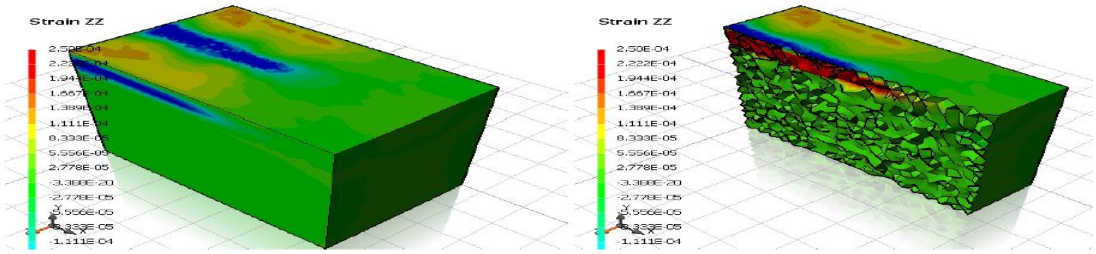

Figure G69. Horizontal Strain (Longitudinal) Profile for 100% Shredded Tire (Double Base) Section – Treated Subgrade

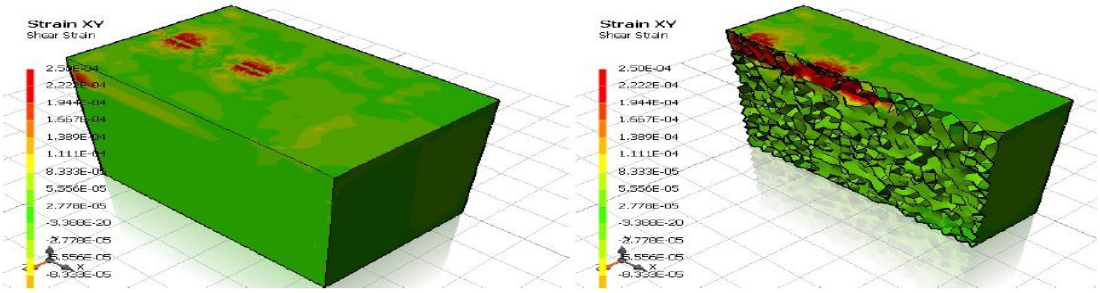

Figure G70. Shear Strain (XY) Profile for 100% Shredded Tire (Double Base) Section – Treated Subgrade

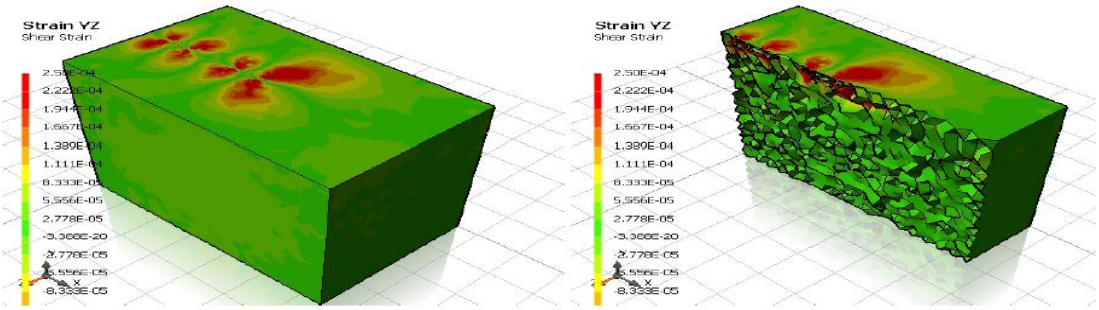

Figure G71. Shear Strain (YZ) Profile for 100% Shredded Tire (Double Base) Section – Treated Subgrade

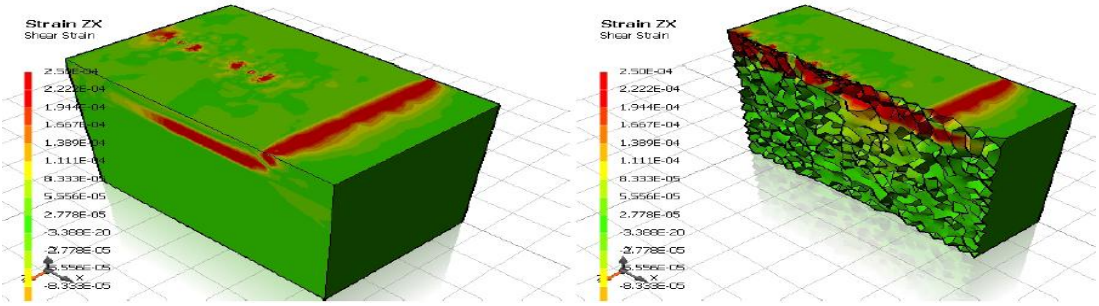

Figure G72. Shear Strain (ZX) Profile for 100% Shredded Tire (Double Base) Section – Treated Subgrade

APPENDIX H.

DESIGN CROSS SECTION & ESTIMATED QUANTITIES AND PRICING FOR ROAD SECTIONS

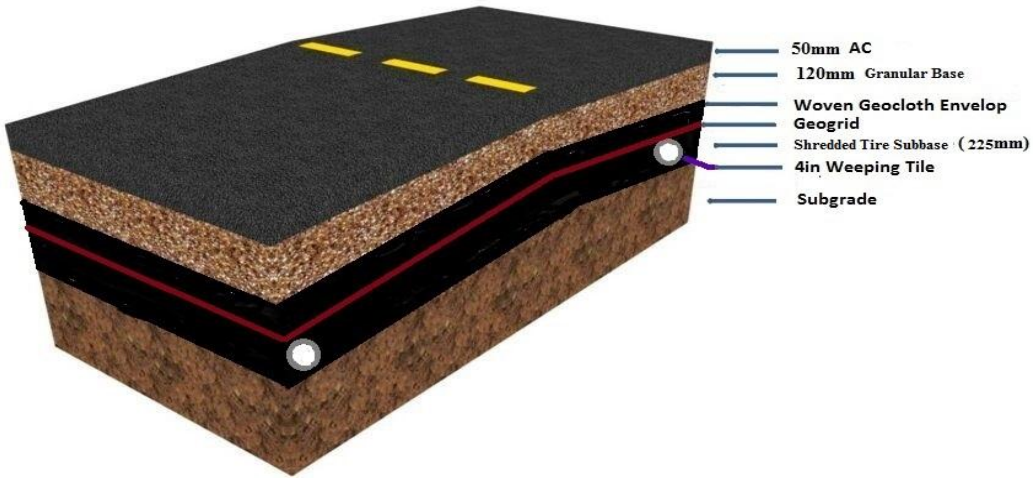

Figure H1. 100% Shredded Tire Road Section

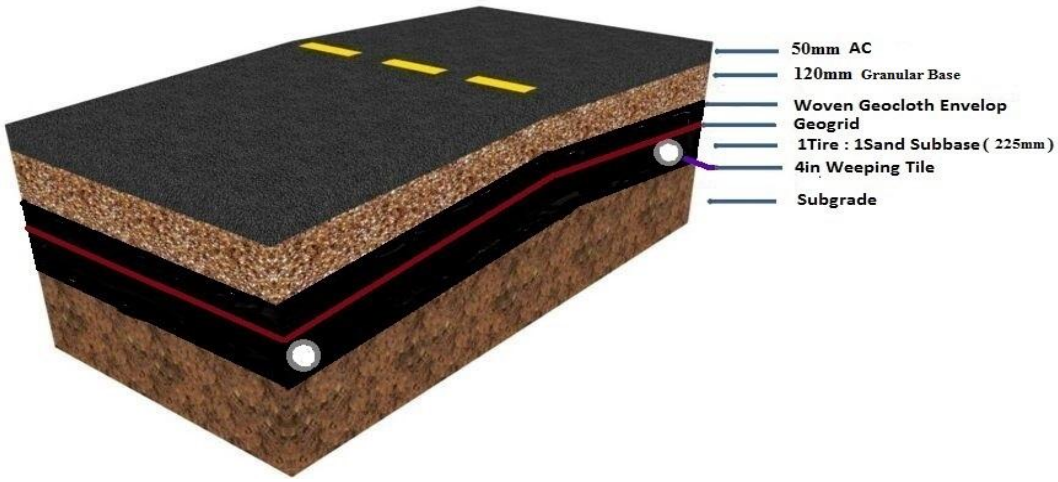

Figure H2. 1Tire:1Sand Road Section

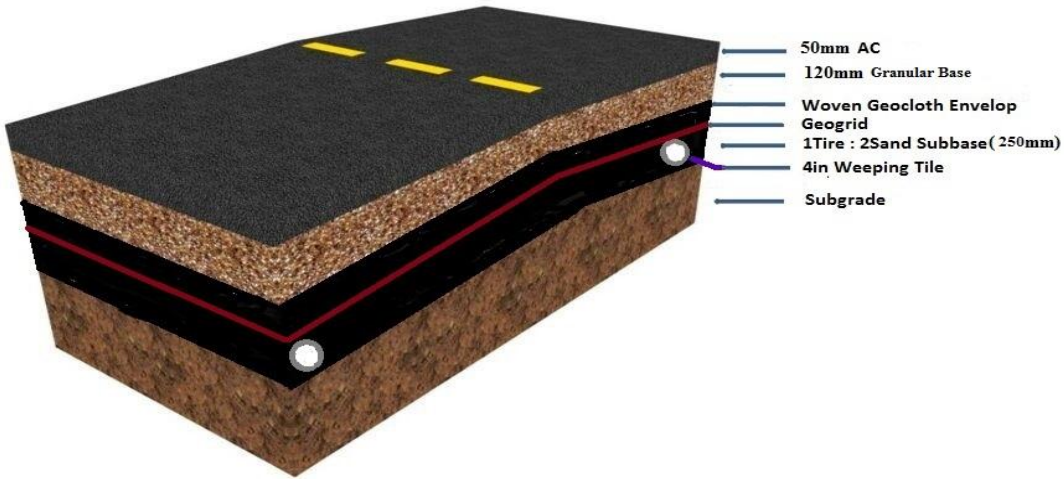

Figure H3. 1Tire:2Sand Road Section

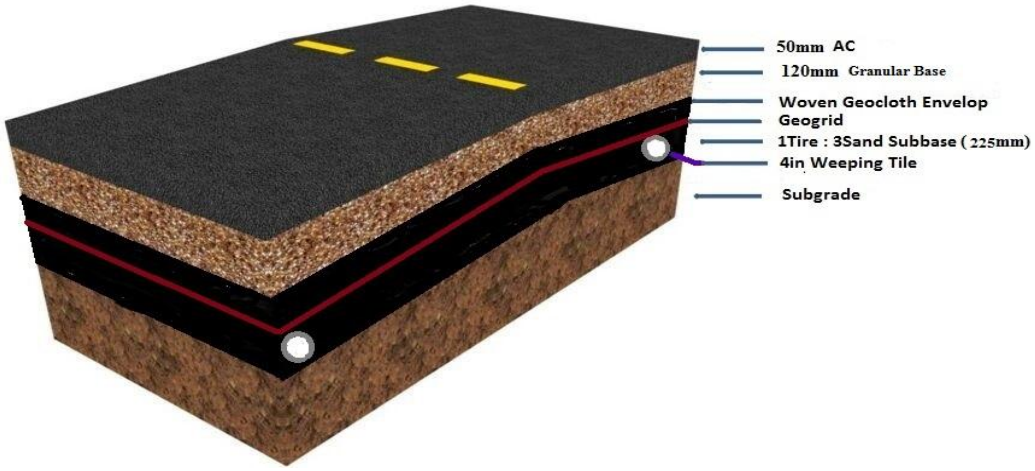

Figure H4. 1Tire:3Sand Road Section

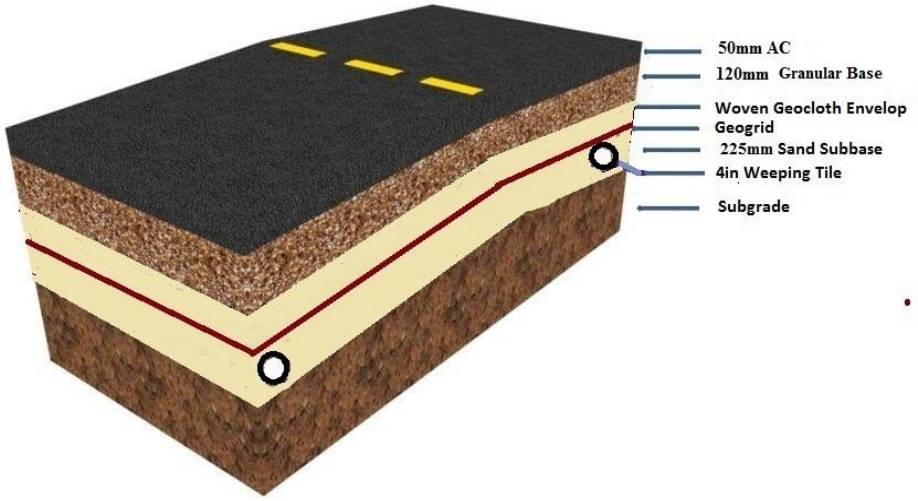

Figure H5. Sand Road Section

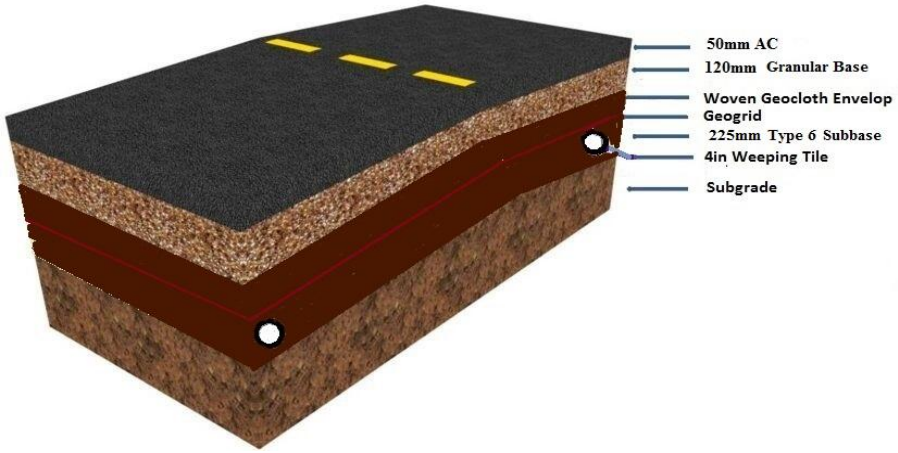

Figure H6. SMHI Type 6 Subbase Road Section

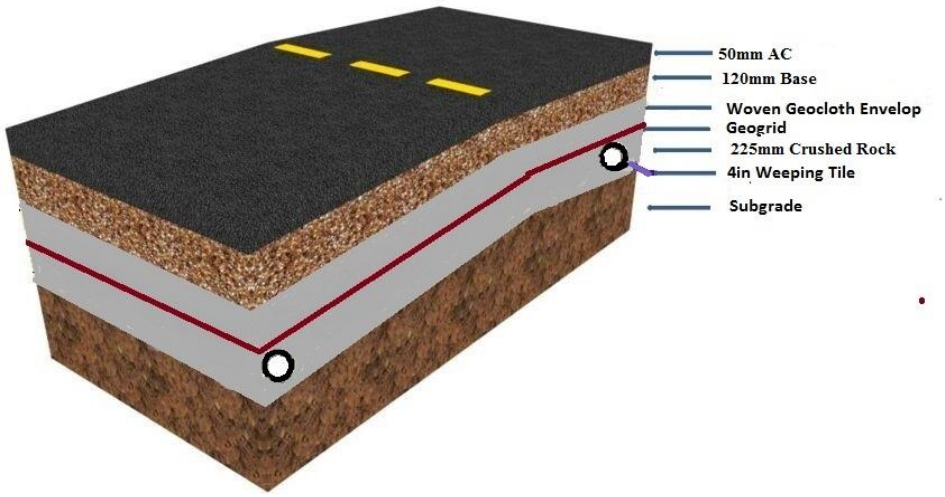

Figure H7. Crushed Rock Road Section

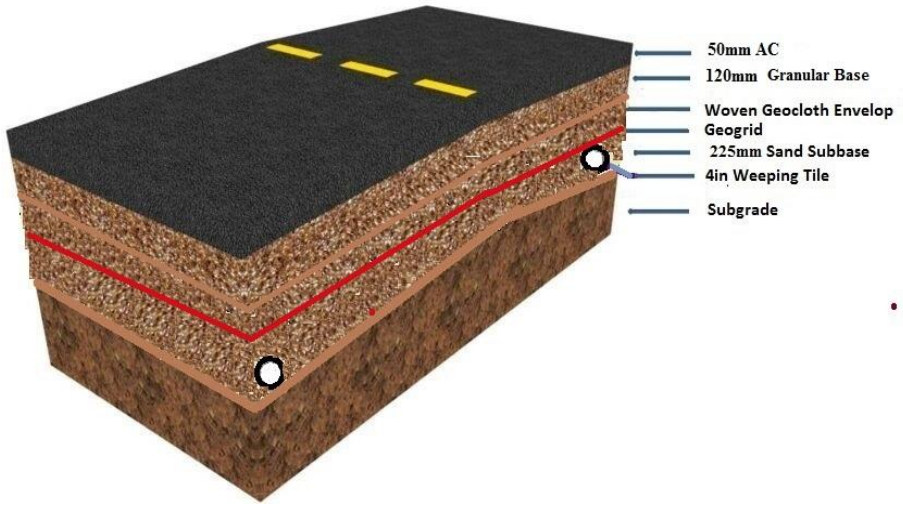

Figure H8. Granular Base Road Section

Table H1. Estimates for 100% Shredded Tire Subbase Layer

No.	Item	Thickness	Unit Price (m^3)	Unit Price $/$m^2$
1	Shredded tire	0.225	13	**2.93**

Table H2. Estimates for 1Tire:1Sand Subbase Layer

No.	Item	Thickness	Unit Price (m^3)	Unit Price $/$m^2$
1	Shredded tire	0.225*(1/2)	13	1.46
2	Sand	0.225*(1/2)	26	2.93
				4.39

Table H3. Estimates for 1Tire:2Sand Subbase Layer

No.	Item	Thickness	Unit Price (m^3)	Unit Price $/$m^2$
1	Shredded tire	0.225*(1/3)	13	0.98
2	Sand	0.225*(2/3)	26	3.9
				4.88

Table H4. Estimates for 1Tire:3Sand Subbase Layer

No.	Item	Thickness	Unit Price (m^3)	Unit Price $/$m^2$
1	Shredded tire	0.225*(1/4)	13	0.73
2	Sand	0.225*(3/4)	26	4.39
				5.12

Table H5. Estimates for Sand Subbase Layer

No.	Item	Thickness	Unit Price (m^3)	Unit Price $/$m^2$
1	Sand	0.225	26	**5.85**

Table H6. Estimates for Type 6 Subbase Layer

No.	Item	Thickness	Unit Price (m^3)	Unit Price $/$m^2$
1	Sand	0.225	26	**5.85**

Table H7. Estimates for Crushed Rock Subbase Layer

No.	Item	Thickness	Unit Price (m^3)	Unit Price $/$m^2$
1	Crushed Rock	0.225	62	**13.95**

Table H8. Estimatess for Granular Base Subbase Layer

No.	Item	Thickness	Unit Price (m^3)	Unit Price $/$m^2$
1	Sand	0.225	40	**9.00**